MARTIN MARIETTA ENERGY SYSTEMS LIBRARIES
3 4456 0250982 7

[redacted]

CENTRAL RESEARCH LIBRARY
DOCUMENT COLLECTION

AEC RESEARCH AND DEVELOPMENT REPORT

ORNL-2115
Vol. III
C-85—Propulsion Systems

ANP

CENTRAL RESEARCH LIBRARY
DOCUMENT COLLECTION
LIBRARY LOAN COPY
DO NOT TRANSFER TO ANOTHER PERSON
If you wish someone else to see this document, send in name with document and the library will arrange a loan.

FIRST SEMIANNUAL ANP SHIELDING INFORMATION MEETING

MAY 7-8, 1956

VOLUME III

DECLASSIFIED
CLASSIFICATION CHANGED TO:
BY AUTHORITY OF: AEC 11-19-65
BY: C. Wells 6/17/66

[redacted]

OAK RIDGE NATIONAL LABORATORY
OPERATED BY
UNION CARBIDE NUCLEAR COMPANY
A Division of Union Carbide and Carbon Corporation
UCC
POST OFFICE BOX P · OAK RIDGE, TENNESSEE

[redacted]

LEGAL NOTICE

This report was prepared as an account of Government sponsored work. Neither the United States, nor the Commission, nor any person acting on behalf of the Commission:

A. Makes any warranty or representation, express or implied, with respect to the accuracy, completeness, or usefulness of the information contained in this report, or that the use of any information, apparatus, method, or process disclosed in this report may not infringe privately owned rights; or

B. Assumes any liabilities with respect to the use of, or for damages resulting from the use of any information, apparatus, method, or process disclosed in this report.

As used in the above, "person acting on behalf of the Commission" includes any employee or contractor of the Commission to the extent that such employee or contractor prepares, handles or distributes, or provides access to, any information pursuant to his employment or contract with the Commission.

[redacted]

C-85, Propulsion Systems

ORNL-2115 - Vol. III

This document consists of 192 pages. Copy 4 of 150 copies. Series A.

Papers Presented at the

FIRST SEMIANNUAL ANP SHIELDING INFORMATION MEETING, May 7-8, 1956,

VOLUME III

Date Issued

JUL 3 1956

Sponsored by
AIRCRAFT REACTORS BRANCH
Division of Reactor Development, USAEC

at

OAK RIDGE NATIONAL LABORATORY
Operated by
UNION CARBIDE NUCLEAR COMPANY
A Division of Union Carbide and Carbon Corporation
Post Office Box P
Oak Ridge, Tennessee

[redacted]

[redacted]

MARTIN MARIETTA ENERGY SYSTEMS LIBRARIES

3 4456 0250982 7

[redacted]

ORNL-2115
Reactors-Aircraft Nuclear
Propulsion Systems
M-3679 (18th ed.)

INTERNAL DISTRIBUTION

1. C. E. Center
2. Biology Library
3. Health Physics Library
4-5. Central Research Library
6. Reactor Experimental Engineering Library
7-31. Laboratory Records Department
32. Laboratory Records, ORNL R.C.
33. A. M. Weinberg
34. L. B. Emlet (K-25)
35. J. P. Murray (Y-12)
36. J. A. Swartout
37. E. H. Taylor
38. E. D. Shipley
39. A. H. Snell
40. M. L. Nelson
41. W. H. Jordan
42. S. J. Cromer
43. G. E. Boyd
44. R. A. Charpie
45. S. C. Lind
46. F. L. Culler
47. A. Hollaender
48. K. Z. Morgan
49. C. E. Winters
50. D. S. Billington
51. A. J. Miller
52. E. P. Blizard
53. D. D. Cowen
54. W. M. Breazeale (consultant)
55. M. J. Skinner
56. R. R. Dickison
57. A. Simon
58. F. C. Maienschein
59. A. D. Callihan
60. C. E. Clifford
61. F. L. Keller
62. R. W. Peelle
63-64. ORNL - Y-12 Technical Library, Document Reference Section

EXTERNAL DISTRIBUTION

65. AF Plant Representative, Baltimore
66-67. AF Plant Representative, Burbank
68. AF Plant Representative, Marietta
69-71. AF Plant Representative, Santa Monica
72-73. AF Plant Representative, Seattle
74. AF Plant Representative, Wood-Ridge
75. Air Research and Development Command (RDGN)
76. Air Research and Development Command (RDZPA)
77. Air Technical Intelligence Center
78. Air University Library
79-81. ANP Project Office, Fort Worth
82. Argonne National Laboratory
83. Armed Forces Special Weapons Project, Sandia
84. Armed Forces Special Weapons Project, Washington
85. Assistant Secretary of the Air Force, R&D
86-91. Atomic Energy Commission, Washington
92. Bureau of Aeronautics
93. Bureau of Aeronautics General Representative
94. Chicago Operations Office
95. Chicago Patent Group

[redacted]

96. Chief of Naval Research
97. Convair-General Dynamics Corporation
98-101. General Electric Company (ANPD)
102. Hartford Area Office
103. Headquarters, Air Force Special Weapons Center
104. Lockland Area Office
105. Los Alamos Scientific Laboratory
106. National Advisory Committee for Aeronautics, Cleveland
107. National Advisory Committee for Aeronautics, Washington
108. Naval Air Development and Material Center
109. Naval Research Laboratory
110. North American Aviation, Inc. (Aerophysics Division)
111. Nuclear Development Corporation of America
112. Office of the Chief of Naval Operations (OP-361)
113. Patent Branch, Washington
114-117. Pratt & Whitney Aircraft Division (Fox Project)
118. Sandia Corporation
119. School of Aviation Medicine
120. USAF Project Rand
121. University of California Radiation Laboratory, Livermore
122-139. Wright Air Development Center (WCOSI-3)
140-149. Technical Information Service Extension, Oak Ridge
150. Division of Research and Development, AEC, ORO

[redacted]

[redacted]

PREFACE

The papers presented at the First Semiannual ANP Shielding Information Meeting are published in three volumes. Volumes I and II are also identified as ORNL-2115.

[redacted]

[redacted]

TABLE OF CONTENTS

Volume III

	Paper No.
Effect of Core Diameter on Shield Requirements for Cylindrical Reactors ..... M. A. Capo, J. G. Carver, General Electric Co., ANP Dept., Cincinnati	III-A
Modification of the Procedure for Using TSF Data for the Optimization of a Divided Neutron Shield ..... S. K. Penny, Oak Ridge National Laboratory	III-B
A Shield Shaping Method ..... T. R. Strayhorn, R. J. Klotz, Convair, Ft. Worth	III-C
Martin Unit Shield Design Procedure ..... B. L. Byrum, J. A. Biggerstaff, Martin, Baltimore	III-D
Shield Design Study for a Circulating Fuel Reactor Utilizing a Fuel-to-Air Radiator ..... L. B. Holland, S. K. Penny, D. K. Trubey, Oak Ridge National Laboratory	III-E
Shielding Materials for Aircraft Application ..... S. A. Szawlewicz, H. C. Sullivan, Wright Air Development Center	III-F
Full Scale Turbojet Activation Experiment -- Preliminary Results ..... J. Moteff, General Electric Co., ANP Dept., Evendale	III-G
The Shield Mockup Reactor ..... L. B. Holland, Oak Ridge National Laboratory	III-H
Current and Future ORNL Shielding Projects ..... E. P. Blizard, Oak Ridge National Laboratory	III-I
Some Aspects of the Long Term Effects of Radiation ..... N. I. Berlin, Armed Forces Special Weapons Project, Washington, D. C.	III-J

[redacted]

[redacted]

Paper III-A

EFFECT OF CORE DIAMETER ON SHIELD REQUIREMENTS FOR CYLINDRICAL REACTORS

M. A. Capo and J. G. Carver
General Electric Company - ANP Dept., Cincinnati

[redacted]

[redacted]

[redacted]

EFFECT OF CORE DIAMETER ON SHIELD REQUIREMENTS FOR CYLINDRICAL REACTORS

by

M. A. Capo, J. G. Carver

General Electric Company
Aircraft Nuclear Propulsion Department
Cincinnati, Ohio

Any abbreviation in the design procedures for a reactor shield assembly would certainly be of benefit to the field of shielding in general. For this reason, the shielding effect of varying the diameter of the core in a reactor-shield assembly possessing cylindrical geometry was investigated. It should first be of interest to note that one result of changing the core diameter will be a change in the shielding requirements at the side of the RSA. This change is independent of variations in power, permissible dose rates, or any of the other design parameters involved. If this effect of variation in core diameter on the thicknesses of shielding material required at the side of the RSA could be determined, it may be possible to avoid some of the trial-and-error procedures used in modifying an existing shield design for a reactor of different diameter.

COMPUTATIONS INVOLVED

The basic core composition and shield design were taken as those for a direct air-cycle power plant presently under study at GE-ANP.[1] This reactor has a cross section which is approximately cylindrical and has a diameter of 48 inches. The side shielding materials are as follows:

MATERIAL	THICKNESS, cm.	
Core	60.96	
Be	10.16	including 10% void for cooling
U	2.90	including 10% void for cooling
LiH	34.11	
Pentalene	9.95	

The power distribution was assumed to be uniform along the axis of symmetry of the reactor.

[redacted]

[redacted]

Digital computer programs were used to calculate fast neutron and gamma dose rates at 50 feet from the side of the reactor center for both constant total power and constant power density in the reactor for cores of radii 30 inches down to 1 inch (for the sake of completeness). In all computations the radial thickness of the side shielding material was constant at the values just mentioned. Similar calculations were performed for two other conditions — (1) a shielded, non-absorbing core, and (2) a bare, unshielded core. Thus we have three sets of data to study:

1. Bare core
2. Shielded non-absorbing core — "transparent core"
3. Complete RSA

All the calculations discussed here were line-of-sight calculations employing point kernels for homogeneous infinite media. The validity of this approach has been discussed in Reference 2. For our present study, it is felt that any errors inherent in this point kernel approach would be in the same direction and of comparable magnitude for all of the core radii considered, and that any such errors would tend to cancel out in comparisons between reactors of different diameters.

QUALITATIVE DISCUSSION

To understand the discussion of results which will follow, it will be well to examine a sketch of a cross section taken perpendicular to the core axis (Figure 5). The receiver point is 50 feet from the side, lies in the plane of the diagram, and is sufficiently remote that the lines connecting the receiver point to the various source points in the core may be considered approximately parallel. It is at once evident that radiations from different source points are attenuated by different thicknesses of both reactor and shield materials. It can also be proven algebraically that for a source point located, as shown here, both l_1 and l_2 increase as "a" decreases or for a fixed "a", both l_1 and l_2 increase as R increases.

There are three characteristics of the RSA that should be noted: (1) for a core of constant diameter, the radiation from a given source point undergoes less attenuation from the core and more from the shielding as the source point is moved out along a radial line perpendicular to the line joining source and receiver points; (2) for a source point located on this line at a constant fraction of the core radius away from the center, both core and shield introduce more and more attenuation as the core diameter is increased; (3) as the core radius increases, the attenuation in the core increases more rapidly than the attenuation in the shield for most source points within the core of an RSA of typical design.

These properties of the RSA are sufficient to explain qualitatively the behavior of the curves given in Figures 1 and 2 for the case of constant total reactor power. (It should be noted that all curves have been normalized to unity for the 30 inch core.) In this case, the reactor may be considered as an array of radiation source points

[redacted]

[redacted]

which expands or contracts as the core radius is varied. Each source point has a strength that is determined by the uniform radial power density necessary to provide the same total power. By referring to these graphs it should be noticed that even when the attenuation in the core is neglected ("transparent core" case), the effectiveness of the shielding increases as the core radius increases. This variation is in the same direction, but more pronounced, for the bare core case, because the attenuation due to the core increases with core radius more rapidly then does the attenuation due to the shielding. Since both effects operate in the same direction, the fact that the variation of dose rate with core radius is still more pronounced for the complete RSA should be expected.

The graphs in Figures 3 and 4 differ from the previous ones since the power density in the reactor is held constant; hence the total power varies as the square of the core radius. This fact accounts for the order in which the curves exhibit an increasing variation in dose rate with core radius which is the reverse of that for the case of constant total power. The effect is equivalent to multiplying the first two curves by a factor $(R/30 \text{ in})^2$ which would bend all of the curves to new locations below the horizontal axis. As a result, the curves for the "transparent core" case now exhibit the most rapid changes with core radius. It is not surprising that the curves for the transparent core RSA follow quite closely the curve of total reactor power because the dose rate should change in the same manner as the change in power.

QUANTITATIVE DISCUSSION

An attempt was made to separate the attenuating properties of core and shield in studying the total effect of variation of core radius. By setting up a few simple equations (by way of definition), and examining them, it was found that such an attempt failed.

Aside from the mathematical analysis of the variables involved, the difficulty of separating the attenuating properties can be seen for physical reasons. Since the attenuation introduced by the shield is different for different source points (See Figure 5), the average attenuation due to the shield depends on the spatial distribution of the radiation impinging on the inner surface of the shield. This distribution, in turn, depends on the absorption within the core. Thus it is evident that the attenuating properties cannot be separated. It was then calculated that such a separation resulted in an error of the order of 20% in calculations for practical values of core radius (15-30 inches).

POSSIBLE APPLICATION

As stated earlier, the results of this study are expected to be most useful when an existing RSA design is to be modified by changing the diameter (and usually the operating power) of the reactor. In such

[redacted]

[redacted]

cases, a good design for the new reactor shield may be obtained by simple hand-calculated corrections to the shield thicknesses of the existing RSA design. The method to be described is an elaboration of the procedure given in Reference 2 for modifying a shield for a change in reactor power.

Let

Σ = fast neutron removal cross section

μ = pile gamma absorption coefficient

Δt = required change in thickness of a particular shielding material

P = total reactor power

$f(r) = \frac{D(r)}{D(r_o)}$ for constant total power <u>or</u> constant power density

D(r) = dose rate for complete RSA with core radius of r

Subscripts n and γ denote neutron and gamma-ray shielding materials, respectively; o refers to original RSA design.

The required shielding thickness changes at the side are given by:

$$\Sigma_n \Delta t_n + \Sigma_\gamma \Delta t_\gamma = \ln\left[f_n(r)\frac{P}{P_o}\right]$$
$$\mu_n \Delta t_n + \mu_\gamma \Delta t_\gamma = \ln\left[f_\gamma(r)\frac{P}{P_o}\right]$$

where allowance has been made for the general case, i.e., the power has been changed. In the case for constant power density, the ratio $\frac{P}{P_o}$ must be replaced by a ratio of the power densities.

The foregoing procedure is applicable to shielding thicknesses at the side of a reactor having Σ and μ approximately the same as those of the direct air-cycle reactor for which these curves have been computed (Σ = 0.055 cm. and μ = 0.062 cm.). If the reactor under consideration has a substantially different Σ or μ, some revision of the method is necessary. However, for reactors having radii between 15 and 30 inches, the principal effect of changing core radius is due to the change in self-shielding of the reactor itself, as Figures 1 - 4 clearly show. Thus it is indicated that the procedure is applicable provided that compensation can be made for the different values of Σ or μ for the core.

Such compensation may be achieved, at least to a reasonably good approximation, by replotting Figures 1 and 2 (or 3 and 4 if preferred) against an abscissa of core radius, expressed as number of relaxation lengths for the type of radiation in question. For the reactor used in this study, these relaxation lengths are: λ_n = 18.1 cm. and λ_γ = 16.1 cm. The results of such a plot are shown in Figures 6 and 7.

[redacted]

If now the radius of the new core is expressed as a number of relaxation lengths, then the equations stated above are applicable and should yeild reasonably good first-trial design thicknesses.

In a strict sense, the foregoing analysis applies only to a reactor shield with the same thicknesses and materials used in the direct air-cycle reactor that was examined. However, in view of the very weak dependence of dose rate on the inner radius of the shield, if attenuation in the core is neglected, it is expected that the suggested procedure would yield equally good results for a wide range of thicknesses of both neutron and gamma-ray shielding materials. Thus for particular purposes, it should not be necessary to attempt a separation of the shielding effects of core and shield. This circumstance would be welcome in any event and is especially desirable in view of the difficulties, already discussed, of achieving such a separation in any useful manner.

[redacted]

BIBLIOGRAPHY

1. APEX 214, "Nuclear Shield Analysis for the AC-110 Power Plant", J. G. Carver, W. E. Edwards, and J. Moteff, November 11, 1955.

2. APEX 230, "GE-ANPD Methods of Shield Design", J. G. Carver, W. E. Edwards, and J. E. MacDonald, December 30, 1955

[redacted]

[redacted]

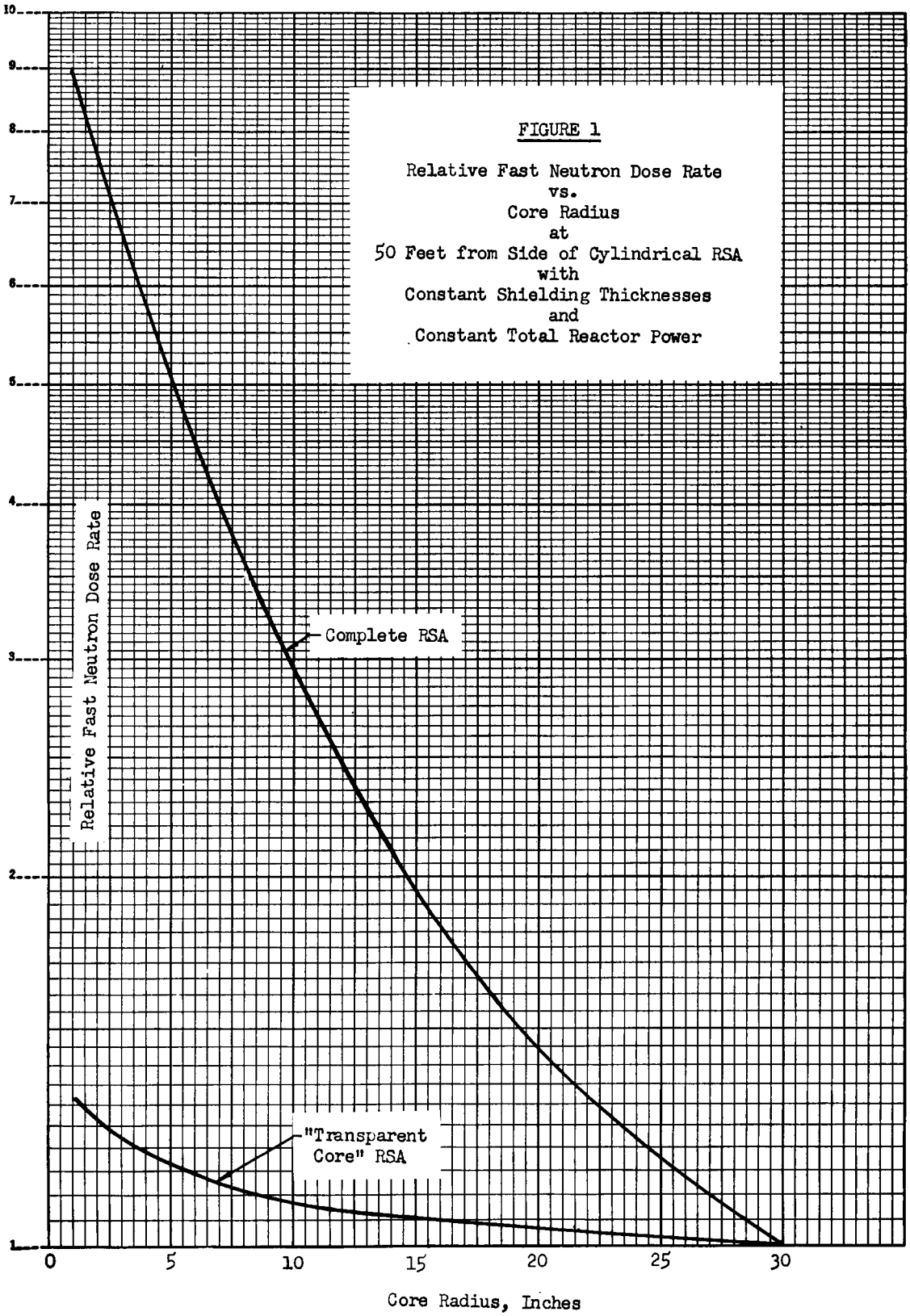

[redacted]

[redacted]

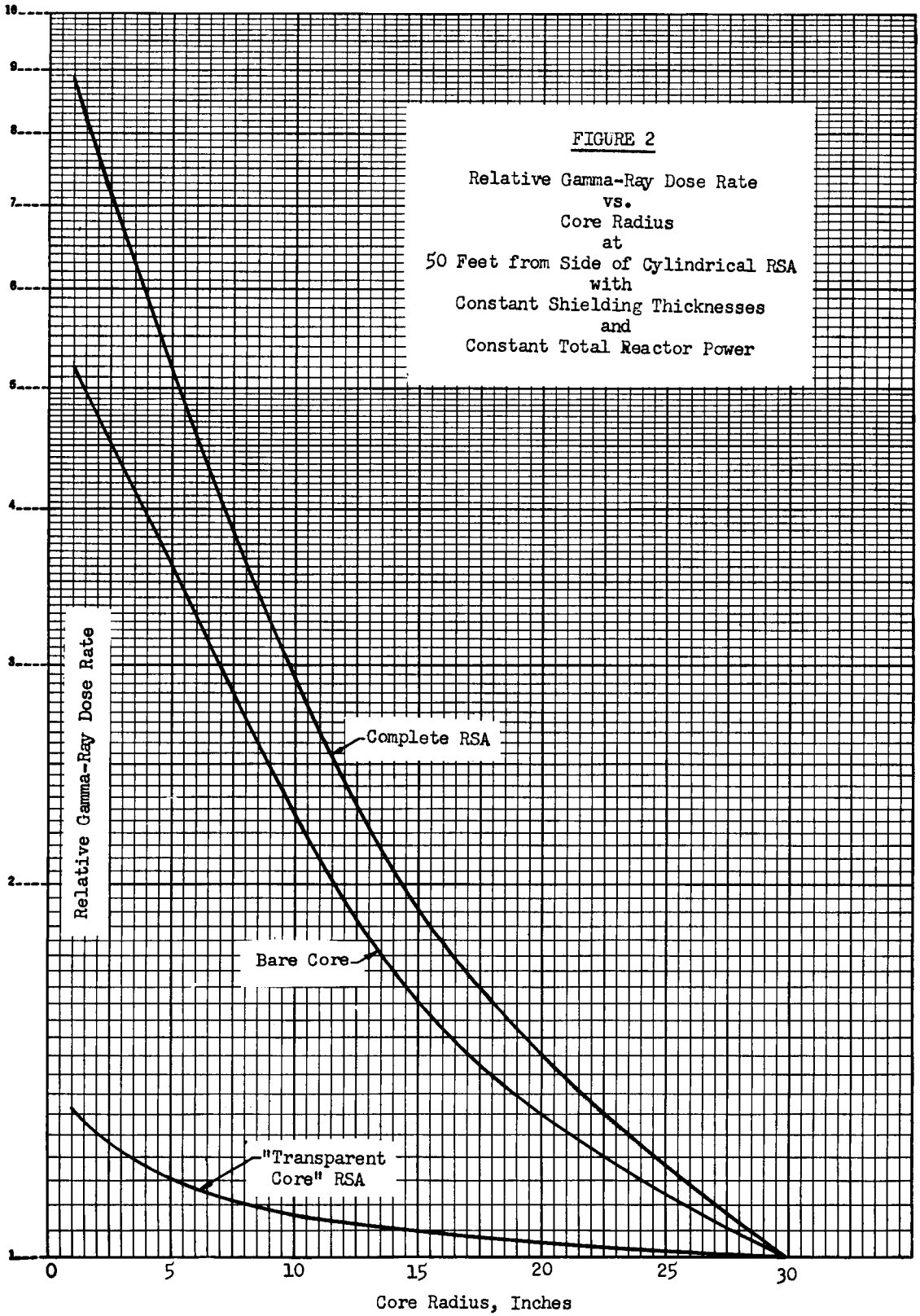

[redacted]

[redacted]

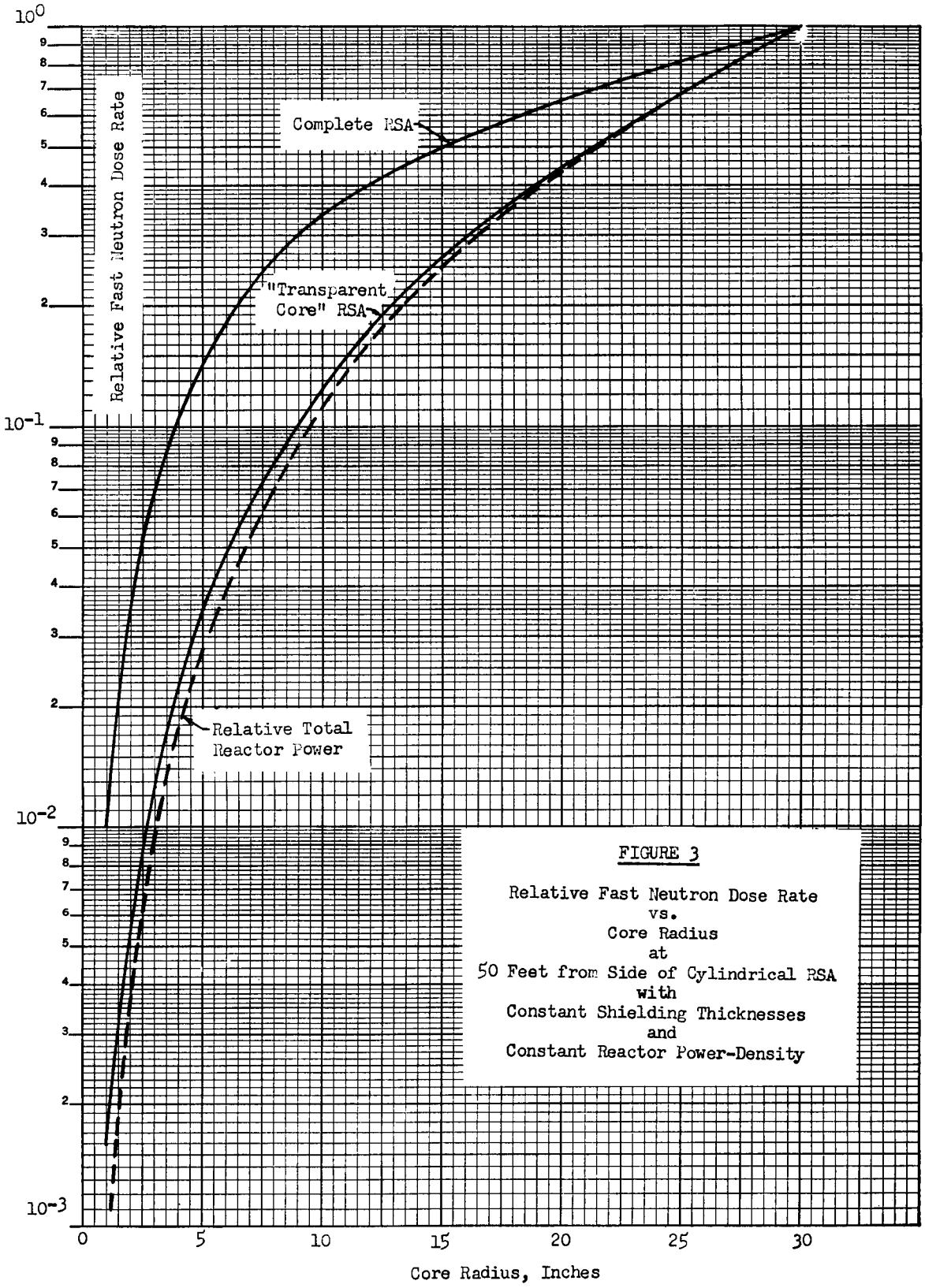

FIGURE 3

Relative Fast Neutron Dose Rate
vs.
Core Radius
at
50 Feet from Side of Cylindrical RSA
with
Constant Shielding Thicknesses
and
Constant Reactor Power-Density

[redacted]

[redacted]

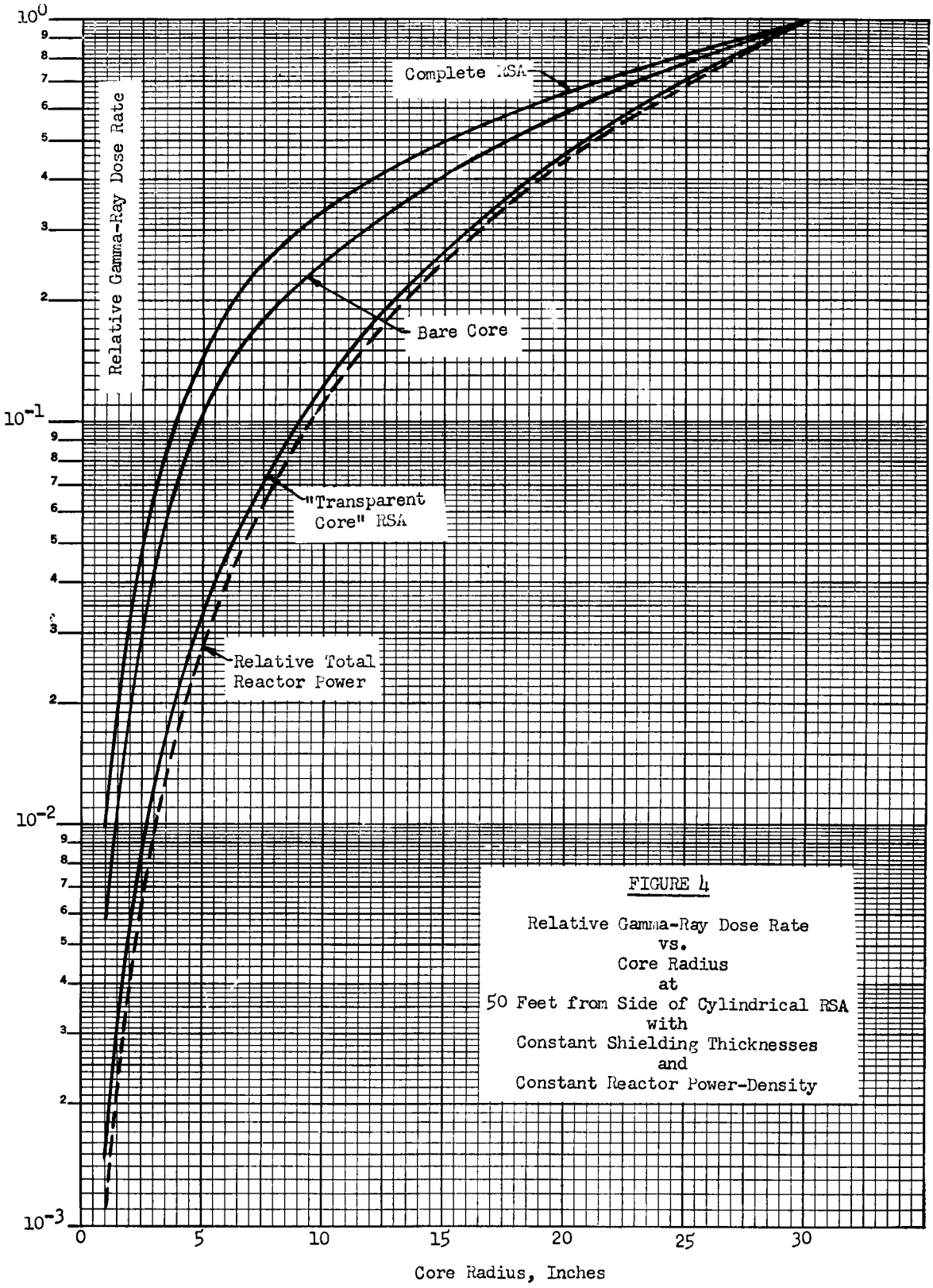

FIGURE 4

Relative Gamma-Ray Dose Rate
vs.
Core Radius
at
50 Feet from Side of Cylindrical RSA
with
Constant Shielding Thicknesses
and
Constant Reactor Power-Density

[redacted]

[redacted]

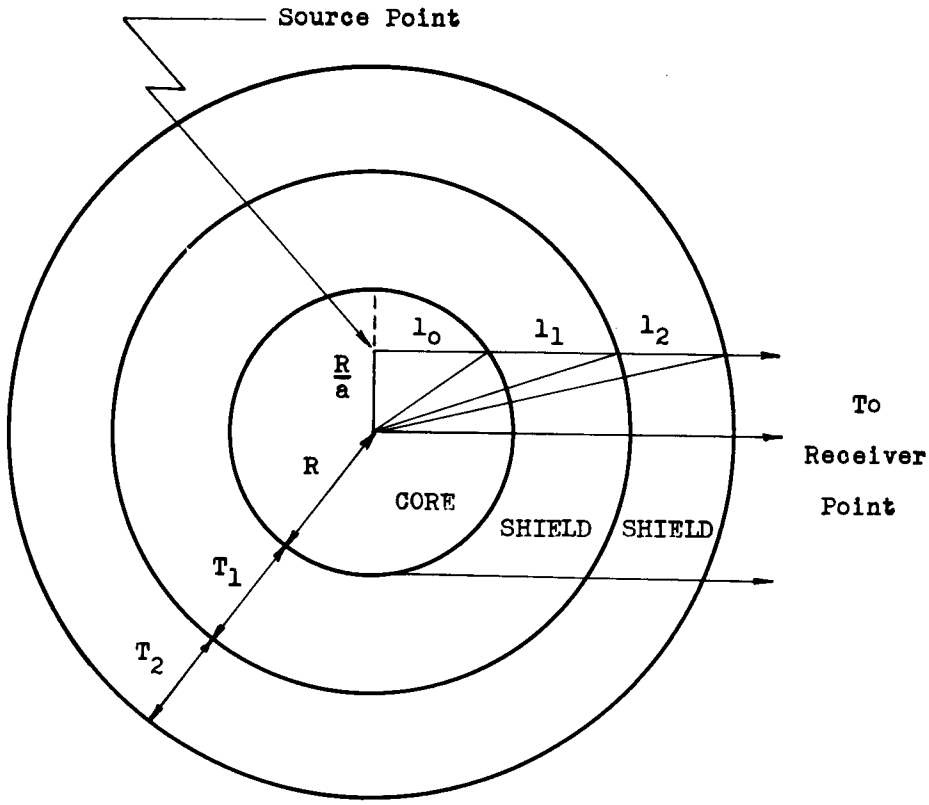

FIGURE 5. Cross Section of Cylindrical Reactor with Side Shielding Materials of Thicknesses T_1 and T_2.

[redacted]

[redacted]

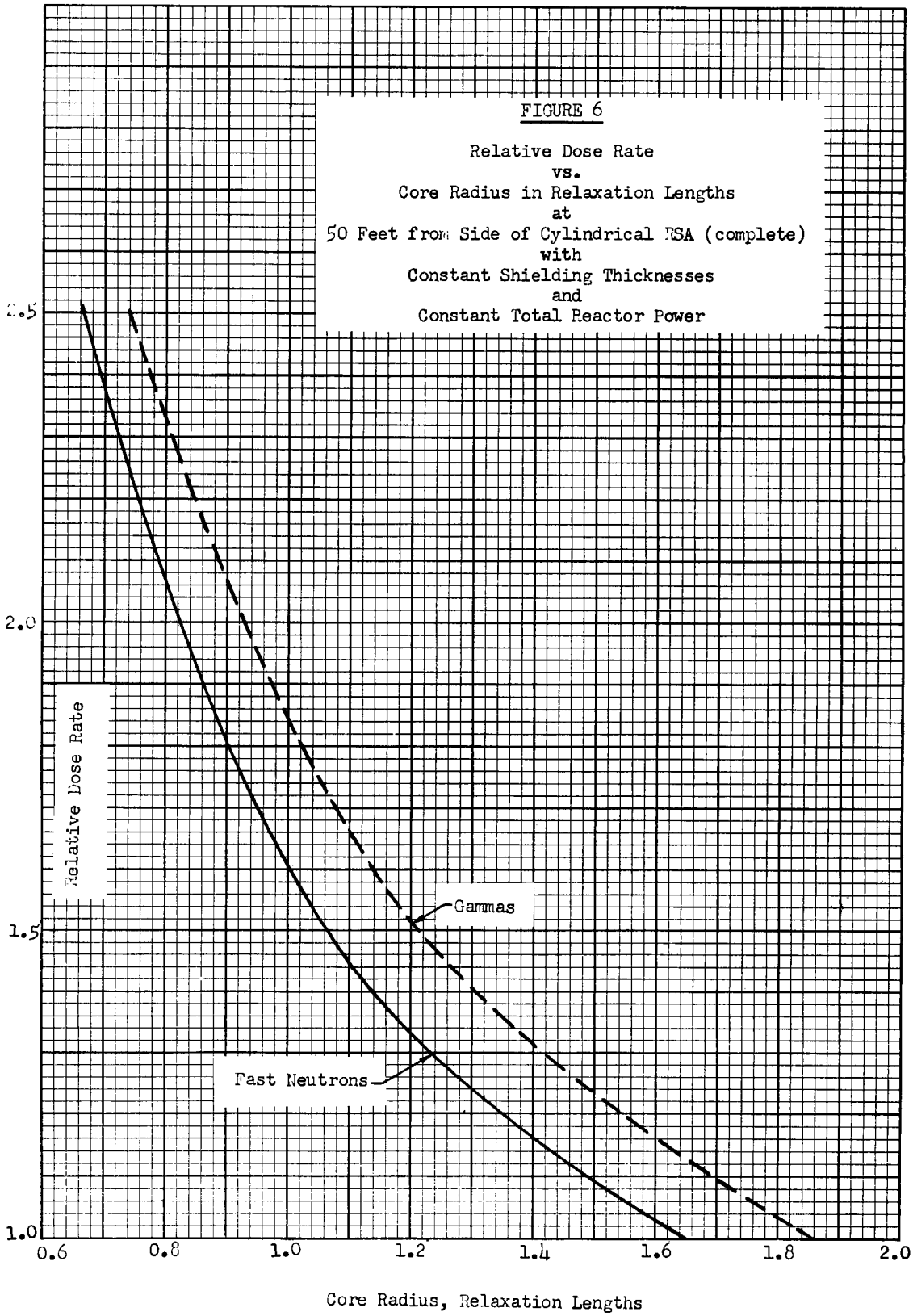

[redacted]

[redacted]

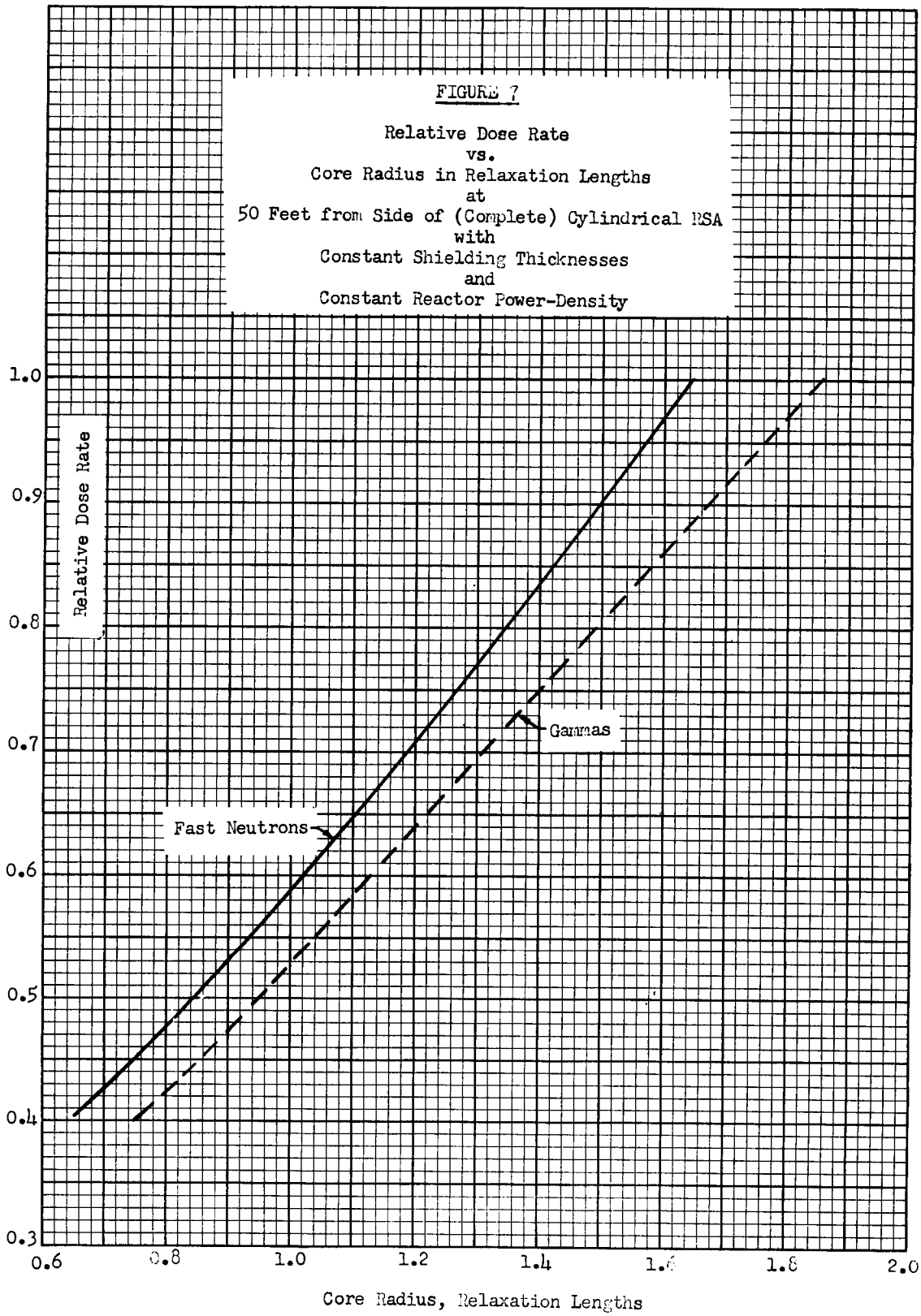

FIGURE 7

Relative Dose Rate
vs.
Core Radius in Relaxation Lengths
at
50 Feet from Side of (Complete) Cylindrical RSA
with
Constant Shielding Thicknesses
and
Constant Reactor Power-Density

[redacted]

SECRET

Paper III-B

MODIFICATION OF THE PROCEDURE FOR USING TSF DATA FOR THE OPTIMIZATION OF A DIVIDED NEUTRON SHIELD

S. K. Penny
Oak Ridge National Laboratory

SECRET

RESTRICTED DATA

"This document contains restricted data as defined in the Atomic Energy Act of 1954. Its transmittal or the disclosure of its contents in any manner to an unauthorized person is prohibited."

[redacted]

MODIFICATION OF THE PROCEDURE FOR USING TSF DATA FOR THE OPTIMIZATION OF A DIVIDED NEUTRON SHIELD

by

S. K. Penny
Oak Ridge National Laboratory
Oak Ridge, Tennessee

The procedure for the optimization of a divided neutron shield using TSF data has been modified in two respects: (1) a derivative term was included which was neglected before, and (2) the iteration procedure was changed in such a way that one of the Lagrangian multipliers converges more rapidly. The effect these modifications have on the shield thicknesses and weights has been determined by a sample shield calculation for the same reactor and crew compartment system used previously.

The procedure for the optimization of a divided neutron shield using TSF data[1,a] determines the shield which has the minimum weight subject to the condition that the dose rate at the center of the crew compartment be a specified amount. It should be understood that it does not determine a completely optimized neutron shield for a particular reactor and crew compartment configuration. The reactor shield is divided into N conical shells as shown in Fig. 1. The radius a in Fig. 1 is the inner radius of the neutron shield on the reactor and the neutron shield thickness is T_n. The crew shield has a rear thickness, T_r, and a side thickness, T_s. The front thickness, T_f, is assumed to be the same as the side thickness.

The procedure consists of the following: (1) expressing both the total weight of the neutron shield and the dose rate at the center of the cylindrically shaped crew compartment as functions of T_n, T_r, and T_s; (2) using the method of Lagrangian multipliers to obtain the equations which T_n, T_r, and T_s must satisfy in order that the weight be a minimum for a specified total dose rate; and (3) developing an iterative procedure for the solution of these equations.

The total weight of the neutron shield is given by

---

a. The description of the original procedure given in this paper was largely lifted from Ref. 1.

[redacted]

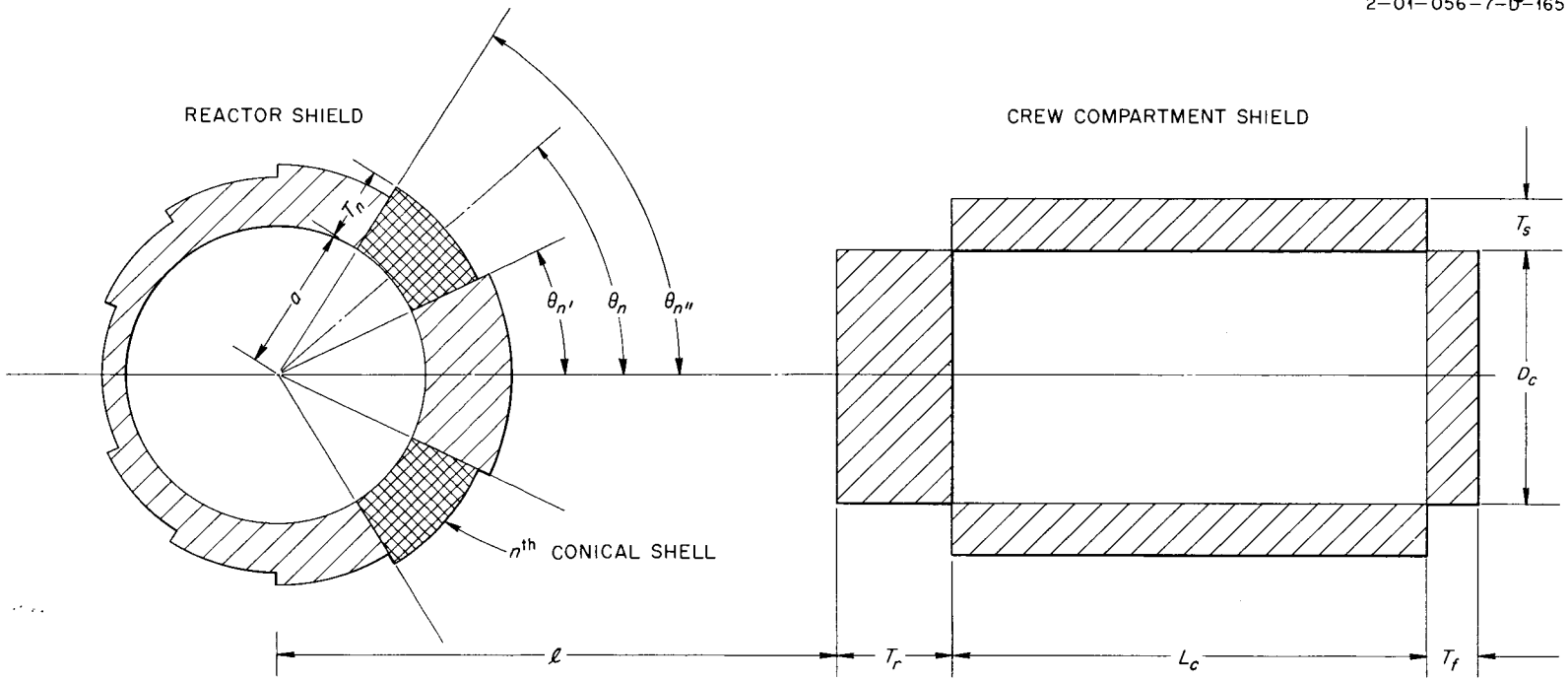
REACTOR SHIELD
CREW COMPARTMENT SHIELD
T_n
a
$\theta_{n'}$
θ_n
$\theta_{n''}$
n^{th} CONICAL SHELL
T_s
D_c
ℓ
T_r
L_c
T_f

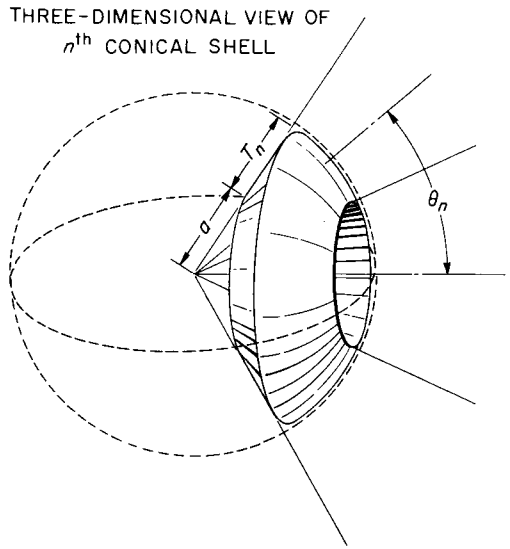
THREE-DIMENSIONAL VIEW OF
n^{th} CONICAL SHELL
T_n
a
θ_n

Fig. 1

[redacted]

$$W_{total} = \sum_{n=1}^{N} \frac{2\pi\rho_R}{3} (\cos\theta_n' - \cos\theta_n'') \left[(T_n + a)^3 - a^3 \right]$$

$$+ \frac{\pi\rho_{cs}}{4} \left\{ D_c^2 (T_r + T_s) + \left[(D_c + 2T_s)^2 - D_c^2 \right] L_c \right\} \quad (1)$$

where

ρ_R = density of the shielding material at the reactor,

ρ_{cs} = density of the shielding material at the crew compartment.

The angles θ_n' and θ_n'', D_c and L_c are defined in Fig. 1. The contribution to the dose rate at the center of the crew compartment by neutrons which leave the nth conical shell and scatter into the side of the crew compartment is given by

$$D_n^{s,side} = (\cos\theta_n' - \cos\theta_n'') D_d(a,\ell)\, e^{-\int_0^{T_n} \left(\frac{1}{\lambda_d}\right) dt}$$

$$\times\ \ell^2 P_{side}^s(\theta_n) f_s^s\, e^{-\int_0^{T_s} \left(\frac{1}{\lambda_s^s}\right) dt} \quad (2)$$

where

$D_d(a,\ell)$ = the direct-beam dose rate at a distance ℓ from the unshielded sphere of radius a,

λ_d = the direct-beam relaxation length which is a function of the depth of penetration of the reactor shield,

$P_{side}^s(\theta_n)$ = the probability of scattering into the crew compartment side from a conical-shell beam,[2]

λ_s^s = the relaxation length for the scattered dose at the side of the crew compartment and is a function of θ_n, T_n and the depth of penetration of the side shielding,

f_s^s = the focusing factor which accounts for the radiation focusing in the center of the crew compartment and depends on the angular distribution of the radiation at the inside surface of the crew compartment side shield.

[redacted]

[redacted]

A similar expression holds for the contribution to the dose rate at the center of the crew compartment by neutrons which leave the nth conical shell at the reactor and scatter into the rear of the crew compartment. The expression is

$$D_n^{s,rear} = (\cos\theta_n' - \cos\theta_n'')\, D_d(a,\ell)\, e^{-\int_0^{T_n} \left(\frac{1}{\lambda_d}\right) dt}$$

$$\times\, \ell^2 P^s_{rear}(\theta_n) f_s^{\,r}\, e^{-\int_0^{T_r} \left(\frac{1}{\lambda_s^{\,r}}\right) dt} \qquad (3)$$

where

$\lambda_s^{\,r}$ = the relaxation length for the scattered dose at the rear of the crew compartment. This is a function of T_n.

The factor $f_s^{\,r}$ accounts for the decrease in the dose rate at the center of the crew compartment caused by the angular distribution of the neutrons leaving the inside surface of the shield at the rear of the crew compartment.

The contribution to the dose rate at the center of the crew compartment by the direct beam through the rear of the crew compartment, assuming an angular distribution at the reactor shield surface of the form $\cos^m \psi$ and that the reactor--crew compartment separation distance is large compared to the outer radius of the reactor shield, is

$$D_n^{d,rear} = (\cos^{m+1}\theta_n' - \cos^{m+1}\theta_n'')\, D_d(a,\ell)\, e^{-\int_0^{T_n} \left(\frac{1}{\lambda_d}\right) dt}$$

$$\times\, f_d^{\,r}\, e^{-\int_0^{T_r} \left(\frac{1}{\lambda_d^{\,r}}\right) dt} \qquad (4)$$

with the stipulation that if the shell is in the hemisphere away from the crew compartment, the contribution of the shell to the direct-beam dose

[redacted]

[redacted]

is zero. λ_d^r is the relaxation length for the direct-beam dose at the rear of the crew compartment and is a function of T_n and the depth of penetration of the rear shielding. f_d^r accounts for the decrease in dose rate at the direct beam at the center of the crew compartment caused by the angular distribution of the direct-beam neutrons leaving the inside surface of the rear of the crew compartment.

Therefore the total dose is

$$D_{total} = \sum_{n=1}^{N} (D_n^{s,side} + D_n^{s,rear} + D_n^{d,rear}) \tag{5}$$

The method of Lagrangian multipliers consists of solving the N + 3 simultaneous equations

$$\left.\begin{aligned}
&\frac{\partial W_{total}}{\partial T_n} + \frac{1}{L}\frac{\partial D_{total}}{\partial T_n} = 0 \qquad (n = 1, 2, \ldots, N)\\
&\frac{\partial W_{total}}{\partial T_r} + \frac{1}{L}\frac{\partial D_{total}}{\partial T_r} = 0\\
&\frac{\partial W_{total}}{\partial T_s} + \frac{1}{L}\frac{\partial D_{total}}{\partial T_s} = 0\\
&D_{total} = \text{(specified constant)}
\end{aligned}\right\} \tag{6}$$

For the purposes of the calculation a subscript is attached to the L although for a solution to the equations all the L's must be the same.

$$L_s = -\frac{\dfrac{\partial D_{total}}{\partial T_s}}{\dfrac{\partial W_{total}}{\partial T_s}} = \frac{1}{\dfrac{\partial W_{total}}{\partial T_s}} \sum_{n=1}^{N} \frac{D_n^{s,side}}{\lambda_s^{s}} \tag{7}$$

[redacted]

[redacted]

$$L_r = -\frac{\dfrac{\partial D_{total}}{\partial T_r}}{\dfrac{\partial W_{total}}{\partial T_r}} = \frac{1}{\dfrac{\partial W_{total}}{\partial T_r}} \sum_{n=1}^{N} \left(\frac{D_n^{s,rear}}{\lambda_s^{\,r}} + \frac{D_n^{d,rear}}{\lambda_d^{\,r}} \right) \tag{8}$$

$$L_n = -\frac{\dfrac{\partial D_{total}}{\partial T_n}}{\dfrac{\partial W_{total}}{\partial T_n}} = \frac{1}{A(\theta_n)(T_n + a)^2} \left\{ D_n^{s,side} \left[\frac{1}{\lambda_d} + \int_0^{T_s} \frac{\partial}{\partial T_n} \left(\frac{1}{\lambda_s^{\,s}} \right) dt \right] \right.$$

$$\left. + D_n^{s,rear} \left[\frac{1}{\lambda_d} + \int_0^{T_r} \frac{\partial}{\partial T_n} \left(\frac{1}{\lambda_s^{\,r}} \right) dt \right] + D_n^{d,rear} \left[\frac{1}{\lambda_d} + \int_0^{T_r} \frac{\partial}{\partial T_n} \left(\frac{1}{\lambda_d^{\,r}} \right) dt \right] \right\}$$

$$(n = 1, 2, \ldots, N) \tag{9}$$

where

$$A(\theta_n) = 2\pi r_R (\cos\theta_n' - \cos\theta_n'')$$

In Eq. 9, the terms involving the integrals were previously neglected. These terms arise from the following functional dependencies of relaxation lengths at the crew compartment on T_n:

$$\lambda_s^{\,s}(T_n, \theta_n, t) = \frac{\lambda_s^{\,s}(45, \theta_n, t)\ \lambda_d(T_n + t)}{1.14\ \lambda_d(45 + t)} \tag{10}$$

$$\lambda_s^{\,r}(T_n) = \frac{7.0\ \lambda_d(T_n + 15)}{1.14\ \lambda_d(45 + 15)} \tag{11}$$

[redacted]

[redacted]

$$\lambda_d{}^r(T_n,t) = \frac{\lambda_d(T_n + t)}{1.14} \tag{12}$$

The factor 1.14 accounts for plastic being used for the crew compartment shielding. For an explanation of these dependencies one may refer to Ref. 1.

The previously neglected terms involving the integrals may be estimated as follows:

$$\frac{\partial}{\partial T_n}\left(\frac{1}{\lambda_s{}^s}\right) = -\frac{1}{\left(\lambda_s{}^s\right)^2}\frac{\partial\lambda_s{}^s}{\partial T_n} = -\frac{1.14\ \lambda_d(45 + t)}{\lambda_s{}^s(45,\theta_n,t)\lambda_d{}^2(T_n + t)}\frac{\partial\lambda_d(T_n + t)}{\partial T_n} \tag{13}$$

$$\frac{\partial}{\partial T_n}\left(\frac{1}{\lambda_s{}^r}\right) = -\frac{1}{\left(\lambda_s{}^r\right)^2}\frac{\partial\lambda_s{}^r}{\partial T_n} = -\frac{1.14\ \lambda_d(45 + 15)}{7.0\ \lambda_d{}^2(T_n + 15)}\frac{d\lambda_d(T_n + 15)}{dT_n} \tag{14}$$

$$\frac{\partial}{\partial T_n}\left(\frac{1}{\lambda_d{}^r}\right) = -\frac{1}{\left(\lambda_d{}^r\right)^2}\frac{\partial\lambda_d{}^r}{\partial T_n} = -\frac{1.14}{\lambda_d{}^2(T_n + t)}\frac{\partial\lambda_d(T_n + t)}{\partial T_n} \tag{15}$$

$$\frac{\partial\lambda_d(T_n + t)}{\partial T_n} = \frac{d\lambda_d(T_n + t)}{d(T_n + t)} \tag{16}$$

Thus the partial derivative in Eq. 16 may be evaluated from the slope of the plot of $\lambda_d(x)$ vs. x. From this one obtains

$$-\int_0^{T_s}\frac{\partial}{\partial T_n}\left(\frac{1}{\lambda_s{}^s}\right)dt \quad \text{which must be evaluated numerically.} \tag{17}$$

$$-\int_0^{T_r}\frac{\partial}{\partial T_n}\left(\frac{1}{\lambda_s{}^r}\right)dt = \frac{1.14\ \lambda_d(60)T_r}{7.0\ \lambda_d{}^2(T_n + 15)}\left.\frac{d\lambda_d(x)}{dx}\right]_{x = T_n + 15} \tag{18}$$

[redacted]

[redacted]

$$-\int_{o}^{T_r} \frac{\partial}{\partial T_n}\left(\frac{1}{\lambda_d{}^r}\right) dt = 1.14\left[\frac{1}{\lambda_d(T_n)} - \frac{1}{\lambda_d(T_n + T_r)}\right] \tag{19}$$

A procedure was devised for an iterative method of solution which converges rapidly enough to be useful for hand calculation.

STEP a. ESTIMATE OF L

The Lagrangian multiplier can be estimated from the thicknesses provided by the previous iteration and using the following definitions:

$$\frac{1}{\bar{\lambda}_s{}^s} \equiv \frac{\sum_{n=1}^{N} \frac{D_n^{s,side}}{\lambda_s{}^s}}{\sum_{n=1}^{N} D_n^{s,side}} \tag{20}$$

$$\frac{1}{\bar{\lambda}_s{}^r} \equiv \frac{\sum_{n=1}^{N} \frac{D_n^{s,rear}}{\lambda_s{}^r}}{\sum_{n=1}^{N} D_n^{s,rear}} \tag{21}$$

$$\frac{1}{\bar{\lambda}_d{}^r} \equiv \frac{\sum_{n=1}^{N} \frac{D_n^{d,rear}}{\lambda_d{}^r}}{\sum_{n=1}^{N} D_n^{d,rear}} \tag{22}$$

By using Eqs. 7 and 8 and $L_s = L_r = L$ one obtains

[redacted]

[redacted]

$$L = \frac{D_{total} + \left(\frac{\bar{\lambda}_d{}^r}{\bar{\lambda}_s{}^r} - 1\right) \sum_{n=1}^{N} D_n^{s,rear}}{\bar{\lambda}_s{}^s \frac{\partial W_{total}}{\partial T_s} + \bar{\lambda}_d{}^r \frac{\partial W_{total}}{\partial T_r}} \tag{23}$$

The second term in the numerator may be neglected since the rear-scattered dose amounts to approximately 1% of the total dose when the shield is nearly optimum. Thus L varies quite slowly from one iteration to the next. Previously $1/\bar{\lambda}_d{}^r$ was not defined and the equation for L was

$$L = \frac{D_{total} + \sum_{n=1}^{N} \left(\frac{\bar{\lambda}_s{}^r}{\lambda_d{}^r} - 1\right) D_n^{d,rear}}{\bar{\lambda}_s{}^s \frac{\partial W_{total}}{\partial T_s} + \bar{\lambda}_s{}^r \frac{\partial W_{total}}{\partial T_r}} \tag{24}$$

Equation 24 is mathematically equivalent to Eq. 23 but is not as close an estimate for L.

STEP b. RELATION BETWEEN T_s AND T_r

Using the thicknesses form the previous iteration one may obtain an approximate relation between T_s and T_r denoted by $T_r = Q(T_s)$. Let

$$\left.\begin{aligned}
B_n &\equiv (\cos\theta_n' - \cos\theta_n'')\, \ell^2 P^s_{side}(\theta_n) f_s{}^s \\
C_n &\equiv (\cos\theta_n' - \cos\theta_n'')\, \ell^2 P^s_{rear}(\theta_n) f_s{}^r \\
J_n &\equiv (\cos^{m+1}\theta_n' - \cos^{m+1}\theta_n'')\, f_d{}^r \\
\alpha &\equiv \frac{\frac{\partial W_{total}}{\partial T_s} \bar{\lambda}_s{}^s}{\frac{\partial W_{total}}{\partial T_r} \bar{\lambda}_d{}^r}
\end{aligned}\right\} \tag{25}$$

[redacted]

[redacted]

$$
\left.
\begin{aligned}
e^{-\frac{T_s}{\bar{\lambda}_s}} &\equiv \frac{\sum_{n=1}^{N} B_n\, e^{-\int_0^{T_n}\left(\frac{1}{\lambda_d}\right)dt}\; e^{-\int_0^{T_s}\left(\frac{1}{\lambda_s}\right)dt}}{\sum_{n=1}^{N} B_n\, e^{-\int_0^{T_n}\left(\frac{1}{\lambda_d}\right)dt}} \\
e^{-\frac{T_r}{\bar{\lambda}_r}} &\equiv \frac{\sum_{n=1}^{N} C_n\, e^{-\int_0^{T_n}\left(\frac{1}{\lambda_d}\right)dt}\; e^{-\int_0^{T_r}\left(\frac{1}{\lambda_s}\right)dt}}{\sum_{n=1}^{N} C_n\, e^{-\int_0^{T_n}\left(\frac{1}{\lambda_d}\right)dt}} \\
e^{-\frac{T_r}{\bar{\lambda}_d}} &\equiv \frac{\sum_{n=1}^{N} J_n\, e^{-\int_0^{T_n}\left(\frac{1}{\lambda_d}\right)dt}\; e^{-\int_0^{T_r}\left(\frac{1}{\lambda_d}\right)dt}}{\sum_{n=1}^{N} J_n\, e^{-\int_0^{T_n}\left(\frac{1}{\lambda_d}\right)dt}}
\end{aligned}
\right\} \quad (26)
$$

By equating L_r and L_s one obtains the approximate relation

[redacted]

[redacted]

$$\frac{1}{\alpha} e^{-\frac{T_s}{\bar{\lambda}_s{}^s}} = \frac{\sum_{n=1}^{N} C_n e^{-\int_0^{T_n} \left(\frac{1}{\lambda_d}\right) dt}}{\sum_{n=1}^{N} B_n e^{-\int_0^{T_n} \left(\frac{1}{\lambda_d}\right) dt}} \frac{\bar{\lambda}_d{}^r}{\bar{\lambda}_s{}^r} e^{-\frac{T_r}{\bar{\lambda}_s{}^r}}$$

$$+ \frac{\sum_{n=1}^{N} J_n e^{-\int_0^{T_n} \left(\frac{1}{\lambda_d}\right) dt}}{\sum_{n=1}^{N} B_n e^{-\int_0^{T_n} \left(\frac{1}{\lambda_d}\right) dt}} e^{-\frac{T_r}{\bar{\lambda}_d{}^r}} \qquad (27)$$

A qualitative plot would be

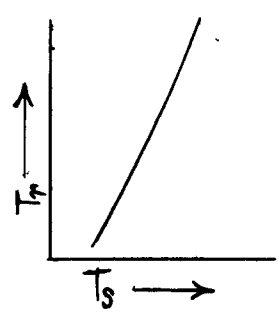

STEP c. RELATION BETWEEN T_s AND T_n's

Using the T_n's from the previous iteration, the relationship $T_r = Q(T_s)$ from Step b and $L = L_n$, one obtains from Eq. 9 the relation $T_n = F_n(T_s)$

[redacted]

[redacted]

$$\frac{\lambda_d (T_n + a)^2}{D_d(a,\ell) e^{-\int_0^{T_n} \left(\frac{1}{\lambda_d}\right) dt}} = \frac{1}{LA(\theta_n)} \left\{ B_n e^{-\int_0^{T_s} \left(\frac{1}{\lambda_s}\right) dt} \left[1 + \lambda_d \int_0^{T_s} \frac{\partial}{\partial T_n} \left(\frac{1}{\lambda_s}\right) dt \right] \right.$$

$$+ C_n e^{-\int_0^{Q(T_s)} \left(\frac{1}{\lambda_s^r}\right) dt} \left[1 + \lambda_d \int_0^{Q(T_s)} \frac{\partial}{\partial T_n} \left(\frac{1}{\lambda_s^r}\right) dt \right] + J_n e^{-\int_0^{Q(T_s)} \left(\frac{1}{\lambda_d^r}\right) dt}$$

$$\left. \times \left[1 + \lambda_d \int_0^{Q(T_s)} \frac{\partial}{\partial T_n} \left(\frac{1}{\lambda_d^r}\right) dt \right] \right\} \tag{28}$$

The left side of Eq. 28 is a function of T_n only so that by using the T_n's from the previous iteration in the right side the relation is obtained. A qualitative plot is

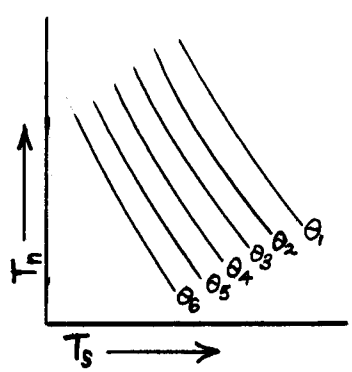

[redacted]

[redacted]

STEP d. RELATION BETWEEN T_s AND L_s

Using the relations from Steps b and c, $T_r = Q(T_s)$ and $T_n = F_n(T_s)$, one may obtain a relation between L_s and T_s from Eq. 7 denoted by $T_s = \Lambda(L_s)$

$$L_s = \frac{1}{\frac{\partial W_{total}}{\partial T_s}} \sum_{n=1}^{N} \frac{B_n e^{-\int_0^{F_n(T_s)} \left(\frac{1}{\lambda_d}\right) dt} e^{-\int_0^{T_s} \left(\frac{1}{\lambda_s}\right) dt}}{\lambda_s^{s}} \tag{29}$$

A qualitative plot is

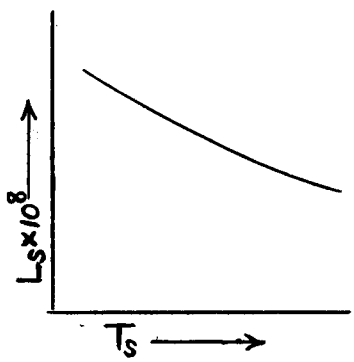

By using the estimate for L obtained in Step a, one obtains all the thicknesses for the next iteration.

$$T_s = \Lambda(L); \; T_n = F_n\left[\Lambda(L)\right]; \; T_r = Q\left[\Lambda(L)\right]$$

One may continue until the convergence of L_s, L_r, and L_n's is nearly complete; however, the total weight does not change a great deal after three iterations. Three iterations usually fixes the dose rate very well.

The results after three iterations, using the new procedure and beginning with the shield thicknesses presented previously,[1] are shown in Table I. The thicknesses on the last two conical shells tended to become negative and thus were dropped from the optimization procedure and set

[redacted]

[redacted]

Table I. Optimization of Neutron Shielding for a 300-Mw Circulating-Fuel Reflector-Moderated Reactor

Shield Region	Old Procedure			New Procedure		
	Shielding Thickness (cm)	Lagrangian Multiplier x 10^8	Weight of Shield (tons)	Shielding Thickness (cm)	Lagrangian Multiplier x 10^8	Weight of Shield (tons
Reactor shield						
$\Delta\theta$* = 0 to 15	43.4	16.8	0.15	36.8	17.7	0.12
$\Delta\theta$ = 15 to 45	39.3	17.0	0.96	32.0	18.7	0.74
$\Delta\theta$ = 45 to 75	28.6	18.3	1.11	20.3	18.7	0.72
$\Delta\theta$ = 75 to 105	21.3	18.9	0.89	12.2	17.3	0.47
$\Delta\theta$ = 105 to 165	10.4	17.8	0.53	0.0	- -	0.00
$\Delta\theta$ = 165 to 180	7.8	18.0	0.02	0.0	- -	0.00
Rear of crew compartment	43.8	11.9	1.47	46.3	17.4	1.54
Side and front of crew compartment	16.8	18.0	4.52	20.6	18.2	5.54
Total weight			9.65			9.13

*Polar angle increment.

[redacted]

[redacted]

equal to zero. The dose rate criterion at the center of the crew compartment was 0.25 rem/hr which is the same as that for the previous system. Some useful curves are shown in Fig. through Fig. which may be an aid in following the procedure. The curves showing the TSF data are also shown in Fig. 2 through Fig. 13 .

[redacted]

[redacted]

2-01-059-63

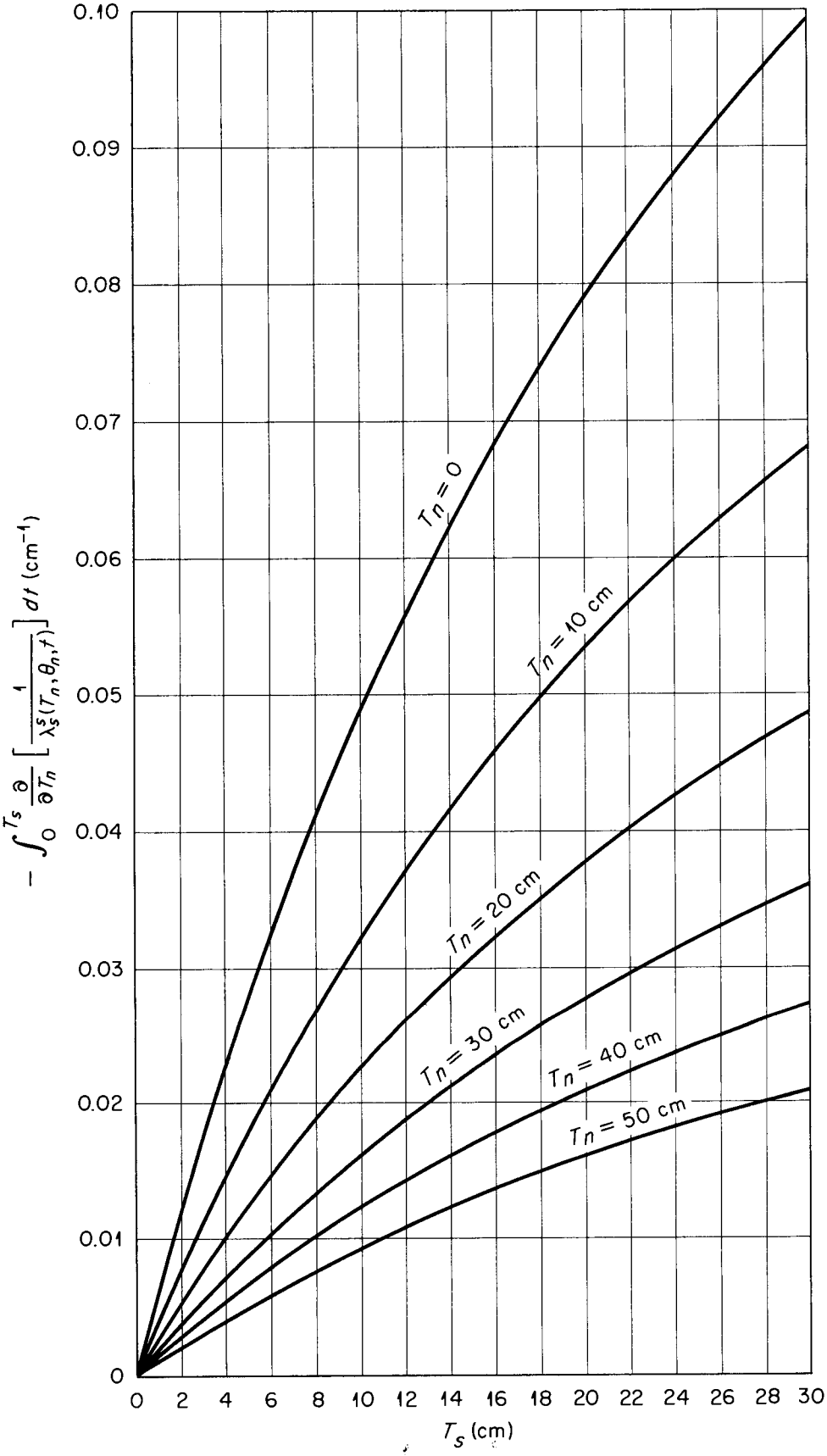

Fig. 2. $\int_0^{T_s} \frac{\partial}{\partial T_n}\left[\frac{1}{\lambda_s^s(T_n,\theta,t)}\right] dt$ as a Function of T_s for $\theta = 0$ to 30 deg.

[redacted]

2-01-059-64

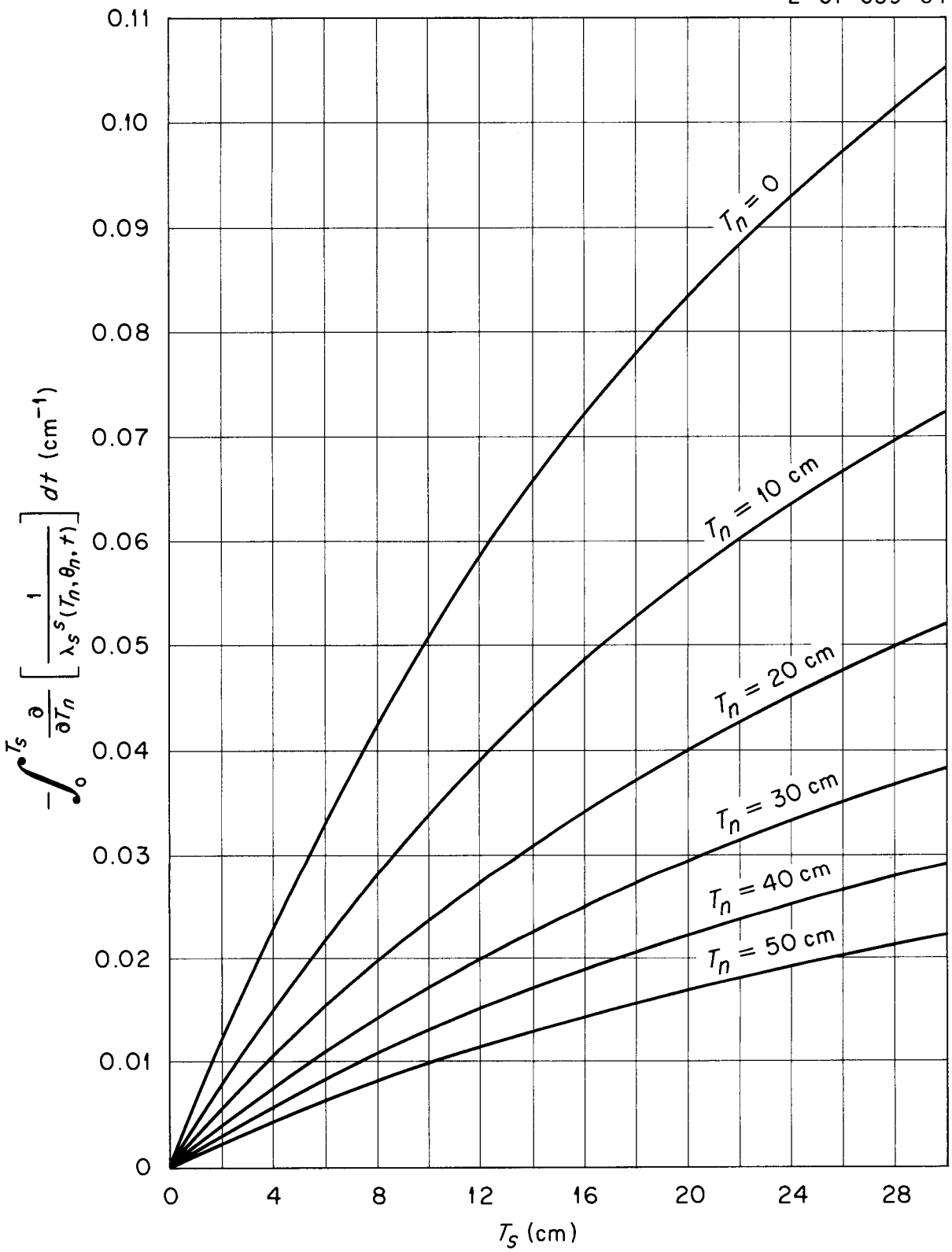

Fig. 3. $\int_0^{T_s} \frac{\partial}{\partial T_n}\left[\frac{1}{\lambda_s{}^s(T_n,\theta,t)}\right] dt$ as a Function of T_s for θ = 60 to 90 deg.

[redacted]

2-01-059-65

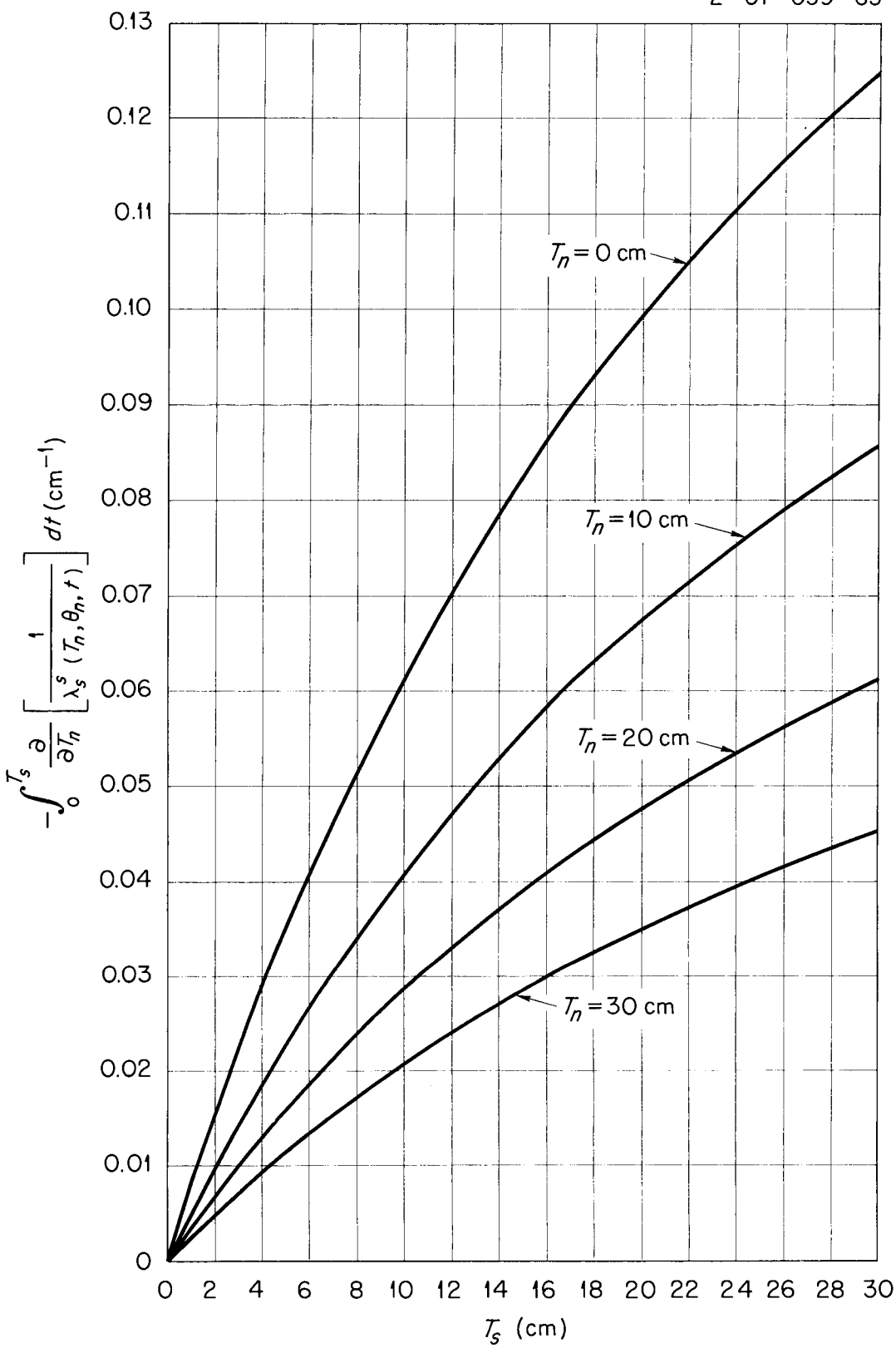

Fig. 4. $-\int_0^{T_s} \frac{\partial}{\partial T_n}\left[\frac{1}{\lambda_s^s(T_n,\theta,t)}\right] dt$ as a Function of T_s for $\theta = 135$ to 180 deg.

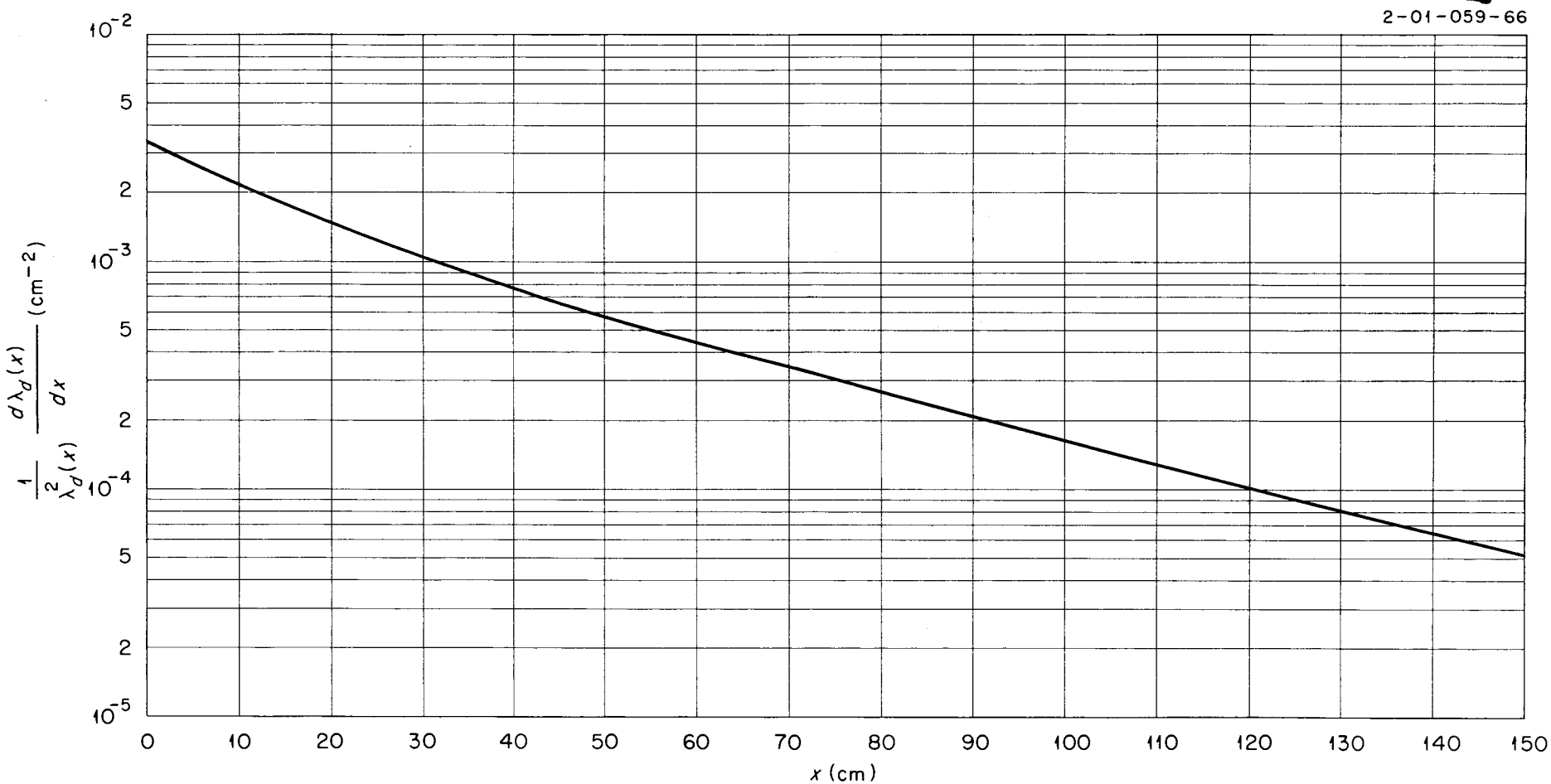

Fig. 5. $\frac{1}{\lambda_d(x)} \frac{d\lambda_d(x)}{dx}$ as a Function of x.

[redacted]

2-01-059-67

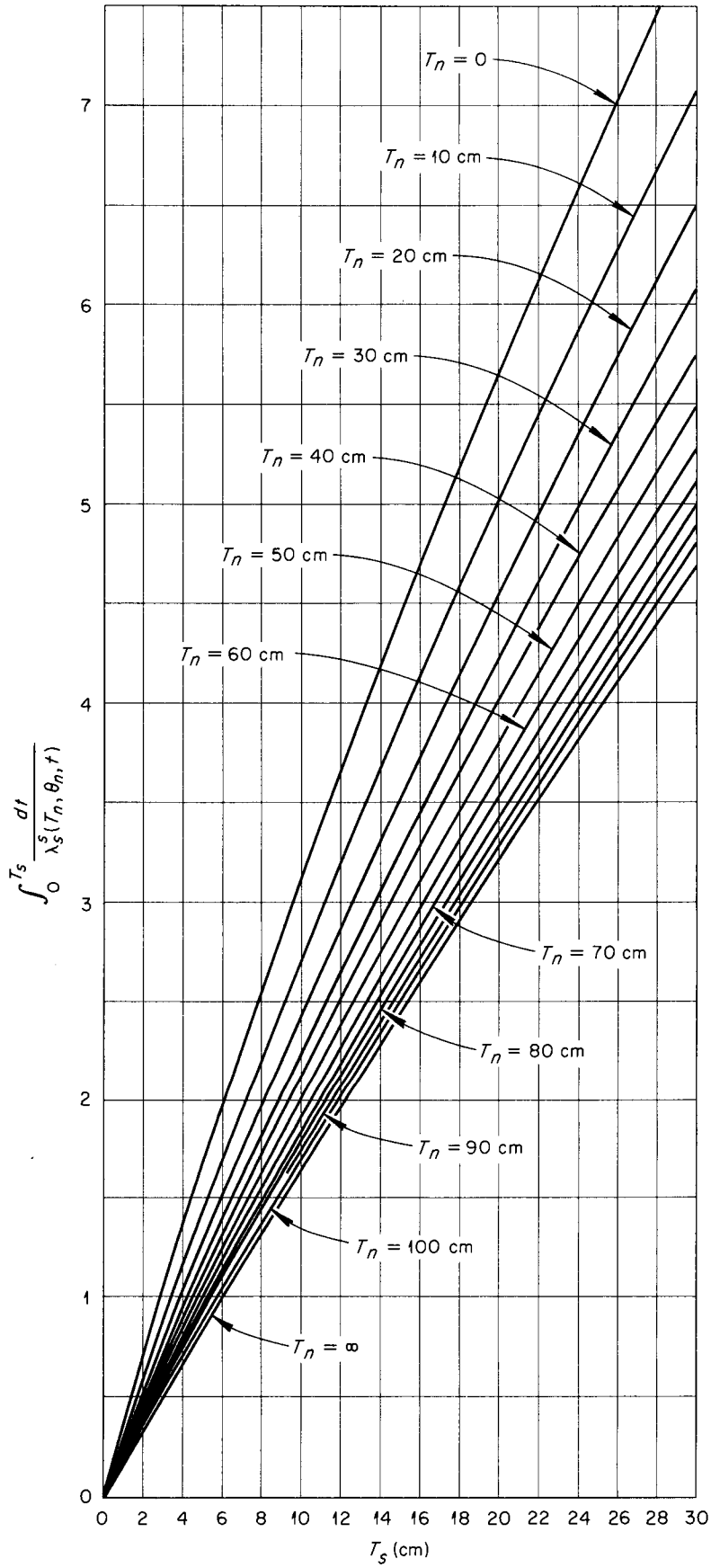

Fig. 6. $\int_0^{T_s} \left[\frac{1}{\lambda_s^s(T_n, \theta, t)}\right] dt$ as a Function of T_s for $\theta = 0$ to 30 deg.

[redacted]

2-01-059-68

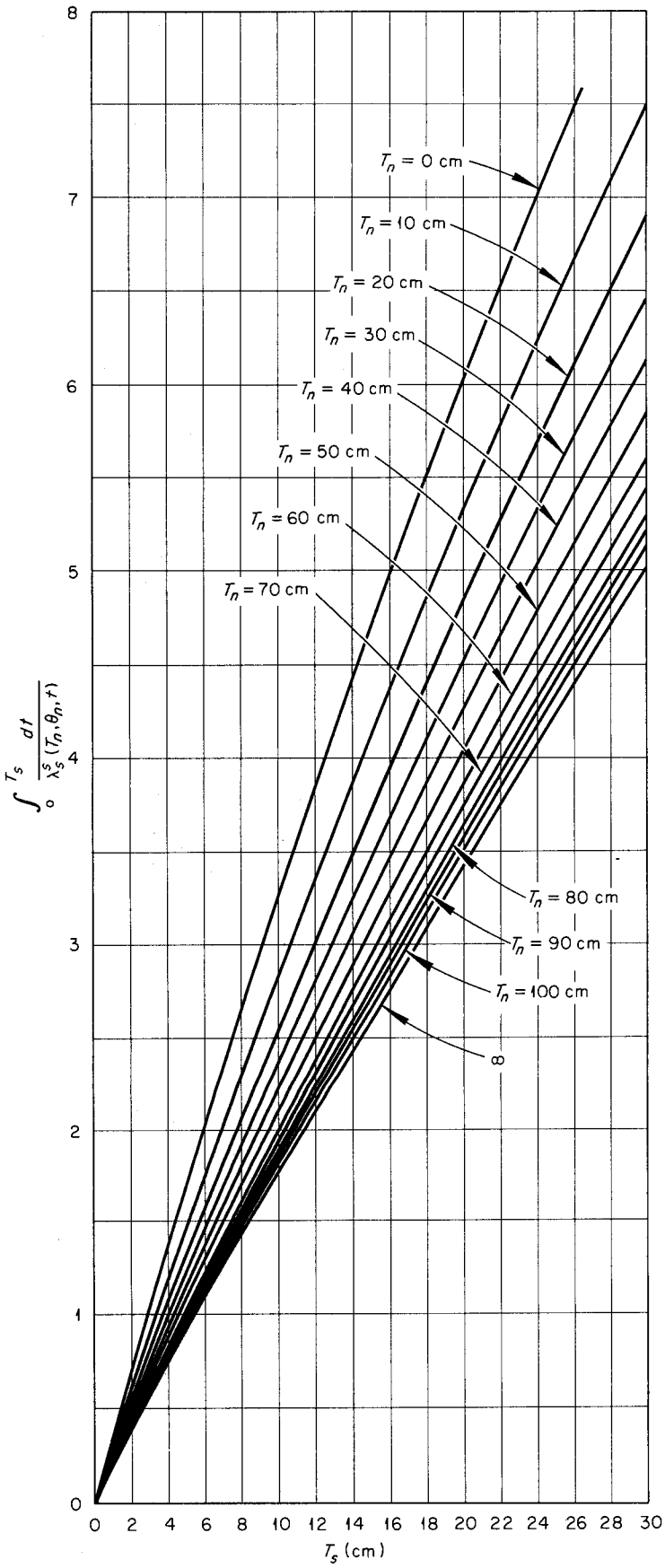

Fig. 7. $\int_0^{T_s} \frac{dt}{\lambda_s^s(T_n,\theta,t)}$ as a Function of T_s for θ = 60 to 90 deg.

[redacted]

2-01-059-69

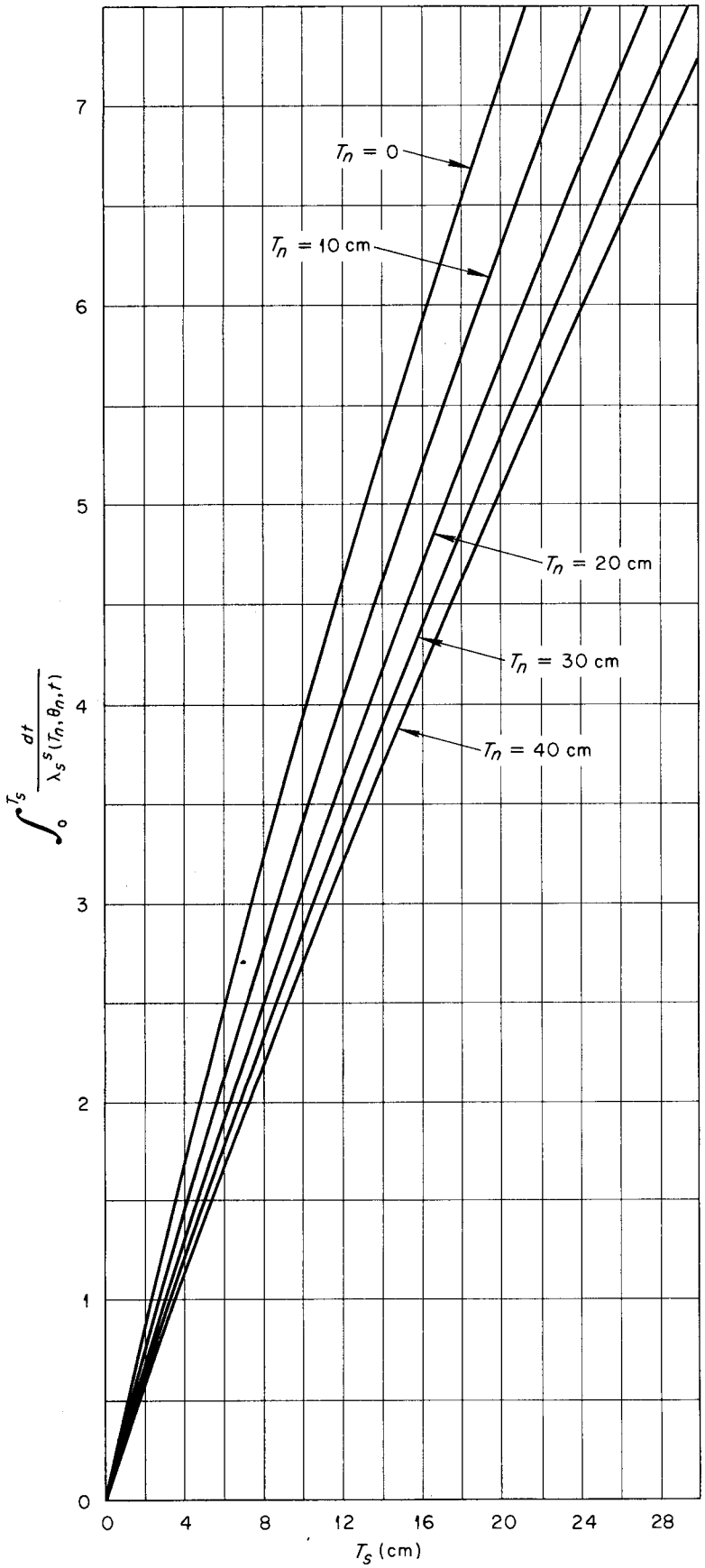

Fig. 8. $\int_0^{T_s} \frac{dt}{\lambda_s^s(T_n, \theta, t)}$ as a Function of T_s for $\theta = 135$ to 180 deg.

[redacted]

2-01-059-70

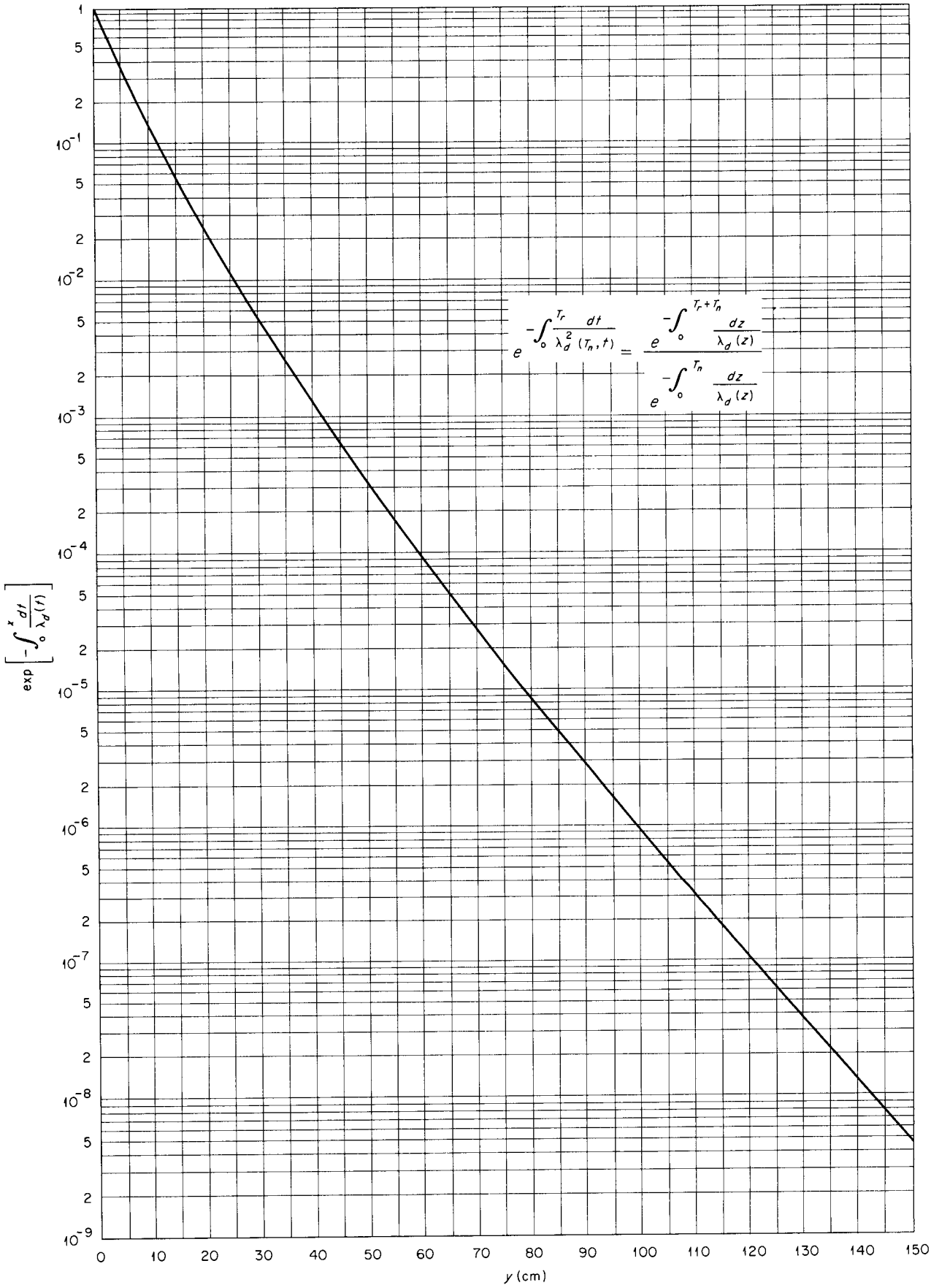

Fig. 9. $\exp\left[-\int_0^y \frac{dt}{\lambda_d(t)}\right]$ as a Function of y.

[redacted]

2-01-056-7-A-166

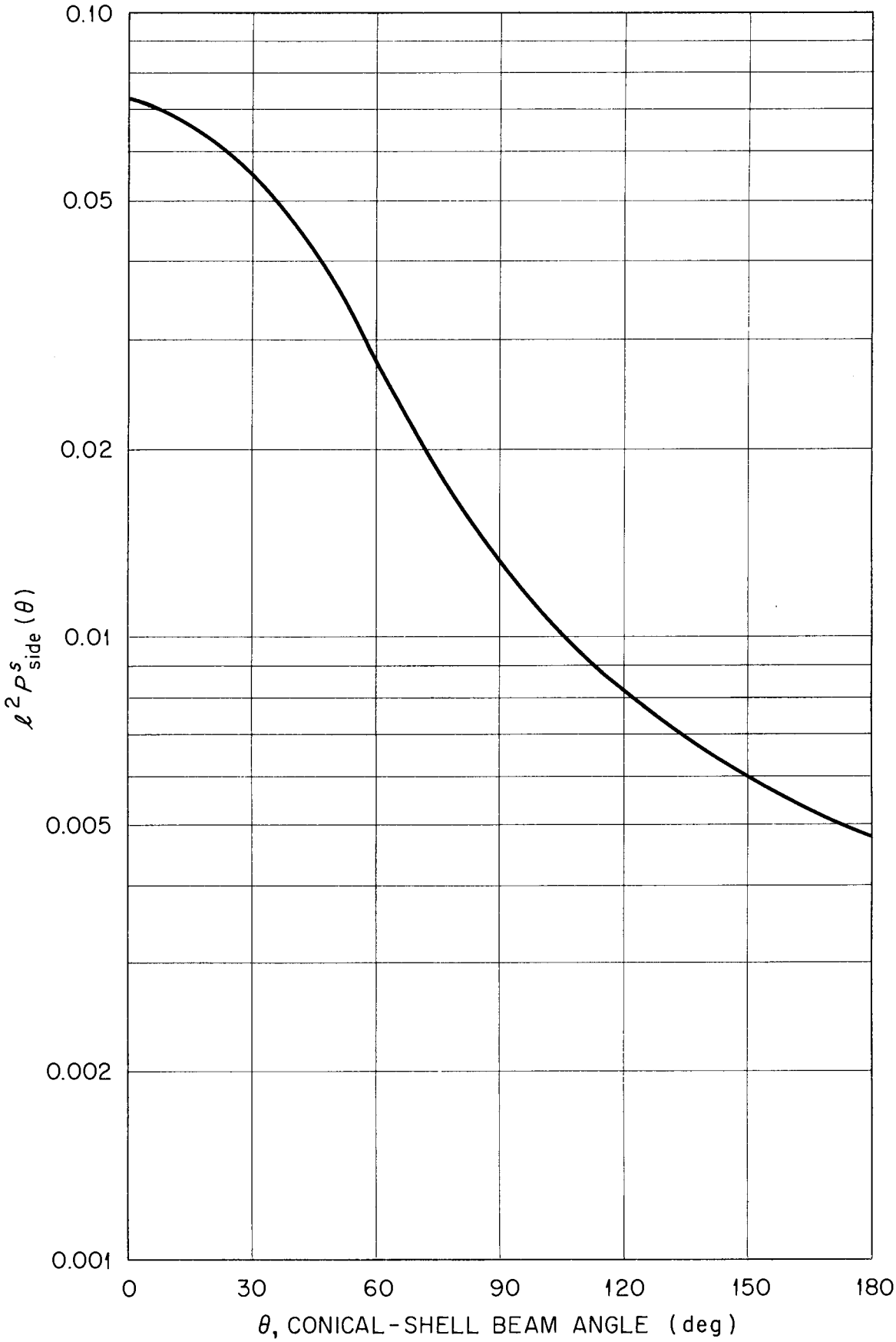

Fig 10.

[redacted]

2-01-056-7-A-167

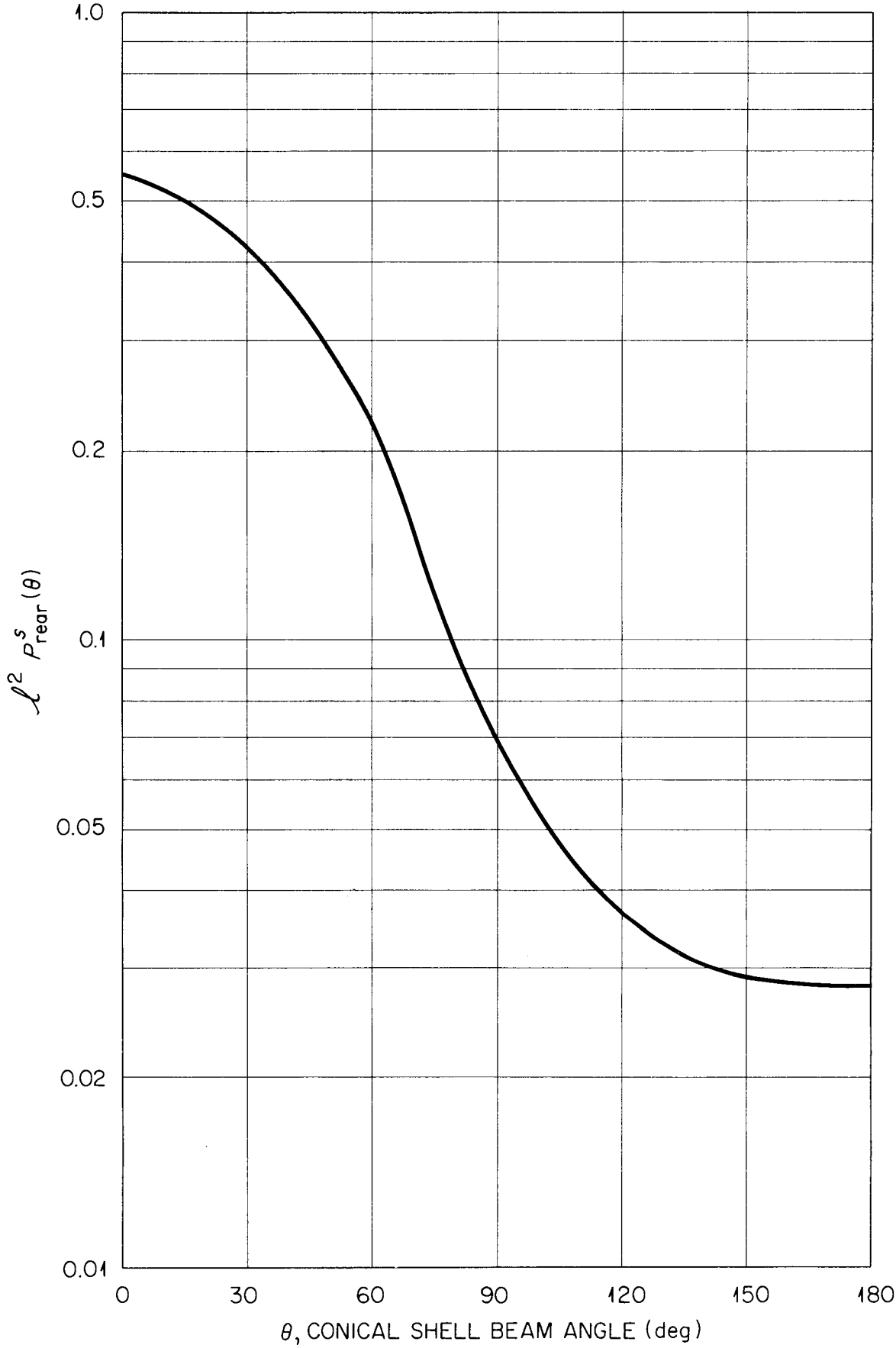

Fig. 11.

[redacted]

2-01-056-7-A128

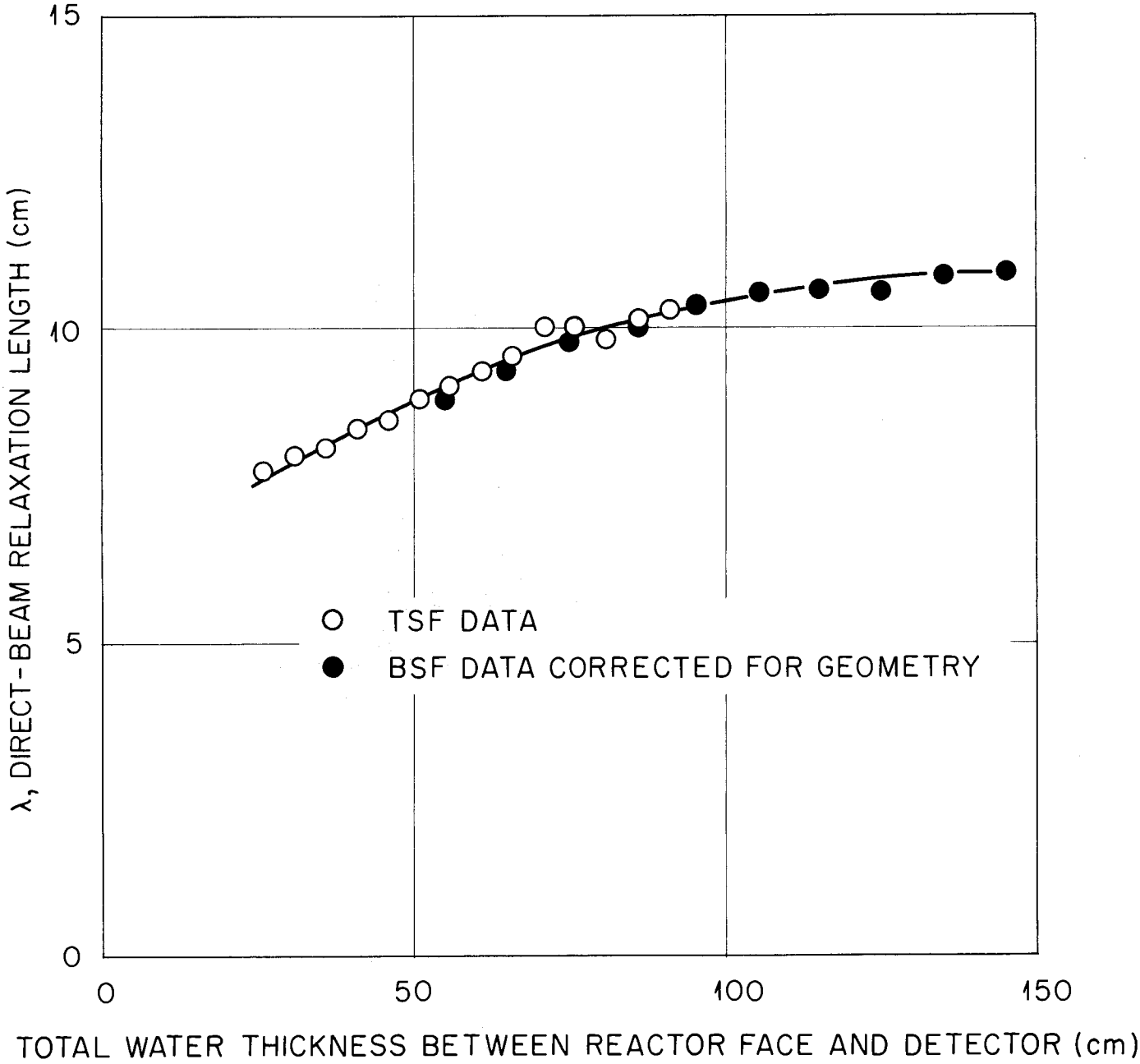

Fig. 12. Relaxation Length (λ) for Fast-Neutron Dose

[redacted]

2-01-056-7-A-168

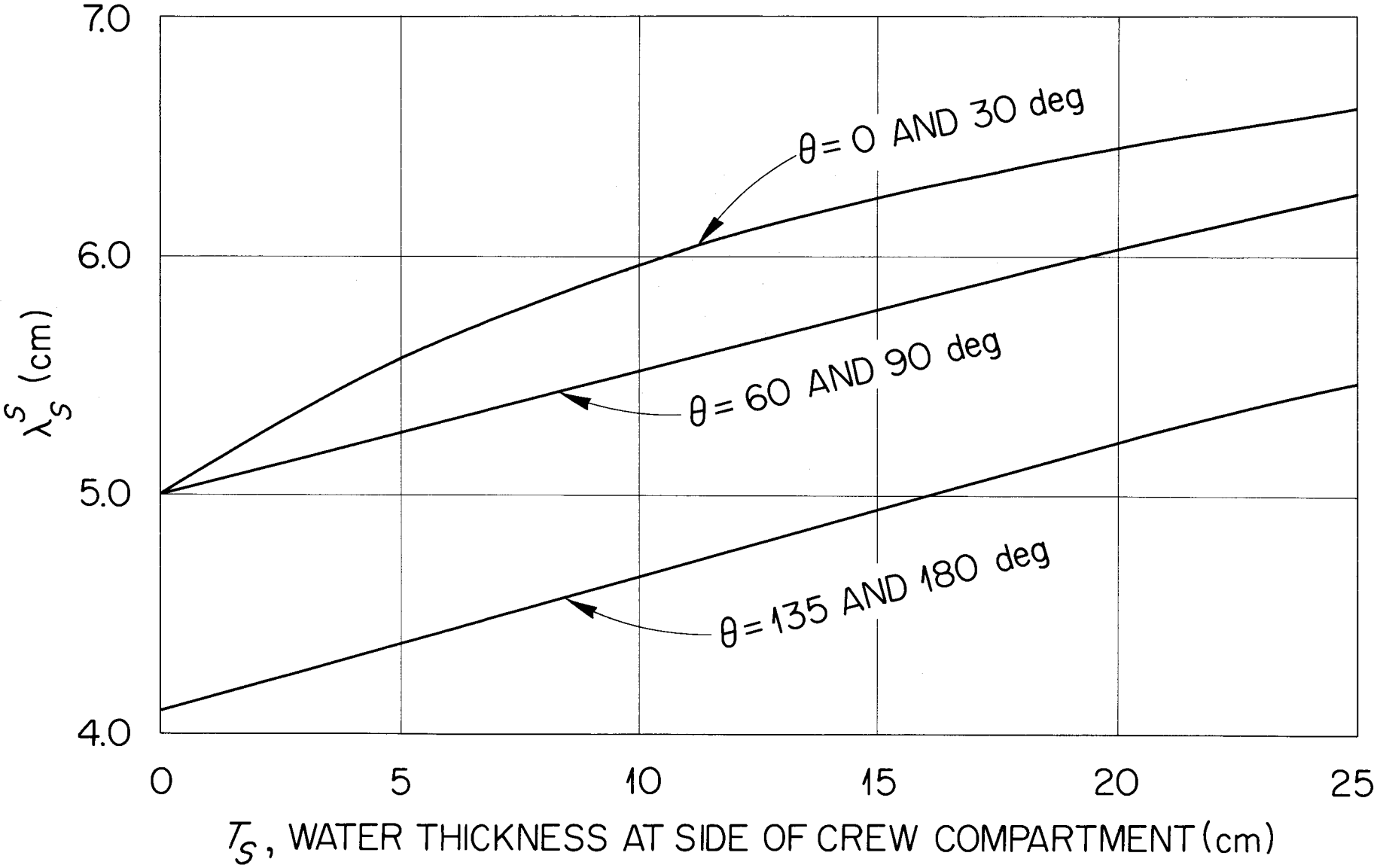

Fig. 13.

[redacted]

REFERENCES

1. C. E. Clifford et al., ANP Quar. Prog. Rep. Sept. 10, 1955, ORNL-1947, p. 205.

2. M. F. Valerino, ANP Quar. Prog. Rep. June 10, 1955, ORNL-1896, p. 206.

[redacted]

SECRET

Paper III-C

A SHIELD SHAPING METHOD*

T. R. Strayhorn and R. J. Klotz
Convair, Ft. Worth

*Published at Convair, Ft. Worth, as Report No. FZM-439.

SECRET

[redacted]

A SHIELD SHAPING METHOD
(Title Unclassified)

by

T. R. Strayhorn and R. J. Klotz

Convair, A Division of General Dynamics Corporation, Fort Worth, Texas

A method by which the shielding weight of a nuclear powered aircraft may be minimized is presented. Results indicating possible weight savings are shown to illustrate the worth of the method.

GENERAL OUTLINE OF METHOD

The method described here is one which may be used to determine the shielding required for a nuclear-powered aircraft. While there are many improvements which can be made, this method is relatively simple and lends itself readily to parametric studies. The accuracy, or rather, inaccuracy, has not been completely determined. The assumptions made might be satisfactory approximations in one case but not in another. While it is believed that this method will not give a minimum shielding weight, it will give a lower weight than would be given by a spherically shielded reactor and an arbitrary selection of relative percentages of dose rate components in the crew compartment.

In section B, there is indicated a method whereby the relative dose-rate components can be determined in the crew compartment, so that the crew compartment has a minimum weight. If the desired total crew dose rate is known, then the dose-rate components can be found.

Crew compartment side-shield thicknesses are then selected. This will usually be a lead layer followed on the outside by a layer of hydrogenous material. For the selected altitude and the reactor-crew compartment separation distance, the single-scattering probabilities for radiation emerging

AEC-3313-CVAC

[redacted]

ATOMIC ENERGY ACT - 1954

from the reactor are calculated. These scattering probabilities include scattered radiation penetration through the sides of the crew compartment.

These scattering probabilities, together with the desired scattered dose-rate components in the crew compartment, are used in section C, to determine the required thicknesses of shielding on the reactor.

This reactor shielding is shaped to give a minimum reactor shield weight for a selected dose rate in the crew compartment.

After the reactor shielding has been determined, the direct-beam dose rates at the outside rear of the crew compartment are calculated. Using these dose rates outside the rear of the crew compartment and the desired direct-beam dose-rate components in the crew compartment, one can calculate required direct-beam shielding. This shielding is to be placed on the rear of the crew compartment.

When all the shield thicknesses have been calculated, the reactor shield weight and crew shield weight are calculated. These are added together to get the total shield weight for a given crew compartment side-shield thickness. A different thickness of shielding is then selected for the crew-compartment sides and the above process is repeated. The results can be expressed in the form of total shield weight vs. crew compartment side-shield thickness. If the calculations are carried out for thickness variations for both types of materials on the crew compartment sides, there may be plotted the total weight versus the thickness of one type of material parameterized in the thicknesses of the other material. The curves may indicate a minimum total shield weight for certain thicknesses of shielding on the crew compartment sides. This would be the case to use for the given conditions.

Figure 1 indicates the steps outlined above.

OPTIMIZATION OF CREW SHIELD

The crew shield weight optimization method used is outlined in detail in CVAC-200T. It is possible using this method to find the scattered and direct dose rate components that will lead to a minimum weight crew shield.

[redacted]

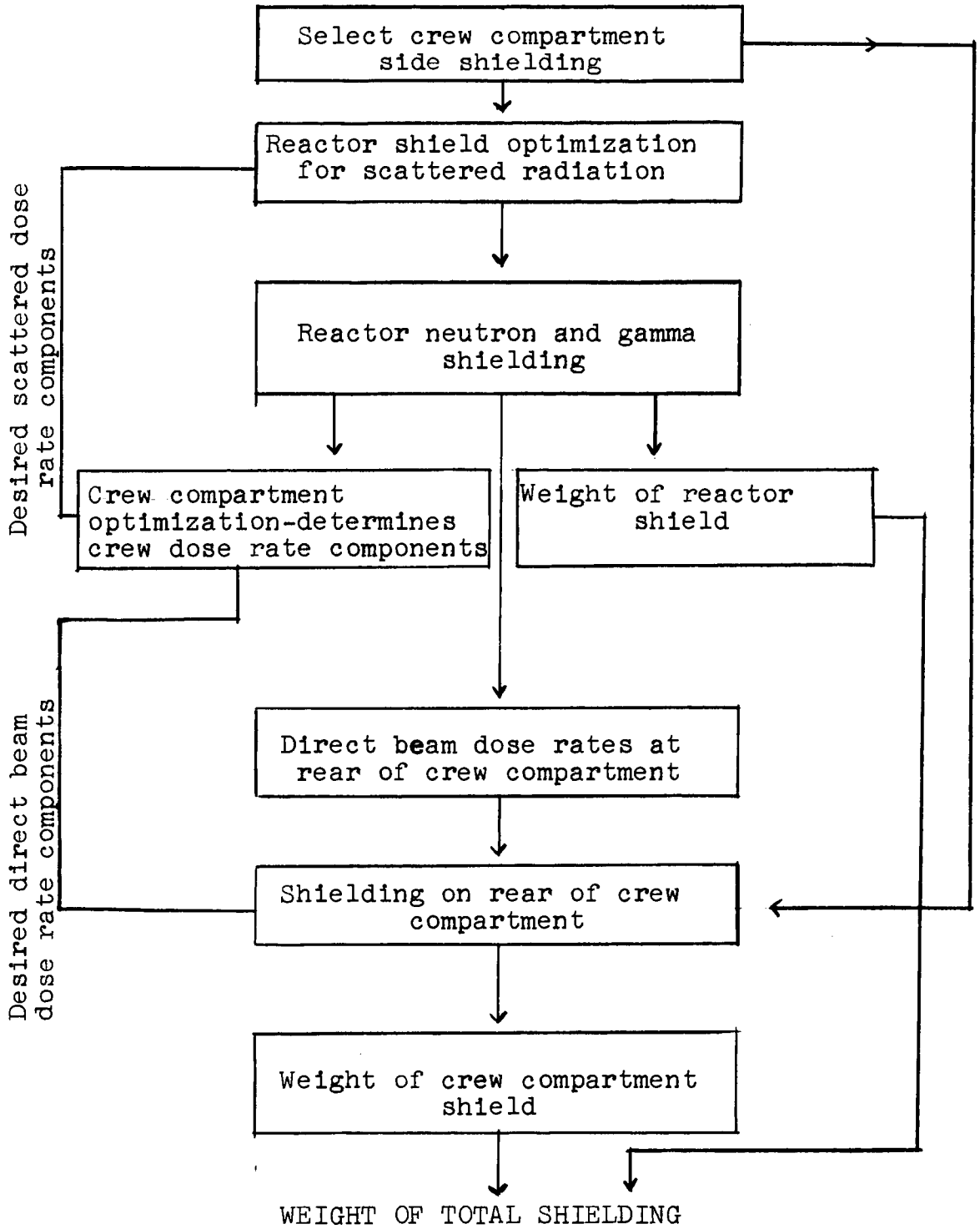

Figure 1

AEC-3313-CVAC

[redacted]

[redacted]

[redacted]

For an Area of Sides to Area of Rear ratio of 8, and with the use of lead and polyethylene plastic shielding, the dose rate components are as follows:

scattered neutrons = 25%

scattered gammas = 36%

direct neutrons = 2%

direct gammas = 37%

These dose rate components have been found to be relatively insensitive to variations of radiation incident on the crew compartment.

REACTOR SHIELD SHAPING METHOD

In an attempt to get away from the arbitrary shaping of reactor shields, a simplified analytical method has been set up for calculating the shape of the shielding around a reactor. The following method is not rigorous with regard to finding the minimum-weight reactor shield. The method can be made more rigorous and would then involve more work for a solution. The shielding is shaped on the reactor with regard to the scattered dose rates only.

As a first approximation, it may be assumed that the radiation emerges from the center of a sphere whose surface represents the interior surface of the reactor shielding. The reactor is assumed to be spherical in shape. If D_A represents the crew dose rate which results from radiation passing through the unit area A on the reactor surface with no shielding present, the contribution with shielding is then $D_A^* = D_A\, e^{-tA/\lambda}$. Likewise for another area, B, $D_B^* = D_B\, e^{-tA/\lambda}$. Then the total dose rate from both areas is:

$$D_{AB}^* = D_A^* + D_B^*$$

[redacted]

[redacted]

[redacted]

If the thicknesses are sufficiently small the weight of the shielding on the two areas may be represented by

$$W_{AB} = W_A + W_B$$

$$W_{AB} = At_A\rho + Bt_B\rho$$

where ρ is the density of shielding material, t is the thickness, and A and B are the areas. Now, since A and B are unit areas,

$$W_{AB} = t_A\rho + t_B\rho .$$

It is now desired to find the minimum weight of shielding for a constant total dose rate D^*_{AB}.

since

$$t_A = \lambda \ln(DA/DA^*)$$

$$t_B = \lambda \ln\left[D_B/(D^*_{AB} - D^*_A)\right]$$

then

$$W_{AB} = \rho\lambda \ln(DA/D^*_A) + \rho\lambda \ln\left[DB/(D^*_{AB} - D^*_A)\right] .$$

For W_{AB} to have a minimum with respect to variation of D^*_A, $\frac{dW_{AB}}{dD_A^*}$ must equal zero.

$$\frac{dW_{AB}}{dD_A^*} = \rho\lambda\left(\frac{D^*_A}{D_A}\right)\left(-\frac{D_A}{(D^*_A)^2}\right) + \rho\lambda\frac{(D^*_{AB} - D^*_A)}{D_B}\frac{D_B}{(D^*_{AB} - D^*_A)^2}$$

$$0 = -\frac{1}{D^*_A} + \frac{1}{(D^*_A - D^*_A)}$$

and $D^*_A = D^*_{AB} - D^*_A$

then $D^*_A = D^*_B$.

In other words, the minimum weight exists when equal increments of crew dose rate are received in the crew compartment from equal solid angles from the reactor.

[redacted]

ATOMIC ENERGY ACT - 1954

[redacted]

The geometry of the situation is as follows:

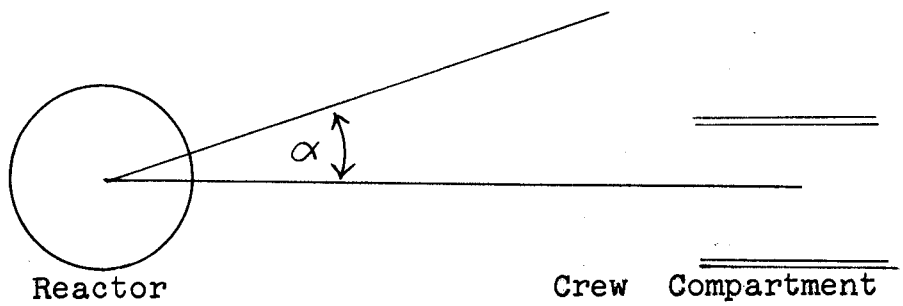

The following symbols are used:

I_{sn} is the scattered neutron dose rate in the crew compartment (rem/hr).

I_{sg} is the scattered gamma dose rate in the crew compartment (rem/hr).

S_n is the neutron source term (n/sec) without reactor shielding and is considered isotropic.

S_g is the gamma source term without reactor shielding and is considered isotropic (photons/sec).

$e^{-x(\alpha)}$ is the neutron shielding attenuation, where $x(\alpha)$ is the number of relaxation lengths of neutron shielding in the direction α

$e^{-y(\alpha)}$ is the gamma shielding attenuation, where $y(\alpha)$ is the number of relaxation lengths of gamma shielding in the direction α.

F_n is the conversion factor from neutron flux to dose rate (rem/hr)/(n/cm^2-sec)

F_g is the conversion factor from gamma photon flux to dose rate (rem/hr)/(photons/cm^2-sec)

Also, $f_n(\alpha)$ is defined by $I_{sn} = \int_0^{\pi} S_n e^{-x(\alpha)} F_n \, f_n(\alpha) \, d\alpha$
and $f_g(\alpha)$ is defined by $I_{sg} = \int_0^{\pi} S_g \, e^{-y(\alpha)} F_g \, f_g(\alpha) \, d\alpha$
Both $f_n(\alpha)$ and $f_g(\alpha)$ will include scattering probabilities and attenuation through the crew shield. The units of $f_n(\alpha)$ are (n/cm^2-sec)/(radian-n/sec). The units of $f_g(\alpha)$ are (photons/cm^2-sec)/(radian-photo/sec).

[redacted]

[redacted]
ATOMIC ENERGY ACT--1954

[redacted]

Now $$I_{sn} = \int_0^{\pi} S_n \, e^{-x(\alpha)} \, F_n \, f_n(\alpha) \, d\alpha \tag{19}$$

then $$\frac{dI_{sn}}{d\alpha} = S_n \, e^{-x(\alpha)} \, F_n \, f_n(\alpha) \tag{20}$$

Now $$\frac{d\alpha}{d\omega} = \frac{1}{2\pi \sin \alpha} \tag{21}$$

where ω is the solid angle, $\omega = 2\pi(1-\cos \alpha)$ (22)

then $$\frac{dI_{sn}}{d\omega} = \frac{1}{2\pi \sin \alpha} S_n \, e^{-x(\alpha)} F_n \, f_n(\alpha) \tag{23}$$

Now, since equal crew dose rates are to come from equal increments of solid angles, it is true that

$$\frac{dI_{sn}}{d\omega} = \text{constant} = \frac{I_{snt}}{4\pi} \tag{24}$$

where I_{snt} is the total allowable scattered neutron dose rate (rem/hr) in the crew compartment.

Then, $$\frac{I_{snt}}{4\pi} = \frac{S_n F_n}{2\pi} e^{-x(\alpha)} \frac{f_n(\alpha)}{\sin \alpha} \tag{25}$$

Solving for $x(\alpha)$ we get:

$$x(\alpha) = \ln \frac{2 \, f_n(\alpha) \, S_n \, F_n}{I_{snt} \sin \alpha} \tag{26}$$

Likewise it is found that

$$y(\alpha) = \ln \frac{2 \, f_g(\alpha) \, S_g \, F_g}{I_{sgt} \sin \alpha} \tag{27}$$

where I_{sgt} is the total allowable scattered gamma dose rate (rem/hr) in the crew compartment.

It may be necessary to place a constraint, usually an upper limit, on the radiation coming from the reactor. This means that there are minimum values of $x(\alpha)$ and $y(\alpha)$ which will be allowed.

Let us consider the scattered neutron dose rate in the crew compartment. Assume there is a minimum number of relaxation lengths of neutron shielding material, x_o, from $\alpha = \alpha_1$, to $\alpha = \pi$ and that for $\alpha < \alpha_1$, $x(\alpha) > x_o$.

Now $$I_{snt} = \int_0^{\alpha_1} e^{-x(\alpha)} S_n F_n f_n(\alpha) d\alpha + \int_{\alpha_1}^{\pi} e^{-x_o} S_n f_n(\alpha) F_n d\alpha \tag{28}$$

If ϕ_{on} (R) is the maximum allowed neturon flux at a distance R from the center of the reactor, then

$$\phi_{on}(R) = \frac{S_n \, e^{-x_o}}{4\pi \, R^2} \text{ (n/cm}^2\text{-sec)}$$

and $$S_n e^{-x_o} = 4\pi R^2 \phi_{on}(R) \tag{29}$$

[redacted]

ATOMIC ENERGY ACT - 1954

[redacted]

Substituting Equation 29 into Equation 28 we get

$$I_{snt} = \int_0^{\alpha_1} e^{-x(\alpha)} S_n F_n f_n(\alpha) d\alpha + \int_{\alpha_1}^{\pi} 4\pi R^2 \phi_{on}(R) F_n f_n(\alpha)\, d\alpha \quad (30)$$

As in the unconstrained case, we shall assume that for the minimum weight arrangement $dI_{sn}/d\omega$ must equal a constant between $\alpha = 0$ and $\alpha = \alpha_1$. This, however, cannot be the case between α_1 and π, since the value of $x(\alpha)$ is required to be constant, x_o.

$$\left[\frac{dI_{sn}}{d\omega}\right]_{o\to\alpha_1} = \text{constant} \equiv \overline{\left[\frac{dI_{sn}}{d\omega}\right]}_{o\to\alpha_1} \quad (31)$$

Then Equation 30 can be written as

$$I_{snt} = \omega_1 \overline{\left[\frac{dI_{sn}}{d\omega}\right]}_{o\to\alpha_1} + \int_{\alpha_1}^{\pi} 4\pi R^2 \phi_{on}(R) F_n f_n(\alpha) d\alpha \quad (32)$$

and from Equation 32 we get

$$\left[\frac{dI_{sn}}{d\omega}\right]_{o\to\alpha_1} = \overline{\left[\frac{dI_{sn}}{d\omega}\right]}_{o\to\alpha_1} = \frac{1}{\omega_1}\left[I_{snt} - \int_{\alpha_1}^{\pi} 4\pi R^2 \phi_{on}(R) F_n f_n(\alpha) d\alpha\right] \quad (33)$$

where $\omega_1 = 2\pi(1 - \cos \alpha_1)$

Now Equation 23 holds for all values of α, from 0 to π. At $\alpha = \alpha_1$, $x(\alpha) = x_o$, and Equation 5 becomes

$$\left[\frac{dI_{sn}}{d\omega}\right]_{\alpha_1} = \left[\frac{dI_{sn}}{d\omega}\right]_{o\to\alpha_1} = \overline{\left[\frac{dI_{sn}}{d\omega}\right]}_{o\to\alpha_1} = \frac{S_n F_n e^{-x_o} f_n(\alpha_1)}{2\pi \sin \alpha_1} \quad (34)$$

Equations 33 and 34 constitute two simultaneous equations in unknowns, $\overline{[dI_{sn}/d\omega]}_{o\to\alpha_1}$ and α_1. These equations can be solved for the unknowns implicitly. Now since $dI_{sn}/d\omega$ is to be constant between $\alpha = 0$ and $\alpha = \alpha_1$, Equation 23 can also be written as:

$$\frac{dI_{sn}}{d\omega} = \left[\frac{dI_{sn}}{d\omega}\right]_{o\to\alpha_1} = \overline{\left[\frac{dI_{sn}}{d\omega}\right]}_{o\to\alpha_1} = \frac{S_n F_n e^{-x(\alpha)} f_n(\alpha)}{2\pi \sin \alpha} \quad (35)$$

Solving for $x(\alpha)$, we obtain

$$x(\alpha) = \ln\left[S_n F_n f_n(\alpha) \Big/ \overline{\left[\frac{dI_{sn}}{d\omega}\right]}_{o\to\alpha_1} 2\pi \sin \alpha\right] \quad (36)$$

Likewise, for shaping gamma ray shielding, we obtain the equations

$$\overline{\left[\frac{dI_{sn}}{d\omega}\right]}_{o\to\alpha_2} = \frac{1}{\omega_2}\left[I_{sgt} - \int_{\alpha_2}^{\pi} 4\pi R^2 \phi_{og}(R) F_g f_g(\alpha)\, d\alpha\right] \quad (37)$$

[redacted]

[redacted]

ATOMIC ENERGY ACT - 1954

[redacted]

$$\left[\frac{dI_{sn}}{d\omega}\right]_{o\to\alpha_2} = \frac{S_g F_g e^{-y_o} f_g(\alpha_2)}{2\,\pi \sin \alpha_2} \tag{38}$$

and

$$y(\alpha) = \ln\left[S_g F_g f_g(\alpha) \Big/ \left[\frac{dI_{sg}}{d\omega}\right]_{o\to\alpha_2} 2\pi \sin \alpha\right] \tag{39}$$

From $\alpha=\alpha_2$ to $\alpha=\pi$, the gamma ray shielding is restricted to the value y_o. This value can be determined from the following equation:

$$S_g e^{-y_o} = 4\pi R^2 \, \phi_{og} \, (R) \tag{40}$$

After the values of $x(\alpha)$ and $y(\alpha)$ have been determined, the thicknesses may be found if the function $x(\alpha) = f(t_g, t_n)$ and $y(\alpha) = g(t_g, t_n)$, may be expressed in terms of the thicknesses. The t_g and t_n are the thicknesses of the gamma and neutron shielding materials respectively.

Then

$$x(\alpha) = \frac{t_g}{\lambda_{n_1}} + \frac{t_n}{\lambda_{n_2}} \tag{41}$$

and

$$y(\alpha) = \frac{t_g}{\lambda_{g_1}} + \frac{t_n}{\lambda_{g_2}} \tag{42}$$

where λ_{n_1} is the relaxation length of neutrons in the gamma shielding material.

λ_{n_2} is the relaxation length of neutrons in the neutron shielding material.

λ_{g_1} is the relaxation length of gammas in the gamma shielding material.

λ_{g_2} is the relaxation length of gammas in the neutron shielding material.

[redacted]

[redacted]

ATOMIC ENERGY ACT - 1954

The two simultaneous equations, Equations 41 and 42, can then be solved for the thicknesses of neutron and gamma shielding material at each angle α . These thicknesses can then be used to determine (1) dose rates at the rear of the crew shield and (2) weight of the reactor shielding.

There are a number of items which, if considered, would improve this method.

The radiation emerging from the reactor is assumed to have a radial distribution at the surface of the reactor shield. This causes a spike to appear at $\alpha = 0$. Use of an angular distribution would reduce the spike.

For air scattering and crew shield penetration calculations, only one energy is used as that of the radiation emerging from the reactor. If the correct spectrum were used the results would be more accurate.

In the derivation of the method, it was assumed that the reactor shielding weight is proportional to the area and thickness. This is not a good approximation for all cases. This is conservative, however, as it leads to thicknesses which over-estimate the reactor shielding weight.

A TYPICAL SHAPED REACTOR SHIELD

The Shaped Reactor Shield Method has been applied to a spherical reactor-cylindrical crew shield to show how one applies the method to obtain a minimum weight shield system. Also, a minimum weight isotropically shielded reactor system has been calculated so a comparison of the final weight could be made.

The geometry of the reactor-crew shield system to be shielded is shown in Figure 2. The design data is as follows:

Neutron source term = 5.0×10^{15} n/sec

Gamma source term = 1.72×10^{17} photon/sec

Neutron constraint at 50' = 10,000 rem/hr

Gamma constraint at 50' = 10,000 rem/hr

Crew dose rate = 1 rem/hr

Altitude = 0 feet

Reactor shielding materials - lead and water

Crew shielding materials - lead and plastic

[redacted]

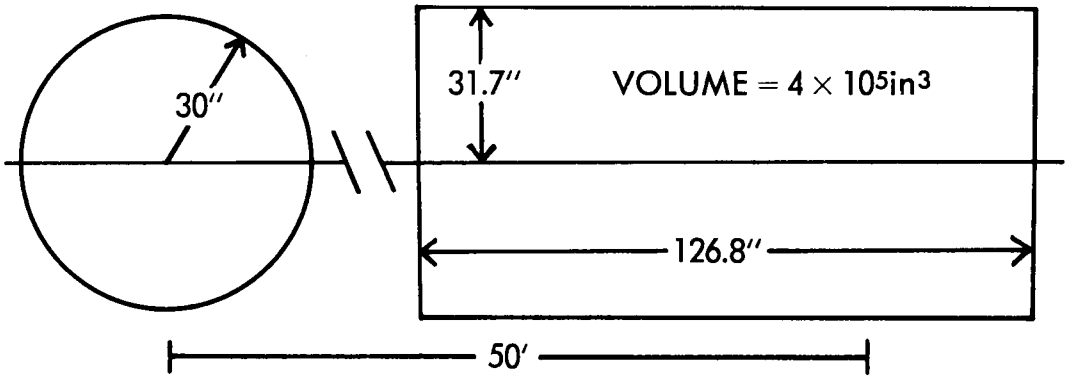

Figure 2. Geometry of Reactor Crew Shield System

[redacted]

AEC-3313-CVAC
[redacted]
ATOMIC ENERGY ACT - 1954

[redacted]

The dose rate components are those calculated in Section B for a minimum weight crew shield.

The outline shown in Figure 1 along with proper equations is used to determine separately the crew shield weight and the corresponding shaped reactor shield weight. These weights are found for several crew shield plastic thicknesses and result in a set of curves as shown in Figure 3. The total shielding weight obtained by adding the reactor shield weight and crew shield weight shows a very definite minimum weight shield system. In the shield system shown in Figure 3, 0.254 cm of lead was placed on the crew shield to reduce the low energy gammas in the crew compartment.

Since a weight penalty of a large magnitude could be imposed by setting the lead thickness at 0.254 cm a calculation was carried out to find at which lead thickness a true minimum shield weight would be determined. Also what the magnitude of this weight penalty would be. The results are shown in Figures 4 and 5. The minimum weight lead thickness was found to be 0.210 cm and the weight penalty for setting the lead thickness on the crew shield at 0.254 cm was 300 pounds.

The resulting shielding placement about the reactor shield and crew compartment for the minimum weight shield system is shown in Figure 6. The thicknesses as a function of α are shown in Table I as are the resulting weight of the lead and water on the reactor.

To give some idea of the weight savings realized by shaping a reactor shield as compared to an isotropic shield a comparison was made for the reactor crew shield system. So as not to penalize unduly the isotropic reactor shield system a minimum weight shield system was determined for the comparison. The weight saved by shaping the reactor shield is 30,100 pounds.

[redacted]

[redacted]

[redacted]

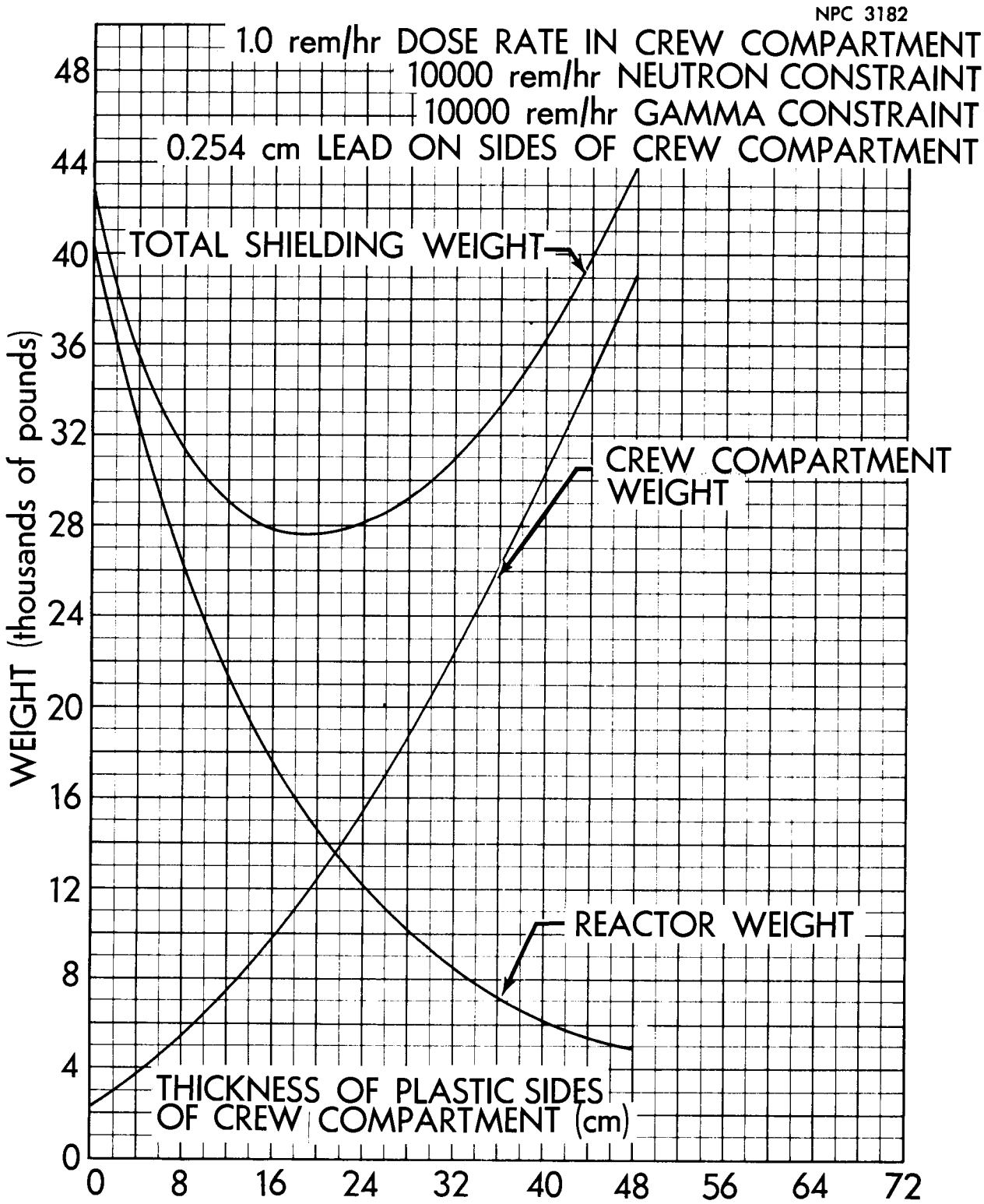

Figure 3. Shielding Weights as a Function of Crew Compartmentside Plastic Thickness

[redacted]

AEC-3313-CVAC
[redacted]
ATOMIC ENERGY ACT - 1954

[redacted]

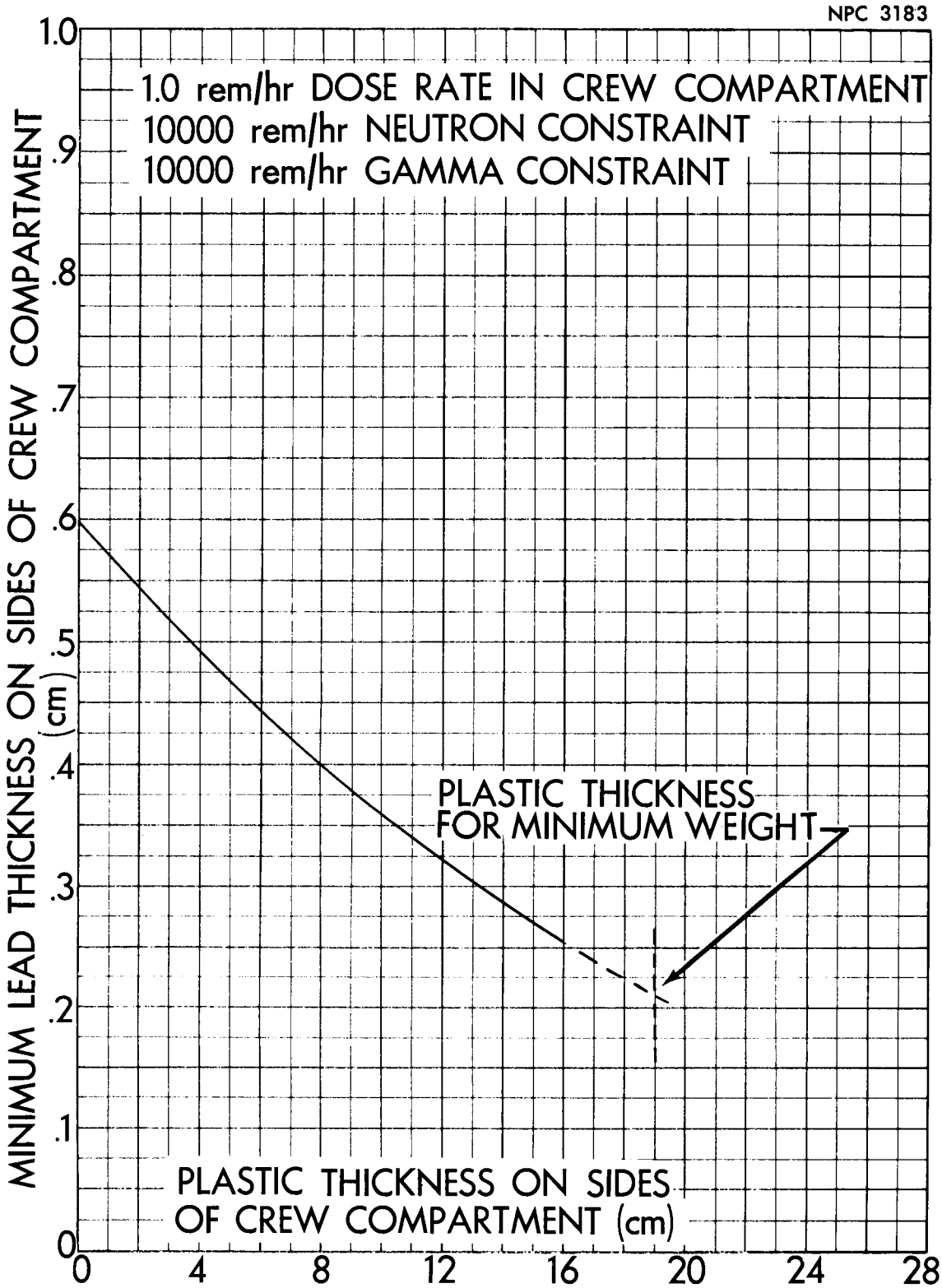

Figure 4. Lead Thickness for Minimum Shield Weight

[redacted]

AEC-3313-CVAC
[redacted]
ATOMIC ENERGY ACT - 1954

[redacted]

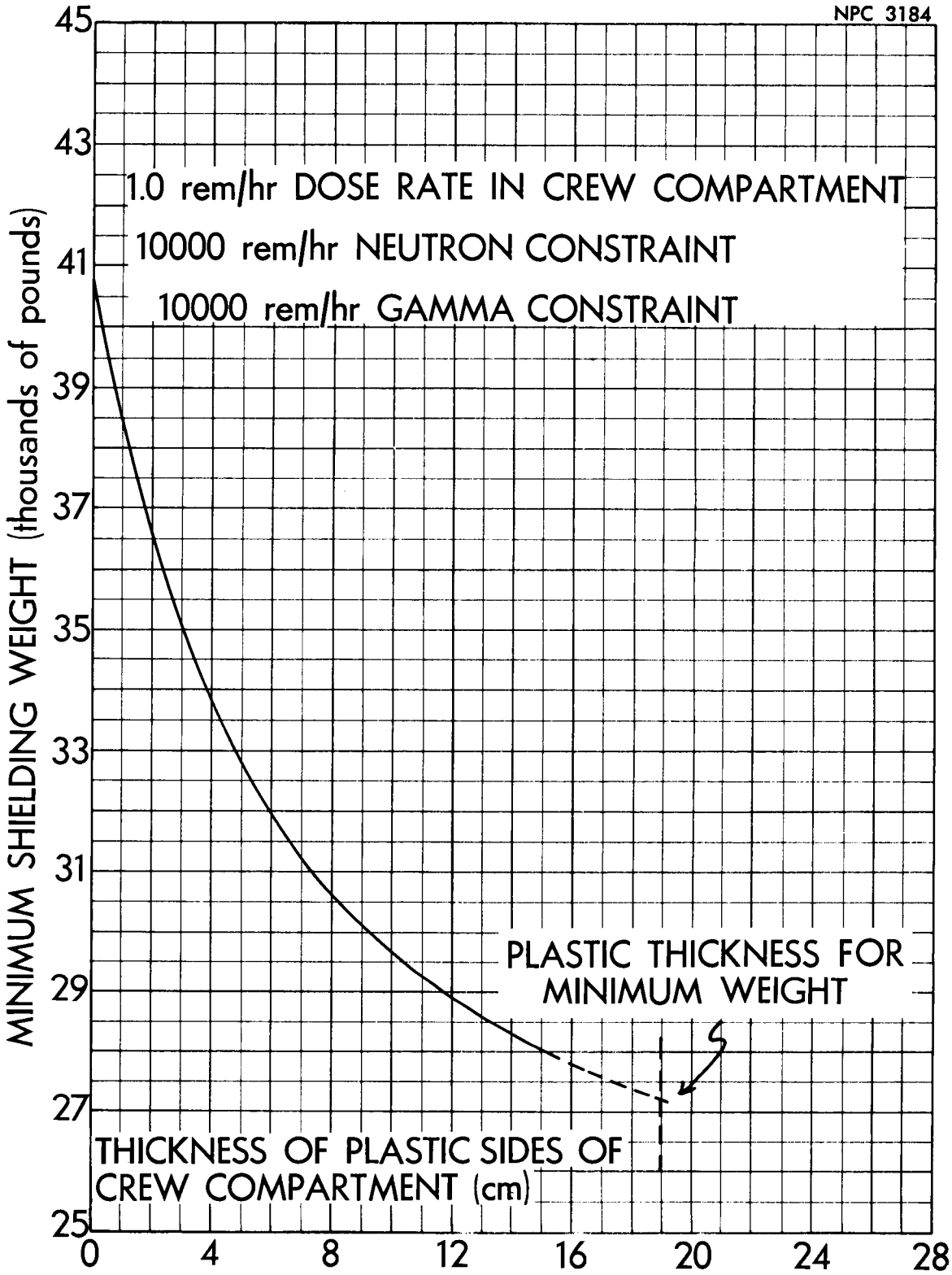

Figure 5 Shielding Weight for Minimum Lead Thickness

[redacted]

AEC-3313-CVAC
[redacted]
ATOMIC ENERGY ACT - 1954

[redacted]

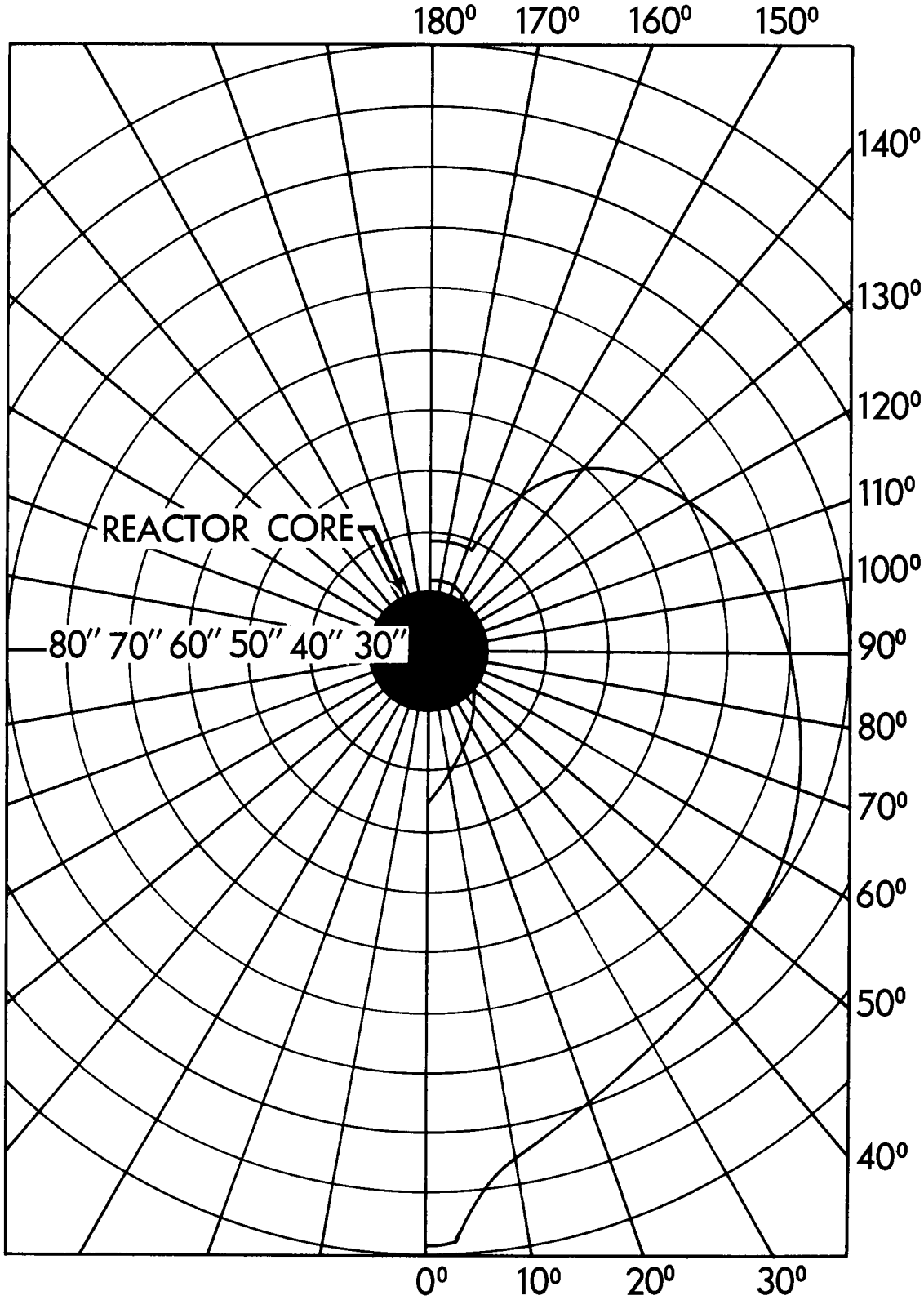

Figure 6. Shaped Reactor Shield

[redacted]

AEC-3313-CVAC
[redacted]
ATOMIC ENERGY ACT - 1954

[redacted]

TABLE I

SHIELDING THICKNESSES (cm)

(degrees)	P_b on Reactor	H_2O on Reactor
2.5	14.5	74.1
7.5	11.38	67.4
12.5	9.35	64.7
17.5	7.68	63.3
22.5	6.2	62.4
27.5	5.0	61.8
32.5	3.70	61.2
37.5	7.62	60.7
42.5	1.57	60.3
47.5	.62	59.9
52.5	0	59.5
57.5	0	59.1
62.5	0	57.5
67.5	0	56.0
72.5	0	54.4
77.5	0	53.3
82.5	0	51.9
87.5	0	50.4
92.5	0	49.0
97.5	0	47.8
102.5	0	46.3
107.5	0	44.7
112.5	0	43.1
117.5	.1	41.4
122.5	.2	39.1
127.5	.3	36.6
132.5	.3	33.4
137.5	.3	30.7
142.5	.3	27.4
147.5	.4	22.0
152.5	.9	15.2
157.5	1.61	6.40
162.5	1.61	6.22
167.5	1.61	6.22
172.5	1.61	6.22
177.5	1.61	6.22

Weight of Lead = 1,600 lbs

Weight of Plastic = 14,000 lbs

[redacted]

[redacted]
ATOMIC ENERGY ACT - 1954

SECRET

Paper III-D

MARTIN UNIT SHIELD DESIGN PROCEDURE*

B. L. Byrum and J. A. Biggerstaff
Martin, Baltimore

*Published at Martin as Report No. ER No. 8017.

SECRET

ERRATA SHEET FOR ER 8017

Page 2. Near the middle of the last equation:

$A(\theta, B, a)$ should be $A(E, \theta, B, a)$

Page 3. Third definition from the bottom of the page:

$A(\theta, B, a)$ should be $A(E, \theta, B, a)$

Page 4. Equation (7):

$1 - K(1 - \cos\theta)$ should be $1 + K(1 - \cos\theta)$

Page 12. Second line from the bottom of the page:

D should be D'

Page 17. Last equation on the page:

Φ should be Φ'

Page 23. End of last equation on the page:

$[\quad](\Delta t)_K$ should be $[\quad](\Delta t)_K \Delta\alpha)_K$

Page 24. The line following Equation 26:

$\underline{v}$ should be $\underline{v}'$

[redacted]

FOREWORD

The report has been prepared in accordance with the requirements of Contract Number Nonr-1612(00) under the direction of the Bureau of Aeronautics and the Office of Naval Research.

The report substantiates the investigation discussed under RADIATION AND SHIELDING in Martin Report ER 7784, where studies of a nuclear-powered seaplane (M331-1) are presented.

ACKNOWLEDGEMENTS

The authors wish to thank Mr. Gerald J. Rausa for his participation in the incipient phases of development of this work, and for the helpful information which he has forwarded to them in connection with his present Martin assignment at the Oak Ridge Tower Shielding Facility.

The authors would also like to express their gratitude to Mr. George T. Dib (presently with Blaw Knox, Pittsburgh, Pa.) for his presentation of the initial work at the Convair Shielding Symposium during August, 1955.

[redacted]

ABSTRACT

A procedure for designing an aircraft reactor shield system is formulated and the underlying theory is summarized in this report. The procedure is predicated upon the fact that, until more sophisticated methods of shield design evolve and are verified by experiments, maximum utilization of information derived directly from shield mockups will yield the most reliable design data. Although the method presented is directly applicable to preliminary unit shield design, the equations and procedures are amenable to the modifications required for extension to divided shields and to consideration of angular and energy spectra when they become known.

The authors wish to remind the reader that the Martin shield design method is constantly being modified to improve its accuracy and range of applicability. Due to its present utility, however, and to profit from the comments of others engaged in "aeronuclear" work, the underlying concepts and the current details of the Martin shield design technique are presented here. The word "aeronuclear", coined by the authors, is defined as pertaining to aeronucleonics, the branch of aerophysics concerned with nuclear science and technology.

The interested reader is encouraged to also read the material presented in Martin Report ER 7784, which presents a number of the aeronuclear problems confronting scientists and engineers in the early study and development phases of an operational nuclear-powered weapons system.

I. INTRODUCTION

The shield design method discussed in this paper was developed at the Martin Company, and was presented in rough form at the Convair Shielding Symposium during August, 1955. (Ref 1).

A. DESIGN PROCEDURE USING SHIELD MOCKUPS

Until more sophisticated methods of shield design evolve and are verified by experiments, it is evident that maximum utilization of information derived directly from shield mockups will yield the most reliable design data. The design procedure discussed in this report is predicated upon this fact. For example, the mathematical form of an anisotropic source strength must be approximated through discretionary utilization of pertinent experimental data which, at the present time, are generated largely with the Lid Tank Facility (LTF) and the Bulk Shielding Facility (BSF) at the Oak Ridge National Laboratory (ORNL).

When designing a shield for the Circulating Fuel Reactor (CFR), the LTF is the logical source of experimental data at the present time. Information derived from the LTF will also be useful for other reactor types such as the Air Cycle Reactor (ACR) when an appropriate series of experiments have been completed. The basic information derived from the BSF reactor can be applied to various reactor types, in particular to the ACR in the absence of appropriate LTF data.

As a conceptual aid in analyzing the influence of air scattering on shield design, the reactor-shield system for any given asymmetric shield design may be replaced by an anisotropic point source of strength $q(\alpha)$. The source strength is defined such that the unscattered radiation intensity at a distance $\underline{r}$ from the source and at an angle $\underline{\alpha}$ from the axis of symmetry is given by $q(\alpha)/4\pi r^2$. Thus, in actual practice, $q(\alpha)$ may be found from the conventional equations used in direct beam calculations. The quantity $q(\alpha)$ has the following physical significance: it is the integrated leakage of the type under consideration which <u>would</u> emanate from a spherically symmetric reactor-shield system of dimensions equal to those of the actual system at $\underline{\alpha}$. This concept has been incorporated into the shield design technique used in this report.

B. GAMMA RAYS

The contribution to the total dose rate by single-collision air-scattered radiation may be determined from the following expression (Ref 2):

$$D(a, b) = \int_{E=0}^{\infty} S(E) \int_{\alpha=0}^{\pi} N(E, \alpha)\, f(E, \alpha, a, b)\, d\alpha\, dE \qquad (1)$$

where

$S(E) \equiv$ energy radiated per unit time from the source per unit energy interval at energy $\underline{E}$

$\alpha \equiv$ linear angle emergent ray or particle makes with the source-receiver axis

$\frac{N(E, \alpha)}{4\pi} \equiv$ fraction of radiation at energy $\underline{E}$ which is emitted at linear angle $\underline{\alpha}$ per unit solid angle

$a \equiv$ source-receiver separation distance

$b \equiv$ symbol representing composition and thickness of shielding material located around the receiver

$\frac{2}{\sin \alpha} f(E, \alpha, a, b) \equiv$ dose rate due to single-collision air scattering at separation distance $\underline{a}$ and receiver shield $\underline{b}$ due to a unit source emitting radiation of energy $\underline{E}$ at angle $\underline{\alpha}$ only

The functions $\underline{N}$ and $\underline{S}$ are intrinsic properties of the source and its shield. The function $\underline{f}$, which is supposed to describe all the phenomena occuring after the radiation leaves the source, may be written as follows:

$$f(E, \alpha, a, b) = \frac{n}{2a\epsilon} \int_{\theta=\alpha}^{\pi} A(\theta, \beta, a)\, \frac{E'(\theta, E)}{2\pi E \sin\theta}\, \frac{d\sigma(\theta, E)}{d\theta}\, C(E, \theta, \beta, b)\, d\theta \qquad (2)$$

where, for gamma rays, the new symbols are defined as follows:

$n \equiv$ volume density of electrons in air at the altitude of interest; e.g., average altitude over the flight profile

$\epsilon \equiv$ conversion factor between energy flux and dose rate, assumed independent of energy

$\theta \equiv$ scattering angle $= \alpha + \beta$

$\beta \equiv$ angle of incidence of the scattered gamma rays on the receiver, measured between the line segment connecting source and receiver and the path of the scattered ray intersecting the receiver ($0 \leq \beta \leq \pi$)

$E'(\theta, E) \equiv$ energy of a gamma ray after having been scattered from an energy $\underline{E}$ through angle $\underline{\theta}$ (3)

$$= \frac{E}{1 + k\,(1 - \cos\theta)}$$

$k \equiv E/mc^2$, where mc^2 represents the rest mass energy of an electron

$= E/0.511$, if $\underline{E}$ is in MeV

$\frac{d\sigma(\theta, E)}{d\theta} \equiv$ Klein-Nishina differential scattering cross section for scattering through angle $\underline{\theta}$ at energy $\underline{E}$, cm^2/ radian-electron

$A(\theta, \beta, a) \equiv$ air attenuation factor

$$= \exp\left(\frac{-a}{\sin\theta}\left[\frac{\sin(\theta - \beta)}{\lambda'} + \frac{\sin\beta}{\lambda}\right]\right) \qquad (4)$$

$\lambda, \lambda' \equiv$ gamma ray mean free paths in air before and after primary scattering, respectively

$C(E, \theta, \beta, b) \equiv$ attenuation suffered by the scattered gamma rays in penetrating through the shield at the receiver

$$\cong B\left(\sum_i \mu_i b_i \csc \beta\right) \prod_i \exp(-\mu_i b_i \csc \beta) \tag{5}$$

See pertinent comments under FORMULATION

$B\ (E', b_i, \beta) \equiv$ buildup factor for gamma rays penetrating the shield around the receiver

$\mu_i(E') \equiv$ absorption coefficient of ith material in the receiver shield for gamma rays of energy $E'(E, \theta)$

$b_i \equiv$ thickness of ith shielding material at the receiver

There is experimental and theoretical evidence (Refs 3 & 4) that multiple scattering effects compensate for attenuation in air, hence the absorption term A is set equal to unity. Although it is known that certain features of the two principal aircraft nuclear powerplants presently under development preclude any efficient unit shield design, the term C is also set equal to unity. Under these conditions, Eq. (1) simplifies to

$$D(a) = \frac{n}{2\epsilon a} \int_{E=0}^{\infty} dE \int_{\alpha=0}^{\pi} q(\alpha, E)\ \Gamma\ (\alpha, E)\ d\alpha \tag{6}$$

where

$$\Gamma\ (\alpha, E) \equiv \int_{\theta=\alpha}^{\pi} \frac{1}{2\pi \sin\theta} \frac{d\sigma\ (\theta, E)}{d\theta} \frac{d\theta}{1 - k\ (1 - \cos\theta)} = \left[\frac{cm^2}{\text{radian-electron}}\right]$$

$$q(\alpha, E) \equiv S(E)\ N(E, \alpha) = \left[\frac{\text{photon}}{\text{sec}}\right] \tag{7}$$

Eq. (7) is integrated in Chapter VI and $\Gamma(\alpha)$ is illustrated in Fig. 5.

Since the energy distribution of the radiation leakage from an arbitrary reactor design varies with shield thickness, which, in turn, varies with the angle of emission, and there is no satisfactory theoretical treatment describing this dependence, an experimental determination of $q(\alpha, E)$ is required to integrate Eq. (6). For the purposes of preliminary design, it is logical and expedient to proceed as follows. Let

$$\Gamma(\alpha, \bar{E}) \equiv \frac{\int_{E=0}^{\infty} q(\alpha, E)\, \Gamma(\alpha, E)\, dE}{\int_{E=0}^{\infty} q(\alpha, E)\, dE} \tag{8}$$

then Eq. (6) becomes

$$D(a) = \frac{n}{2\,\epsilon\, a} \int_{\alpha=0}^{\pi} q(\alpha)\, \Gamma(\alpha, \bar{E})\, d\alpha \tag{9}$$

where

$$q(\alpha) \equiv \int_{E=0}^{\infty} q(\alpha, E)\, dE = \left[\text{MeV/sec}\right]$$

may be determined from pertinent experimental data. Furthermore, Maienschein (Ref 5) has shown that for a typical shield design (Ref 2), most of the emitted gamma radiation lies in the range from 1.5 MeV to 6MeV, peaking at about 2MeV to 3MeV. Since the shield designs considered in this paper are neither typical nor extreme deviators, 3.066 MeV is assumed to be a satisfactory value for $\bar{E}$.

NEUTRONS

If the various symbols used in the preceding discussion were known for neutrons, Eq. (1) could be used to calculate the single-collision air-scattered neutron contribution to the total dose rate. Due to the absence of an adequate theory describing the behavior of neutrons in the scattering process, however, designers must turn to approximations which seem to yield conservatively designed shields, the validity of which must eventually be judged by comparison with experimental results.

Differential scattering cross section data for neutrons in air are intensely sought at the present time. Measurements at experimental facilities similar to the Oak Ridge Tower Shielding Facility (TSF) will eventually alleviate this condition, but until the results of such measurements are available it will be necessary to assume an angular distribution for the scattered neutrons. One of the popular current methods for theoretical determination of the angular distribution is based upon predictions from the statistical-continuum model of the nucleus (Ref 6). Recent experimental data generated at the TSF have, however, cast doubt on the validity of this model (Ref 7) and have verified that the assumption of isotropic scattering yields an overestimate of the neutron dose rate. Pending completion of pertinent measurements of the neutron scattering probability at the TSF, isotropic scattering of neutrons in air is assumed adequate for preliminary shield design.

Assuming isotropic scattering in air and no exponential attenuation, it follows from Eq. (1) that the neutron air-scattered contribution to the dose rate at an unshielded point a distance $\underline{a}$ from the source is given by

$$D(a) = \int_{E=0}^{\infty} S(E) \int_{\alpha=0}^{\pi} N(E, \alpha) \frac{\Sigma_s (E)(\pi - \alpha)}{8 \pi a \epsilon (E)} \, d\alpha \, dE \qquad (10)$$

where $\underline{N}$ and $\underline{\epsilon}$ are the neutron correspondents to the original definitions under Eq. (1), and

$\Sigma_s(E)$ ≡ average macroscopic scattering cross section for neutrons of energy E in air at the altitude of interest.

$S(E)$ ≡ number of neutrons emitted per unit time from the source per unit energy interval at the energy E.

Assuming that the conversion factor ϵ is independent of energy, and letting

$$\Sigma_s(\bar{E}) \equiv \frac{\int_{E=0}^{\infty} \Sigma_s(E)\, q(\alpha, E)\, dE}{\int_{E=0}^{\infty} q(\alpha, E)\, dE}$$

it is seen that Eq. (10) may be written

$$D(a) = \frac{\Sigma_s(\bar{E})}{8\pi\epsilon a} \int_{\alpha=0}^{\pi} q(\alpha)\,(\pi - \alpha)\, d\alpha \qquad (11)$$

where

$$q(\alpha) \equiv \int_{E=0}^{\infty} q(\alpha, E)\, dE = \left[\text{neutrons/sec}\right]$$

may be determined from pertinent experimental data. Calculations performed by H. Goldstein, originally discussed in Ref (2) predict that the energy distribution of neutrons leaking from "conventional" reactor shields is practically flat up to 6 MeV, falling off as exp(4.50 - 0.75E) for higher energies. Again, since the shield designs considered in this paper are neither typical nor

extreme deviators, 5 MeV is assumed to be a satisfactorily conservative value for the $\underline{\overline{E}}$ in Eq. (11).

II. FORMULATION

Consider a design reactor similar to the CFR, and let

$D'(Z_k) \equiv$ dose rate measured in the shield at distance Z_k from the surface of the Lid Tank source plate with appropriately selected shield mock-up

$$\equiv \sum_i D'(Z_k - X_k^{\,i})$$

$D'(Z_k - X_k^{\,i}) \equiv$ dose rate due to the ith source (assumed a disc of radius $\underline{b'}$) measured in the appropriate Lid Tank shield mockup at distance ($Z_k - X_k^{\,i}$) from the surface of the source considered ($\underline{k}$ denotes a given value of the emission angle $\underline{\alpha}$ in the design shield, and $\underline{i}$ denotes the position relative to the Lid Tank source plate of a given source of radiation in an appropriate Lid Tank shield mockup)

$h(Z_k - X_k^{\,i}) \equiv$ Hurwitz correction for transforming a disc source to an infinite plane source

$$\cong \frac{1}{2} + \frac{2\lambda_i}{b'^2}\,(Z_k - X_k^{\,i} + \lambda_i)$$

$b' \equiv$ radius of Lid Tank source = 35.6 cm

$\lambda_i \equiv$ relaxation length of radiation corresponding to the ith source observed in the Lid Tank shield mockup (note that $\lambda_1 \equiv$ relaxation length of primary radiation $\cong$ 7.5cm)

$D_{p\ell}(Z_k - X_k^i, \infty) \equiv$ dose rate in the Lid Tank shield mockup at a distance $(Z_K - X_K^i)$ from an infinite plane source, derived from $D'^K(Z_k - X_k^i)$

$D_{SV}(Z_k + R_c, R_c + X_k^i) \equiv$ dose rate in a shield precisely like that of the selected Lid Tank mockup at a distance $(Z_k - X_k^i)$ from the surface of a spherical source of radius $(R_c + X_k^i)$

$R_c \equiv$ core radius of design reactor

$R_c + X_k^i \equiv$ effective radius of the ith source region in the design reactor-shield system at a value of $\underline{\alpha}$ characterized by the subscript $\underline{k}$

$s_i, s_i' \equiv$ effective surface source strengths corresponding to source regions in the design system and Lid Tank mockup, respectively (note that $s_1 \equiv$ source strength of Lid Tank fission source = 9.04×10^{-4} watt cm^{-2} is subject to change)

$m \equiv$ material correction for transforming data from comparison to design system (assumed equal to unity if the shield mockup selected for comparison is very similar to the design shield)

$m_k^\gamma \equiv$ material correction for gamma rays at a value of $\underline{\alpha}$ characterized by subscript $\underline{k}$

$$\cong \frac{B_k\left[\sum_j (t/\lambda)_j\right]}{B_k\left[\sum_j (t/\lambda)'_j\right]} \prod_j \exp\left[\left(\frac{t}{\lambda}\right)'_j - \left(\frac{t}{\lambda}\right)_j\right]_k$$

$m_k^n \equiv$ material correction for neutrons at a value of $\underline{\alpha}$ characterized by the subscript $\underline{k}$

$$\cong \prod_j \exp \left[\left(\frac{t}{\lambda}\right)'_j - \left(\frac{t}{\lambda}\right)_j \right]_k$$

$B_k \equiv$ factor representing the buildup of gamma rays in either the design or mockup shield, assumed a function of the sum of the relaxation lengths of the individual materials and assumed equal to the buildup in the same number of relaxation lengths of the dominant material

$\lambda_j, \lambda'_j \equiv$ relaxation length in the jth material of the design and comparison shields, respectively

$t_j, t'_j \equiv$ thickness of jth material in the design and comparison shield, respectively

$s, d \equiv$ scattered or direct component, respectively, when written as subscripts

$n, \gamma \equiv$ neutron or gamma ray, respectively, when written as subscripts or superscripts

$\lambda_c \equiv$ relaxation length of the radiation in the core

$r_c \equiv$ inner radius of the fission source array (core)

$P(r) \equiv$ source density of core region (assumed to be a function only of the radial distance $\underline{r}$)

$n_\gamma \equiv$ volume density of electrons in air at cruise altitude

$n_n \equiv$ nuclear density of air at cruise altitude

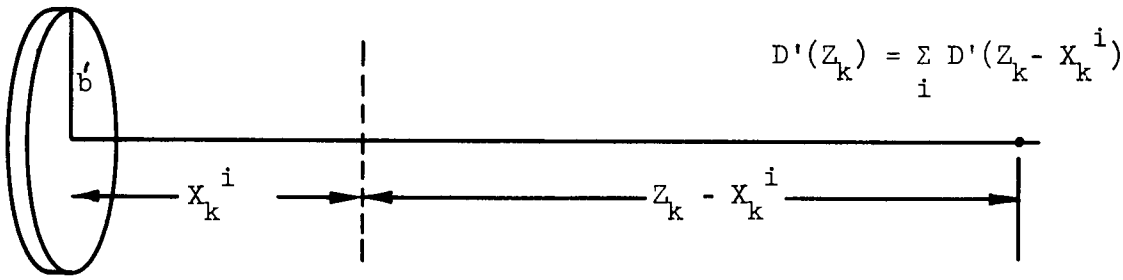

Fig. 1 (a) Lid Tank Source Configuration

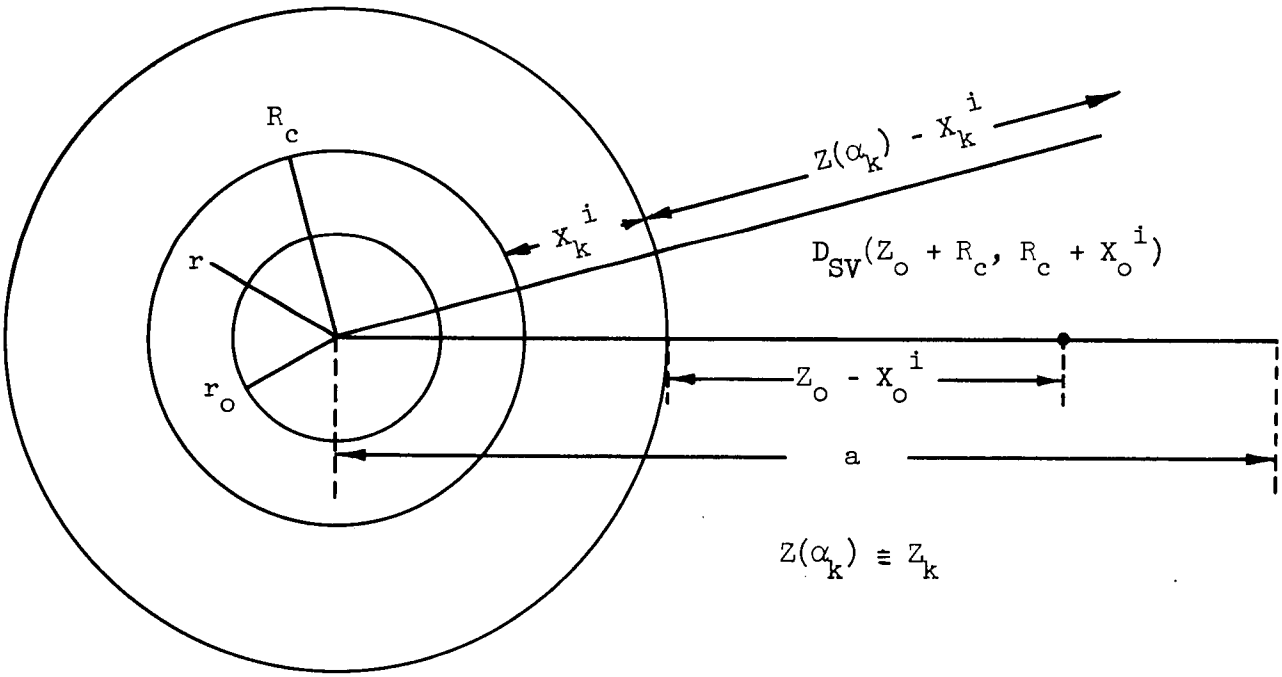

Fig. 1 (b) Circulating Fuel Reactor Source Configuration

With reference to Fig. 1, it is seen that

$$\sum_i h(Z_o - X_o^{\,i})\, D'(Z_o - X_o^{\,i}) = \sum_i D_{p\ell}(Z_o - X_o^{\,i}, \infty) \tag{12}$$

and

$$\sum_i D_{SV}(Z_o + R_c, R_c + X_o^{\,i}) =$$

$$= \sum_i \left(\frac{R_c + X_o^{\,i}}{Z_o + R_c}\right) \left[D_{p\ell}(Z_o - X_o^{\,i},\infty) - D_{p\ell}(Z_o + 2R_c + X_o^{\,i},\infty)\right] \frac{s_i}{s_i'}$$

$$= \sum_i \left(\frac{R_c + X_o^{\,i}}{Z_o + R_c}\right) \Big[h(Z_o - X_o^{\,i})\, D'(Z_o - X_o^{\,i})$$

$$- h(Z_o + 2R_c + X_o^{\,i})\, D\,(Z_o + 2R_c + X_o^{\,i})\Big] \frac{s_i}{s_i'}$$

$$\cong \sum_i \left(\frac{s_i}{s_i'}\right) \left(\frac{R_c + X_o^{\,i}}{Z_o + R_c}\right) h(Z_o - X_o^{\,i})\, D'(Z_o - X_o^{\,i}) \tag{13}$$

assuming that $2R_c + X_o^i$ is much greater than the relaxation length λ_i.

Application of the material and inverse square corrections to Eq. (13) yields the direct contribution to the total dose rate at an unshielded point distance a from the source:

$$D_{\substack{n \text{ or } \gamma \\ \text{direct}}}(a) = m_o \left(\frac{Z_o + R_c}{a^2}\right) \sum_{i=1}^{W} \left(\frac{s_i}{s_i'}\right)\left(R_c + X_o^i\right) h(Z_o - X_o^i) D'(Z_o - X_o^i) \tag{14}$$

where W is the number of disc or spherical shell sources considered. It is noted that

$$s_1 \equiv s_{core} = \frac{\operatorname{csch}(R_c/\lambda_c)}{R_c} \int_{r=r_o}^{R_c} r\, P(r) \sinh\left(\frac{r}{\lambda_c}\right) dr$$

is tabulated on page 300 of (Ref 2) for various CFR core diameters, whereas the quantities to be associated with values of i greater than unity must be ascertained from as yet unpublished data generated in Oak Ridge facilities and evaluated by John Dee and others.

Since

$$q^k_{n \text{ or } \gamma}(\alpha) = 4\pi\epsilon m_k (Z_k + R_c) \sum_{i=1}^{W} \left(\frac{s_i}{s_i'}\right)\left(R_c + X_k^i\right) h(Z_k - X_k^i)\, D'(Z_k - X_k^i) \tag{15}$$

by Eq. (14), it follows from Eqs. (9) and (11), respectively, that

$$D_{\gamma,s}(a) = \frac{2\pi n_\gamma}{a} \sum_{k=0}^{M_\gamma} g_k m_k^{\gamma} (\Delta\alpha)_k (Z_k + R_c)\, \Gamma(\alpha_k, \bar{E}) \qquad (16)$$

and

$$D_{n,s}(a) = \frac{n_n \sigma_s(\bar{E})}{2a} \sum_{k=0}^{M_n} f_k m_k^{n} (\Delta\alpha)_k (\pi - \alpha_k)(Z_k + R_c) \qquad (17)$$

where

$$f_k \equiv \sum_{i=1}^{W_n} \left(\frac{s_i}{s_i'}\right)_n (R_c + X^i_{n,k})\, h(Z_k - X^i_{n,k})\, D_n'(Z_k - X^i_{n,k})$$

$$g_k \equiv \sum_{i=1}^{W_\gamma} \left(\frac{s_i}{s_i'}\right)_\gamma (R_c + X^i_{\gamma,k})\, h(Z_k - X^i_{\gamma,k})\, D_\gamma'(Z_k - X^i_{\gamma,k})$$

$$\pi = \sum_{k=0}^{M_n} (\Delta\alpha)_k = \sum_{k=0}^{M_\gamma} (\Delta\alpha)_k$$

$$n_n \sigma_s(\bar{E}) \equiv \Sigma_s(\bar{E})$$

$i = 1$ = primary (core) source

The value of $(\Delta\alpha)_k$ may be allowed to vary in order to improve accuracy where $\Gamma(\alpha_k, \bar{E})$ is changing rapidly.

If angular distributions of the radiation leakage from the reactor-shield system are not imposed on Eqs. (14), (16) and (17), shield weights calculated therefrom may not be conservative. Recent results derived from investigations at the TSF (Ref 7) permit refinement of Eqs. (14) and (17). Unfortunately, the corresponding information for gamma rays has not yet been generated.

Suppose that in a Lid Tank mockup a fast neutron dose rate $D'(Z_k)$ is measured at a distance Z_k from the source plate, Fig. 1a. Suppose also that it has been shown that the angular distribution of radiation flux reaching the detector is $\Phi'(Z_k, \xi) = \Phi'(Z_k, 0) \cos^{\nu}\xi$, where $\underline{\nu}$ is an integer or zero, Fig. 2a.

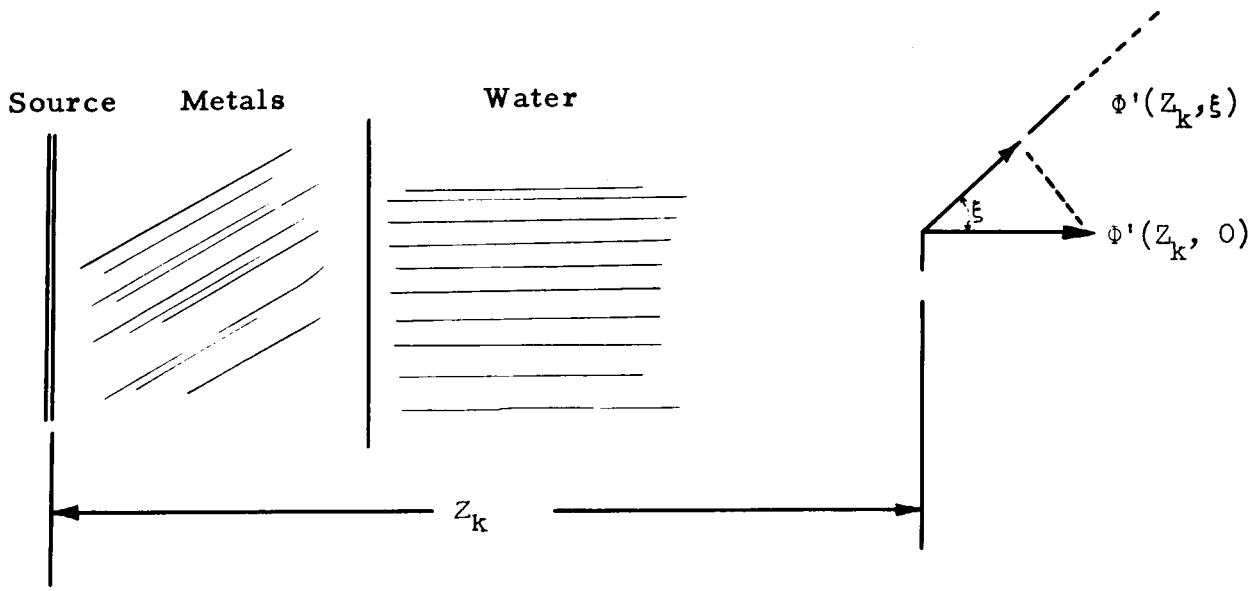

Fig. 2a: Lid Tank Angular Distribution Geometry

[redacted]

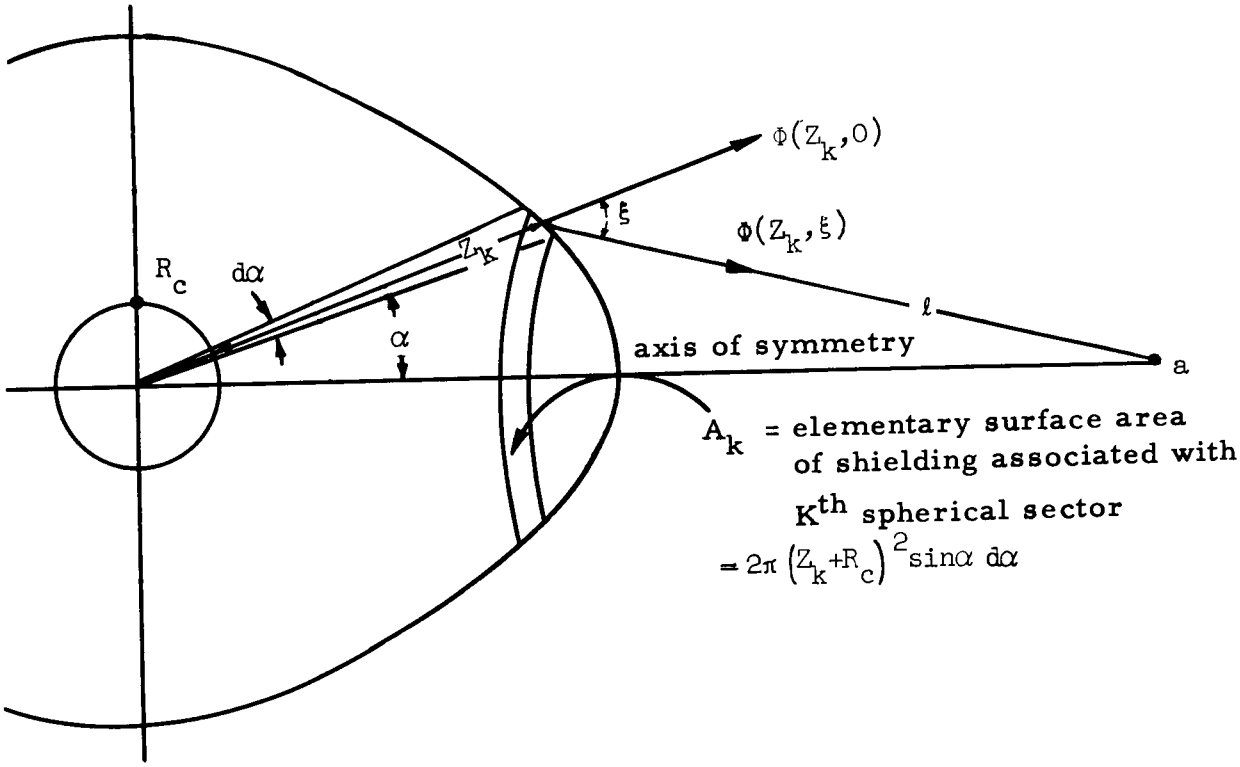

Fig. 2b: Design Shield Angular Distribution Geometry

In a practical design the shielding terminates at a thickness Z_k beyond which the albedo is essentially zero. The contribution $D^k_{n,d}(a)$ to the direct dose rate at a distance a from the center of the design source due to neutrons emitted through the elementary area (A_k) is given by Eq. (19), which is developed below with reference to Fig. 2b and subject to the following assumptions:

(a) Hurwitz and sphere-plane transformations are still valid (effective surface sources were assumed isotropic in Reference 2)

(b) Angular distribution of the leakage from a spherical geometry is given by $\Phi(Z_k, \xi) = \Phi(Z_k, 0) \cos^{\omega} \xi$, where ω is an integer or zero.

(c) Design shield has cylindrical symmetry with respect to the source-receiver axis

(d) Design configuration can be generated from spherical sectors

(e) Radiation flux passing through A_k is the same in every respect as that which would exist if the reactor-shield

[redacted]

system were spherically symmetric with radius equal to the dimension $(Z_k + R_c)$ associated with the given solid angle of the design system

$$D^k_{n,d}(a) = \sum_i \int_{\alpha = \alpha_k}^{\alpha_k + (\Delta\alpha)_k} m_k \frac{d\alpha}{\epsilon} \frac{s_i}{s'_i} 2\pi \left(\frac{Z_k + R_c}{\ell}\right)^2 \left(\frac{R_c + X_k^{\,i}}{Z_k + R_c}\right)$$

$$\times \quad \sin\alpha \quad h(Z_k - X_k^{\,i})\ \Phi'(Z_k, \xi) \tag{18}$$

$$= \frac{2\pi\, m_k (Z_k + R_c)}{a^2} \frac{\Phi'(Z_k, 0)}{\epsilon} \int_{\alpha_k}^{\alpha_k + (\Delta\alpha)_k} \cos^{\omega}\alpha \sin\alpha\, d\alpha$$

$$\times \sum_i \frac{s_i}{s'_i} (R_c + X_k^{\,i})\ h(Z_k - X_k^{\,i})$$

where $\underline{\ell}$ and $\underline{\xi}$ have been assumed equal to $\underline{a}$ and $\underline{\alpha}$, respectively, and $\Phi'(Z_k, \xi)$ has been replaced by $\Phi'(Z_k, 0) \cos^{\omega}\xi$

Since, from Fig. 2a,

$$\sum_i (1 - \eta_k^i)\ D'(Z_k - X_k^{\,i}) = \int_{\xi = 0}^{\frac{\pi}{2}} 2\pi \sin\xi\, d\xi\ \frac{\Phi'(Z_k, \xi)}{\epsilon}$$

which yields

$$\frac{\Phi(Z_k, 0)}{\epsilon} = \frac{\nu + 1}{2\pi} \sum_i (1 - \eta_k^{\,i})\ D'(Z_k - X_k^{\,i})$$

it is seen that Eq. (18) may be written

$$D^k_{n,d}(a) = \frac{\nu + 1}{\omega + 1} \; m_k \; \frac{Z_k + R_c}{a^2} \; (\Delta \cos^{\nu + 1} \alpha_k) \; \sum_i G^i_k \tag{19}$$

where

$$G_k^{\,i} \equiv \frac{s_i}{s'_i} (R_c + X_k^{\,i})(1 - \eta_k^i) \; h(Z_k - X_k^{\,i}) \; D'(Z_k - X_k^{\,i})$$

$\eta_k^{\,i} \equiv$ fraction of neutrons contributing to $D'(Z_k - X_k^i)$ that are back-scattered $(0 \leq \eta_k^{\,i} \leq \frac{1}{2}$

$$\Delta \cos^{\nu + 1}\alpha_k \equiv \cos^{\nu + 1}\alpha_k - \cos^{\nu + 1}\left[\alpha_k + (\Delta\alpha)_k\right]$$

Neglecting the effect of the cosine leakage distribution on Eq. (17), Eqs. (14) and (17) may be replaced by combining Eqs. (17) and (19),

$$D^k_n(a) \equiv D^k_{n,d}(a) + D^k_{n,s}(a)$$

$$= \frac{m_k \, f_k}{a^2} \left[\frac{a \sum_s (\bar{E})(\Delta\alpha)_k \; (\pi - \alpha_k)}{2} + \Delta \cos^{11} \alpha_k \right] (Z_k + R_c) \tag{20}$$

where $\underline{\omega}$ and $\underline{\nu}$ have been set equal to ten (Ref 7), and $D_n(a) \equiv \sum_{k=0}^{M} D^k_n(a) \equiv$ total neutron dose rate at an unshielded point on the axis of symmetry distance $\underline{a}$ from the center of the reactor.

It has also been assumed that $\eta_k^{\,i}$ equals zero, and it is noted that $\Delta \cos^{\nu + 1}\alpha_k$ should be set equal to zero in the range $\frac{\pi}{2} \leq \alpha \leq \pi$.

III. ASYMMETRICAL GEOMETRY

Although the scattered dose rate equations were developed from a cylindrically symmetrical geometry, this assumption was not necessary. It may be shown for cylindrically symmetric source distributions, by a process similar to that used in the section on shield optimization, that an optimum shield will be cylindrically symmetric. The assumed geometry is sufficient, therefore, for preliminary calculation of the shield configuration. However, in order to determine component shielding requirements and to estimate the extent of radiation effects on component performance it is necessary to compute, using a given shield configuration, the dose at points which do not lie on the axis of symmetry. Further, detailed shield design will involve asymmetric shield configurations.

Consider the geometry depicted, Fig. 3, where OX is the axis from the source to the point at which the dose rate is to be determined, OC is the axis from the source to the crew compartment (the axis of symmetry of the reactor-shield assembly) and OP is the axis from the source to an arbitrary point on the shield surface. As in the case of cylindrical symmetry, let α be the angle between OX and OP and define the additional angle ψ necessary to describe OP in this system as the angle between the perpendicular line from P to OX and the plane containing OC and OX.

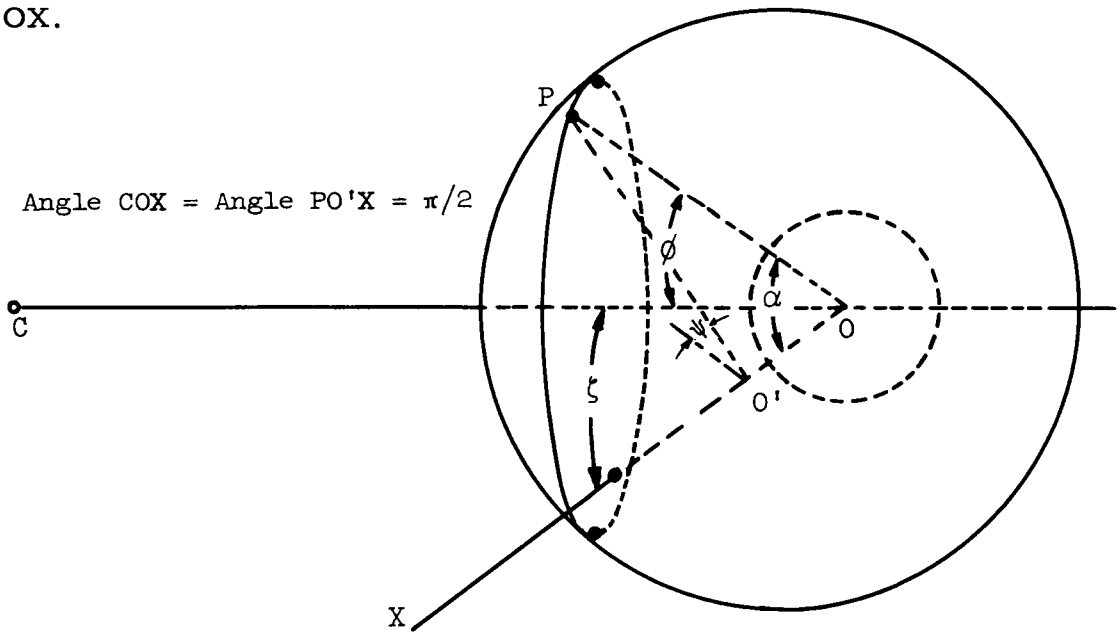

Fig. 3: Geometry for Asymmetric Calculations

Since it is necessary to determine the shield dimensions along the OP axis, the angle between the OP axis and the OC axis is represented by ϕ , and the angle between the OC and OX axis is represented by ζ . It may easily be shown geometrically that:

$$\phi = \arccos\,[\cos\alpha\cos\zeta + \sin\alpha\cos\psi\sin\zeta] \tag{21}$$

Since when $\zeta = 0$, $\alpha = \phi$, the shield dimensions along OP may be determined from those calculated in designing the shield by measuring the values of shield material thicknesses along values of the polar angle (α in the original case) equal to values of ϕ given as solutions to the above equation.

Whereas an integration over the angle here represented by ψ was implicit in Eq. (1) (for there, from symmetry, this integration only introduced a factor 2π), in the asymmetrical case the integration must be performed over both α and ψ . If the shield is cylindrically symmetric however, the integration may be performed in the interval $0 \leq \psi \leq \pi$ and the result doubled.

Denoting values of ψ by the subscript ℓ, i.e. $Z_{\ell k} \equiv$ the value of Z at α_k, ψ_ℓ in the coordinate system of Fig. 3, Eqs. (16), (17) and (20) become:

$$D_{\gamma,s}(a,\ \zeta) = \frac{2n_\gamma}{a} \sum_{k=0}^{M_\gamma} (\Delta\alpha)_k\ \Gamma\ (\alpha_k,\ \bar{E}) \sum_{\ell=0}^{M'_\gamma} g_{\ell k}\ m^{\gamma}_{\ell k} (\Delta\psi)_\ell\ (Z_{\ell k} + R_c) \tag{22}$$

$$D_{n,s}(a,\ \zeta) = \frac{n_n \sigma_s(\bar{E})}{2\pi} \sum_{k=0}^{M_n} (\Delta\alpha)_k\ (\pi - \alpha_k) \sum_{\ell=0}^{M'_n} f_{\ell k}\ m^{n}_{\ell k}\ (\Delta\psi)_\ell\ (Z_{\ell k} + R_c) \tag{23}$$

$$D_n^{\ell,k}(a') = \frac{m_{\ell k}\, f_{\ell k}}{2\pi\, a^2} (Z_{\ell k} + R_c) \left[\frac{a\, \Sigma_s(\bar{E})\, (\Delta\alpha)_k\, (\pi - \alpha_k)}{2} + \Delta \cos^{11} \alpha_k \right] (\Delta\psi)_\ell$$

where, now (24)

$$D_n(a) = \sum_{k=0}^{M} \sum_{\ell=0}^{M'} D_n^{\ell,k}(a)$$

and

$$\sum_{\ell=0}^{M'_\gamma} (\Delta\psi)_\ell = \sum_{\ell=0}^{M'_n} (\Delta\psi)_\ell = \sum_{\ell=0}^{M'} (\Delta\psi)_\ell = \pi$$

IV. OPTIMIZATION CRITERIA

Because of the reduced number of parameters, the optimization of a unit shield may be undertaken at this time with some assurance of success, while the optimization of a divided shield is still a very difficult undertaking (availability of data for both cases assumed).

Since it has been shown (Ref 8) that total shield thicknesses required for neutron shielding are, for reasonably thick hydrogenous layers, independent of thicknesses of gamma shielding, but not vice-versa, consider first a unit shield such as the neutron shielding for the CFR studied in this report. Let the total dose rate in the crew compartment of a given type (neutron dose rate in this case) be specified by radiological requirements and let this quantity be represented by D_n. Assume that it has been possible to describe the contribution to the dose rate D_n arising from each of a number of slices of the reactor-shield assembly (for this case, see Eq. 20). Let the contribution of the kth slice to D_n be designated D_k and further assume that the functional relationship between each D_k and the shield dimensions characteristic of the kth slice has been specified. Then, in order to determine the optimum thickness of shielding for each slice required to reduce the total radiation reaching the crew compartment to the desired level D_n, suppose that through a given small area A_k on a shield surface there is a flux Φ_k which may, in general, be either a particulate or energy flux. The contribution of this flux to the dose rate in the crew compartment is given by $D_k = K_k \Phi_k$ where $\underline{K}$ converts from energy or particle flux to dose rate and contains all the factors which may affect the radiation between the shield and the crew compartment. Thus, neglecting the dependence of the energy spectrum of $\underline{\Phi}$ on shield thickness, K_k is a function only of the coordinate system describing the source-receiver geometry.

If a small thickness of shielding $(\Delta t)_k$ is added, the contribution to the dose rate is changed by an amount

$$(\Delta D)_k = K_k \, (\Delta \Phi)_k = K_k \nu' \Phi_k \, (\Delta t)_k$$

where $\underline{\nu}'$ is the macroscopic removal coefficient of the shielding for the type of radiation being considered.

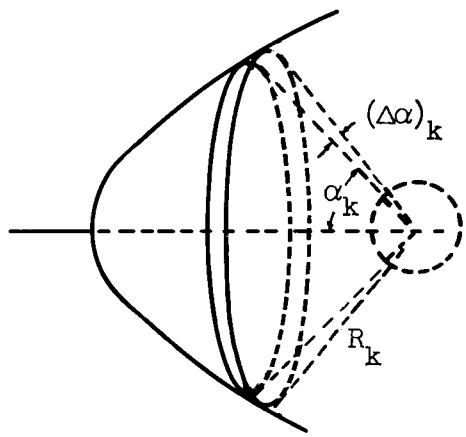

Fig. 4: Shield Optimization Geometry

Assuming that the reactor-shield configuration has cylindrical symmetry with respect to the source-receiver axis and that the configuration can be generated from spherical sectors, consider the condition depicted in Fig. 4 where the shield has been divided into spherical sectors by increasing $\underline{\alpha}$ in steps $(\Delta\alpha)_k$ (here the spherical sector is defined as that region lying between α_k and $\alpha_k + (\Delta\alpha)_k$) and thus:

$$A_k = 2\pi R_k^2 \sin\left[\alpha_k + \frac{(\Delta\alpha)_k}{2}\right](\Delta\alpha)_k$$

The weight added to this area by adding a thickness $(\Delta t)_k$ is

$$(\Delta W)_k = \rho(\Delta V)_k = \rho A_k\,(\Delta t)_k = \rho 2\pi\, R_k^2 \sin\left[\alpha_k + \frac{(\Delta\alpha)_k}{2}\right](\Delta t)_k$$

and the efficiency of the added shielding is, then:

$$\left(\frac{\Delta D}{\Delta W}\right)_k = \frac{K_k \nu' \Phi_k}{\rho\ A_k}$$

Eliminating K_k :

$$\left(\frac{\Delta D}{\Delta W}\right)_k = \frac{\nu' D_k}{2\pi\rho R_k^2 \sin\left[\alpha_k + \frac{(\Delta\alpha)_k}{2}\right](\Delta\alpha)_k} \tag{25}$$

A smaller $\frac{\Delta D}{\Delta W}$ in one place than in another indicates that the weight could be used more effectively in the second location. Therefore, $\Delta D/\Delta W$ should be constant for the most efficient shield.

Shield thicknesses may be calculated, using LT data and Eq. (20), such that:

$$\frac{D_k}{R_k^2 \sin\left[\alpha_k + \frac{(\Delta\alpha)_k}{2}\right](\Delta\alpha)_k} = \text{constant}, \tag{26}$$

if $\underline{\nu}$ is constant over the range of shield thicknesses used,

where

$$\sum_k D_k = D_n \tag{27}$$

Since D_k varies much more rapidly than R_k, R_k may be assumed constant for the first iteration and successively better values found in successive iterations.

Optimization of a divided shield may, in the very special case of the gamma shielding for the CFR studied in this report, be simplified by making the following assumptions:

i) The entire reactor gamma shield is determined solely by the scattered dose, Eq. (16), subject to the limitations placed on gamma shielding thickness by secondary effects (Ref 9).

ii) The crew compartment shield may be a simple slab placed across the rear bulkhead of the crew compartment of sufficient thickness to attenuate the direct beam from the reactor and the contribution from sources outside the reactor (e.g., activated NaK), plus a 1/8" lead shield around the remainder of the crew compartment. This thin lead shield is deemed the minimum crew compartment shield adequate to attenuate unaccounted-for soft gamma radiation.

Although these assumptions prohibit the generation of the minimum weight divided gamma shield, they assure the generation of the most nearly unit shield practicable. While neglecting the attenuation of scattered gammas by the thick lead slab at the rear bulkhead of the crew compartment results in only a slight overestimate of the dose rate in the crew compartment, neglecting the effect of the lead on the sides of the crew compartment might result in a gross overestimate of the dose rate and consequently in an overestimate of the required shield weight. Therefore, the factor $C(E, \theta, \beta, b)$ in Eq. (2) has been reinserted and a new scattering function $\Gamma'(\alpha, \bar{E}, b)$ determined, where

$$\Gamma'(\alpha, \bar{E}, b) = \Gamma(\alpha, \bar{E})\ \bar{C}(\alpha, \bar{E}, b)$$

where $\underline{\overline{C}}$ is the average value of $\underline{C}$ over the integration over $\underline{\theta}$. The quantity $\underline{\overline{C}}$ may be determined by cross-plotting data generated by NDA (Ref 10). It should be noted that the only difference remaining between the scattering function used in these calculations and the function generated at ORNL (Ref 2) is the omission herein of the air absorption term, justified as a compensation for multiple scattering effects (see Fig. 5).

To proceed, let the total dose rate allowable in the crew compartment, specified by radiological requirements, be denoted by D_γ. Write the direct and the scattered components of D_γ as follows:

$$D_{\gamma,\ d} = fD_\gamma \tag{28a}$$

$$D_{\gamma,\ s} = (1 - f)\ D_\gamma \tag{28b}$$

where d and s, as subscripts, denote direct and scattered portions of the dose rate, respectively, and f, the fraction of the dose rate in the crew compartment due to direct beams from the reactor and external sources, is the parameter of optimization.

Since the neutron shielding configuration has already been determined, the required reactor gamma shielding may be calculated by application of Equations (16) and (28b) for any selected value of f.

The direct contribution to the dose rate received in an unshielded crew compartment is composed of two parts; D_r, which is the component due to direct radiation from the reactor, is completely specified since the reactor shielding configuration is known and D_{ex}, the component due to external sources, presumably may be calculated. The attenuation required at the rear surface of the crew compartment may be calculated as follows:

$$\delta = \frac{D_{\gamma,\ d}}{D_r + D_{ex}}$$

where δ is the required attenuation factor. The thickness of shielding required to produce this attenuation may be calculated using gamma absorption coefficients and buildup factors.

Finally, the combined weight of the reactor and crew compartment gamma shielding may be computed for various values of the parameter f and the optimum value selected.

V. SALIENT ASSUMPTIONS

1) Reactor and shield form an infinite homogeneous medium.

2) Effective surface sources are isotropic (the errors introduced hereby will not be small unless: (a) the source-receiver distance is large with respect to the effective radius of the source and (b) the source is practically opaque to the radiation).

3) Attenuation over a small distance in the "infinite homogeneous medium" is practically exponential.

4) Shield leakage consists only of 5 MeV neutrons, thermal neutrons and 3.066 MeV gammas.

5) Isotropic and Klein-Nishina scattering in air of neutrons and gammas, respectively.

6) Contribution to dose rate from multiple scattering is compensated by absorption of radiation in air.

7) Factor for converting to dose rate from energy flux and particle number flux is independent of gamma ray and neutron energy, respectively.

8) Negligible degradation of neutron energy upon scattering interaction with oxygen or nitrogen.

9) Inverse square attenuation in air is valid all the way to the surface of the shield.

10) When estimating the material correction, scattering in the shield may be neglected.

11) Neutron attenuation in gamma shielding is equivalent to that in neutron shielding for sufficiently large hydrogenous backing. (This allows calculation of the neutron shield shape independent of the gamma shielding.)

12) Reactor-shield system is symmetrical about the source-receiver axis.

13) Crew compartment focusing effect may be neglected.

14) Relaxation length of primary radiation observed in the Lid Tank is applicable to neutrons or gammas.

15) Number of scattering nuclei and electrons in air vary as the density of air.

16) Shield leakage distributions are radial for direct gamma rays and scattered neutrons and gamma rays.

17) Shield leakage distribution is proportional to tenth power of cosine for direct neutrons.

VI. GAMMA SCATTERING

Eq. (7) is integrated in this chapter.

Klein and Nishina (Ref 11) derived the following expression for the differential cross section per unit solid angle for the scattered gamma rays in various directions (θ):

$$\frac{d\sigma(\theta, E)}{d\Omega} = \frac{1}{2\pi \sin\theta} \frac{d\sigma(\theta, E)}{d\theta} = C_o \left(\frac{E'}{E}\right)^2 \left(\frac{E}{E'} + \frac{E'}{E} - \sin^2\theta\right) \tag{29}$$

where $E' = E'(\theta, E)$ is given by the Compton equation for the energy of the degraded gamma ray. With reference to Eqs. (3) and (29), Eq. (7) may be written

$$\Gamma(\alpha, \bar{E}) = C_o (\Gamma_1 + \Gamma_2 + \Gamma_3) \tag{30}$$

where

$$\Gamma_1 \equiv \int_{\theta=\alpha}^{\pi} \frac{d\theta}{(C_1 - k\cos\theta)^2} \qquad \Gamma_2 \equiv \int_{\theta=\alpha}^{\pi} \frac{d\theta}{(C_1 - k\cos\theta)^4}$$

$$\Gamma_3 \equiv -\int_{\theta=\alpha}^{\pi} \frac{\sin^2\theta \, d\theta}{(C_1 - k\cos\theta)^3}, \quad C_1 \equiv 1 + k, \qquad K = \bar{E}/mc^2$$

Consider Γ_1, letting $x = \tan\frac{\theta}{2}$: $\theta = 2\tan^{-1} x \quad \cos\theta = \frac{1 - x^2}{1 + x^2}$

$$\Gamma_1 = \Gamma_{1,1} + \Gamma_{1,2} \tag{31}$$

where

$$\Gamma_{1,\,1} \equiv 2 \int_{X_1}^{X_2} \frac{dX}{(A + BX^2)^2} \qquad \Gamma_{1,\,2} \equiv 2 \int_{X_1}^{X_2} \frac{X^2 dX}{(A + BX^2)^2}$$

$$A \equiv C_1 - k = 1 + k - k = 1$$

$$B \equiv C_1 + k = 1 + 2k$$

By a reduction formula it may be shown that

$$\Gamma_{1,\,1} = \frac{X}{A(A + BX^2)} \int_{X_1}^{X_2} + \frac{1}{A} \int_{X_1}^{X_2} \frac{dX}{A + BX^2}$$

$$= \left[\frac{X}{A(A + BX^2)} + \frac{1}{A\sqrt{A\,B}} \tan^{-1}\left(\sqrt{\frac{B}{A}}\, X\right) \right]_{X_1}^{X_2}$$

$$= \frac{\pi}{2\sqrt{B}} - \frac{\tan\alpha'}{\xi'} - \frac{1}{\sqrt{B}} \tan^{-1}(\sqrt{B}\ \tan\alpha')$$

where

$$\alpha' \equiv \frac{\alpha}{2} \qquad \xi' \equiv 1 + B\tan^2\frac{\alpha}{2}$$

then, integration by parts and application of a reduction formula yields

$$\Gamma_{1,\,2} = \frac{\pi}{2B^{3/2}} + \frac{\tan\alpha'}{B\xi'} - \frac{1}{B^{3/2}} \tan^{-1}(\sqrt{B}\ \tan\alpha')$$

Hence, Eq. (31) may be written

$$\Gamma_1 = \frac{\pi(1 + k)}{B^{3/2}} - \frac{2k\tan\alpha'}{B\xi'} - \frac{2(1 + k)}{B^{3/2}} \tan^{-1}(\sqrt{B}\ \tan\alpha') \qquad (32)$$

Consider Γ_2, letting $x = \tan \theta/2$:

$$\Gamma_2 = \Gamma_{2,\,1} + \Gamma_{2,\,2} + \Gamma_{2,\,3} + \Gamma_{2,\,4} \tag{33}$$

where

$$\Gamma_{2,\,1} \equiv 2 \int_{X_1}^{X_2} \frac{dX}{(A + BX^2)^4} \qquad \Gamma_{2,2} \equiv 6 \int_{X_1}^{X_2} \frac{X^2 dX}{(A + BX^2)^4}$$

$$\Gamma_{2,\,3} \equiv 6 \int_{X_1}^{X_2} \frac{X^4 dX}{(A + BX^2)^4} \qquad \Gamma_{2,\,4} \equiv 2 \int_{X_1}^{X_2} \frac{X^6 dX}{(A + BX^2)^4}$$

By repeated application of a reduction formula it may be shown that

$$\Gamma_{2,\,1} = \frac{\pi}{2\sqrt{B}} - \frac{\tan \alpha'}{3\xi'^3} - \frac{5 \tan \alpha'}{12\xi'^2} - \frac{5 \tan \alpha'}{8\xi'} - \frac{1}{\sqrt{B}} \tan^{-1}(\sqrt{B} \tan \alpha')$$

Integration by parts and application of a reduction formula shows that

$$\Gamma_{2,\,2} = \frac{6 \tan \alpha'}{B\xi'^3} + \frac{3}{5B} \Gamma_{2,\,1}$$

Similarly,

$$\Gamma_{2,\,3} = \frac{2 \tan^3 \alpha'}{B\xi'^3} + \frac{1}{B} \Gamma_{2,\,2}$$

Similarly,

$$\Gamma_{2,\,4} = \frac{2 \tan^5 \alpha'}{B\xi'^3} + \frac{5}{3B} \Gamma_{2,\,3}$$

Hence, Eq. (33) may be written

$$\Gamma_2 = \frac{2}{B\xi'^3} \tan^5 \alpha' + \frac{2}{B\xi'^3}\left(1 + \frac{5}{3B}\right) \tan^3 \alpha' + \frac{6}{B\xi'^3}\left(1 + \frac{1}{B} + \frac{5}{3B^2}\right)\tan \alpha'$$

$$+ \left(1 + \frac{3}{5B} + \frac{3}{5B^2} + \frac{1}{B^3}\right) \Gamma_{2,\,1} \tag{34}$$

Consider Γ_3, letting $x = \tan \theta/2$:

$$\Gamma_3 \equiv \frac{-\pi}{2B^{3/2}} + \frac{2 \tan^3 \alpha'}{\xi'^2} - \frac{\tan \alpha'}{B\xi'} + \frac{1}{B^{3/2}} \tan^{-1}(\sqrt{B} \tan \alpha') \tag{35}$$

Therefore, Eq. (30) for a given $\bar{E}$ is simply the sum of the right sides of Eqs. (32), (34) and (35). The function $\Gamma(\alpha,\bar{E})$ for $\bar{E}$ = 3.066 MeV (k = 6) is tabulated in Table 1 and plotted in Fig. 5.

AIR SCATTERING PROBABILITY

TABLE 1

α	$\Gamma(\alpha,\bar{E})/C_o$	$\Gamma(\alpha,\bar{E})$
0°	.89318	3.50×10^{-26}
10	.55662	2.18
20	.32901	1.29
30	.21187	.831
40	.14389	.564
50	.09901	.388
60	.08085	.317
70	.06283	.246
80	.05280	.207
90	.04368	.171
100	.03691	.145
110	.03021	.118
120	.02463	.0965
130	.01992	.0781
140	.01543	.0605
150	.01134	.0445
160	.00745	.0292
170	.00370	.0145
180	.00000	.0000

where $\bar{E}$ = 3.066 MeV

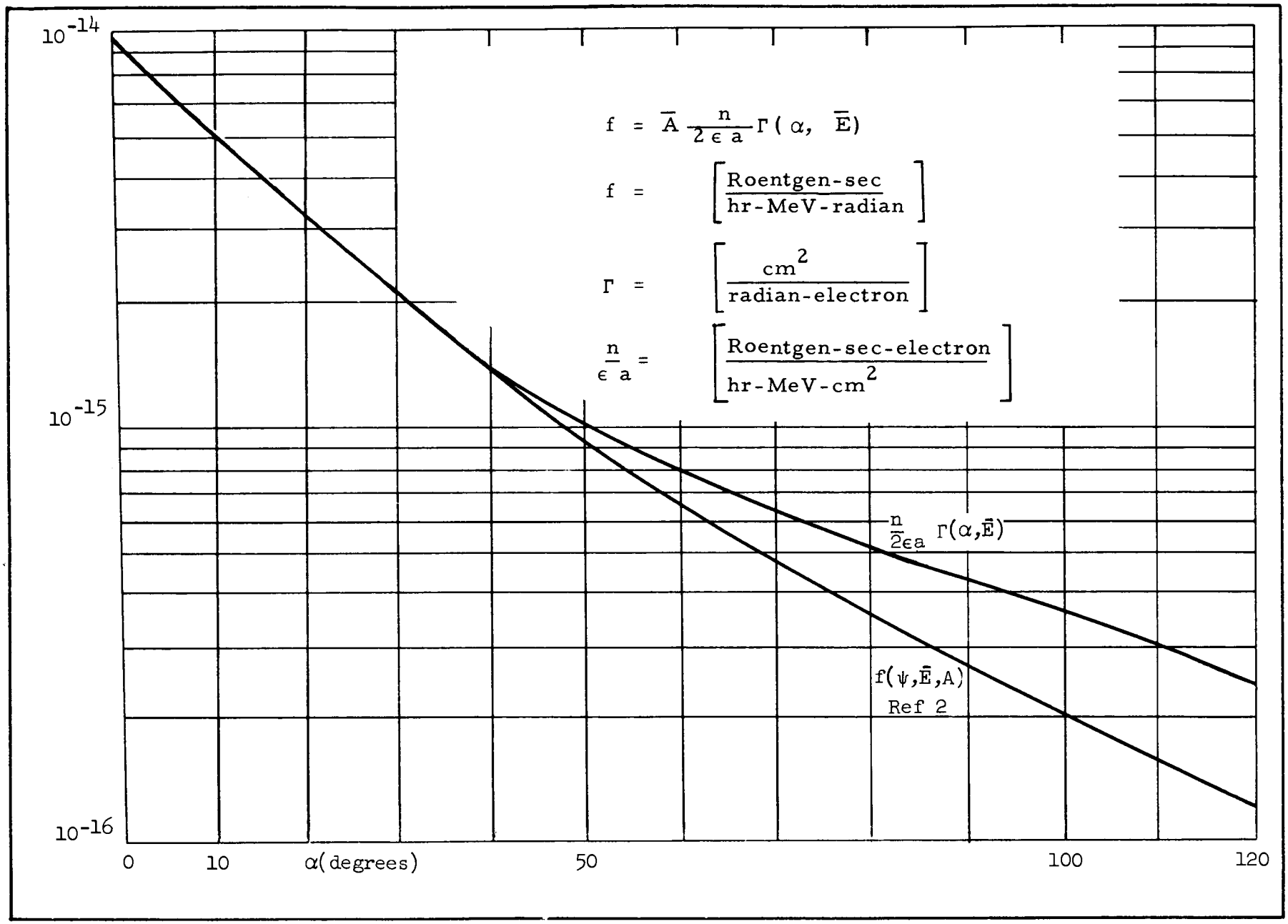

Fig. 5. AIR SCATTERING PROBABILITY FUNCTIONS

VII. REFERENCES

1 "Aircraft Shielding Handbook," Scheduled for publication in July 1957, and "Aircraft Shielding Handbook, (second rough draft)", NARF 55-79T (Convair, Scheduled for publication in December, 1955. SECRET-RESTRICTED DATA

2 E. P. Blizard and H. Goldstein, Editors, "Report of the 1953 Summer Shielding Session," ORNL 1575 (July 12, 1954). SECRET-RESTRICTED DATA

3 B. P. Leonard et al., Private communication (March 1955)

4 A. Simon and R. H. Ritchie, "Background Calculations for the Proposed Tower Shielding Facility," ORNL 1273, Appendix B (November 3, 1952). SECRET-RESTRICTED DATA

5 F. C. Maienschein, "Gamma Ray Spectral Measurements with the Divided Shield Mockup," ORNL CF-52-3-1 (March 3, 1952). SECRET-RESTRICTED DATA

6 B. T. Feld, H. Feschbach, M. L. Goldberger, H. Goldstein, and V. F. Weisskopf, "Final Report of the Fast-Neutron Data Project," NYO 636, Section III (January 31, 1951). SECRET-RESTRICTED DATA

7 J. E. Van Hoomissen, G. J. Rausa and others at the TSF, Private communications (August - November, 1955). SECRET-RESTRICTED DATA

8 F. H. Abernathy et al. at the LTF, "Lid Tank Shielding Tests for the Reflector Moderated Reactor," ORNL 1616 (December, 1954). SECRET-RESTRICTED DATA

9 A. W. Savolainen, Editor, "Aircraft Nuclear Propulsion Project, Quarterly Progress Report," ORNL 1896 (July 28, 1955). SECRET-RESTRICTED DATA

10 H. Goldstein, "Air Scattering of Gamma Rays and Neutrons," NDA Memo 12-3, April 20, 1953 (also appears as chapter 2.9 of "The Reactor Handbook, Volume I"). SECRET-RESTRICTED DATA

11 O. Klein and Y. Nishina, Z. Physik, 52, 853 (1929). UNCLASSIFIED

SECRET

Paper III-E

SHIELD DESIGN STUDY FOR A CIRCULATING-FUEL REACTOR UTILIZING A FUEL-TO-AIR RADIATOR

L. B. Holland
S. K. Penny
D. K. Trubey

SECRET

RESTRICTED DATA

"This document contains restricted data as defined in the Atomic Energy Act of 1954. Its transmittal or the disclosure of its contents in any manner to an unauthorized person is prohibited."

[redacted]

SHIELD DESIGN STUDY FOR A CIRCULATING-FUEL REACTOR UTILIZING A FUEL-TO-AIR RADIATOR

L. B. Holland S. K. Penny
D. K. Trubey

The preliminary shielding study for a 300-Mw circulating fuel aircraft reactor system employing a direct fuel-to-air heat exchanger was completed. Both a wraparound and a tandem heat exchanger arrangement were considered, but no attempt was made to design a heat exchanger or air ducts or to evaluate the increased efficiency for a fuel-to-air heat exchanger system. Divided shield weights were determined for the condition of 1 rem/hr in the crew compartment and 1,000 rep/hr at 50 ft from the reactor. For the wraparound heat exchanger, the total weight was 115,400 lb; for the tandem arrangement the weight was 121,200 lb. When the dose rate for radiation damage and activation was permitted to increase to 100,000 rep/hr at 50 ft from the shielded reactor, the total weights were reduced to 94,700 and 85,700 lb, respectively.

Since the limiting feature of a nuclear powered aircraft system is the weight of the reactor and crew compartment shield, some knowledge of the weight is desirable before a complete investigation of a new system is attempted. A circulating-fuel reactor utilizing a direct fuel-to-air radiator has been considered previously[1] but has been rejected on the assumption that the shield weight would be excessive. There is a possibility, however, that an increase in efficiency and reliability might offset the increase in shield weight; therefore, a shielding study was carried out to determine the feasibility of a more thorough investigation of this type of a system.

Two fuel-to-air radiator configurations were considered in the study. The first configuration employed the standard circulating-fuel wraparound radiator, while the second one consisted of a tandem arrangement of the reactor and radiator. Weights for each arrangement were determined for a total radiation damage limitation of 1,000 and 100,000 rep/hr at 50 ft.

[redacted]

[redacted]

REACTOR, RADIATOR, AND CREW COMPARTMENT

The reactor was assumed to be a 28.5-in.-dia circulating-fuel reflector-moderated reactor with an 8-in.-thick beryllium reflector. It was felt that this reflector thickness was sufficient since there was no NaK activation problem and criticality would not be greatly affected. The reactor dimensions and weights are shown in Tables 1 and 2 respectively.

The radiator volume was estimated to be 200 ft^3,* which included an allowance for the ducting that was not designed into the shield. Design data for a sodium-to-air radiator previously reported[2] were used to determine the volume fractions of the various materials in the radiator, although the selection of materials differed somewhat. In this study Inconel tubes were needed to contain the fuel fluorides, and it was felt that copper fins with stainless steel cladding would give the best performance. The following radiator specifications were assumed:

Fins	
Number per inch	15
Thickness	0.010 in.
Inconel tubes	
Outside diameter	0.1875 in.
Wall thickness	0.015 in.
Spacing (square array)	0.667
Density	98 lb/ft^3 (a)

The volume fractions of the materials in the section of the radiator that contained the fins were determined as follows:

Stainless steel	0.0750
Copper	0.0750
Inconel	0.0287
Fuel	0.0333
Air	0.7880
	1.000

At 3 Mev these volume fractions yield a value of 0.0567 cm^{-1} for the gamma-ray total absorption coefficient.

In order to estimate the gamma-ray flux originating in the heat exchanger, the fraction of the total fuel in the radiator had to be specified. If 3/4 of the 200 ft^3 volume is occupied by fins, the fuel volume is 5 ft^3 (150 ft^3 x 0.0333). The headers were assumed to contain an equal amount.

---

a. A. P. Fraas, private communication.

[redacted]

[redacted]

Table I

Dimensions of Circulating-Fuel Reactor
with Fuel-to-Air Radiator

Reactor Region	Thickness (in.)	Inner Radius (in.)	
		Tandem	Wraparound
Beryllium island	4.0		
Outer sodium annulus of island	0.187	4.0	4.0
Core cladding (Inconel) of island	0.125	4.187	4.187
Core	9.938	4.312	4.312
Inner cladding (Inconel) of beryllium reflector	0.156	14.250	14.250
Inner sodium annulus of reflector	0.187	14.406	14.406
Reflector	8.000	14.593	14.593
Outer sodium passage of reflector	0.066	22.593	22.593
Outer cladding (Inconel) of reflector	0.010	22.659	22.659
Inner cladding (Inconel X) on B_4C-Cu sintered layer	0.01	22.669	22.669
B_4C-Cu sintered layer	0.20	22.679	22.679
Outer cladding (Inconel X) on sintered layer	0.01	22.879	22.879
Sodium passage	0.066	22.889	22.889
Air radiator (including Inconel shells on inside and outside)	23.195		22.955
Thermal shield	1.000	22.955	46.150
Sodium cooling layer	0.035	23.95	47.150
Pressure shell	1.00	23.990	47.185
Insulation	0.250	24.990	48.185
Outer cladding (Inconel X) on insulation	0.032	25.240	48.435

[redacted]

[redacted]

TABLE II

Weights of Circulating-Fuel Reactor* with Fuel-to-Air Radiator

Reactor Region	Weight (lb)	
	Tandem	Wraparound
Inconel	5,870	18,780
Sodium	70	70
Radiator	20,150	20,150
Beryllium	2,430	2,430
Insulation	220	220
Miscellaneous**	2,780	2,780
Total	31,520	44,430

*Spherical shells assumed for calculation.
**Decking, ducting, and expansion tanks, 500 lb; two sodium pumps and drives, 1100 lb; two fuel pumps and drives, 1080 lb; control rod and island support, 100 lb.

[redacted]

[redacted]

DOSE RATE CRITERIA

For this study the permissible total crew compartment dose rate was 1 rem/hr with a gamma-ray--to--neutron ratio of 3 to 1. Since the current radiation damage criterion being used at the Laboratory specified that the total dose rate at 50 ft from the reactor cannot exceed 1,000 rep/hr, shield weights were calculated for this limitation. In addition, weights were calculated for a total dose rate of 100,000 rep/hr at 50 ft. An arbitrary upper limit of the total neutron dose rate at 50 ft was set at 100 rem/hr because of uncertainties in neutron capture in air and neutron activation of structural members. A lower limit of 1/8 in. of lead on the crew compartment was used to compensate for the buildup of soft gamma radiation in the crew compartment plastic.

In the case of the tandem radiator, an arbitrary ratio of the total dose rate from the sides of the radiator and the reactor had to be set because of the uncertainties in the calculation of this ratio for minimum shield weight. The ratio chosen was that of the projected areas of the radiator and reactor.

SHIELD DESIGN FOR CFR WITH WRAPAROUND RADIATOR

The thickness of the wraparound radiator was required by its volume limitation of 200 ft^3 to be 23 in. Since the system is spherical, the shield design was inherently similar to the present RMR design and the methods applied to that reactor could be used.

Neutron Shield. The neutron shield was designed first on the usual assumption that substitution of gamma-ray shielding for some of the neutron shielding would not affect the neutron dose rate since the removal cross section of lead is nearly that of water. This does introduce some error when the neutron shielding is thin. In the design the contribution to the dose rate by delayed neutrons was assumed to be negligible since the radiator and water thicknesses were large.

The design utilized the TSF neutron shield optimization procedure[3] with an assumed $\cos^{10}$ angular distribution of neutrons at the shield surface. The procedure was modified somewhat as shown in another paper (S. K. Penny, "Modification of the Procedure for Using TSF Data for the Optimization of a Divided Neutron Shield", this report). The neutron dose rate used in the procedure was the dose rate a distance (d) of 64 ft from the center of the reactor as a function of water thickness around the reactor. This dose rate was calculated from LTSF CFRMR mockup data[4] as follows:

$$D_R(64\ \text{ft}) = D_{LT}(z)H(a,z)\,\frac{r_c r_s}{d^2}\,\frac{\sigma_R}{\sigma_{LT}}\,C_{HX}C_R$$

[redacted]

where

D_R = neutron dose rate at a distance d from the reactor,

D_{LT} = neutron dose rate at a distance z from the LTSF source plate,

$H(a,z)$ = Hurwitz correction (a = radius of LTSF source plate),

r_c = reactor core radius,

r_s = reactor shield radius,

σ_R = reactor surface source strength,

σ_{LT} = LTSF surface source strength,

C_{HX} = correction for substitution of the reactor radiator for the LTSF heat exchanger mockup on the basis of removal cross sections,

C_R = correction for substitution of the reactor materials, other than for the radiator and reflector, for similar materials in the LTSF mockup on the basis of removal cross sections.

The neutron shield (Table III and Fig. 1) designed by the above procedure allowed the 0.25 rem/hr neutron dose rate specified for the crew compartment and thus was the same for both the 10^3 and 10^5 rep/hr cases. The optimization indicated that no neutron shielding was required on the rear of the reactor. However, the water thickness around the reactor was not allowed to fall below 20 cm in order to prevent the total neutron dose rate at any point 50 ft from the reactor from exceeding the specified 100 rem/hr.

Gamma-Ray Shield. The gamma-ray shield was determined using experimental data from the LTSF CFRMR mockup tests and the optimization procedure described elsewhere (H. C. Woodsum, "Procedure for the Optimization of a Divided Gamma-Ray Shield for Circulating-Fuel Reactors", ANP Quarterly Progress Report, March 10, 1956, ORNL-2061). To maintain a total dose rate of 10^3 rep/hr at 50 ft it was necessary to design both a basic lead shield and a shadow shield. For the 10^5 rep/hr case, however, only the shadow shield was required since the reactor with no shielding only yielded 4.2×10^4 rep/hr at 50 ft.

In the determination of the dose rate to be used in the optimization procedure it was necessary to consider two sources of radiation -- primary and fission-product decay gamma rays. The primary gamma-ray dose rate was calculated using the following expression:

[redacted]

[redacted]

2-01-059-62

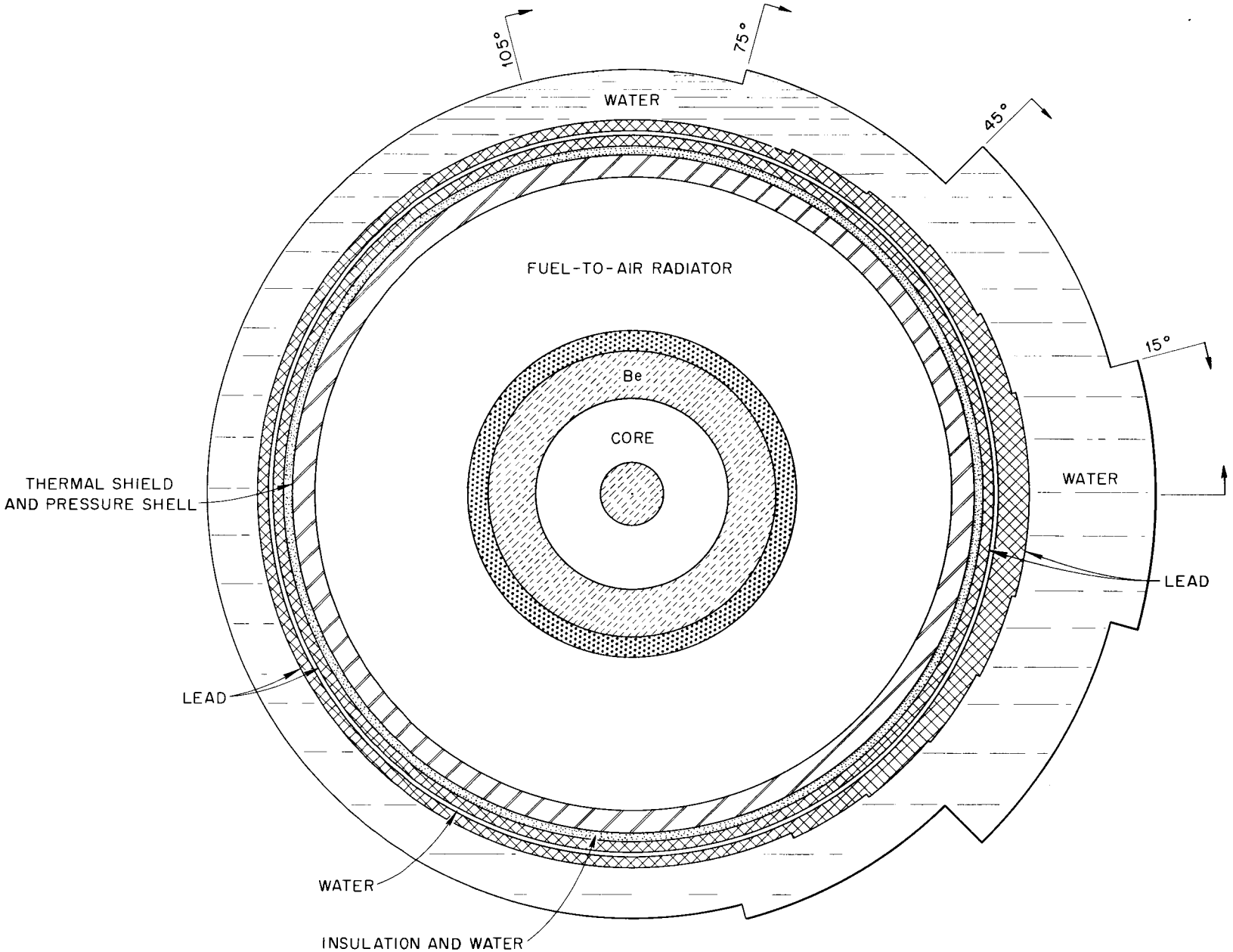

Fig. 1. Shield for a Circulating-Fuel Reactor with a Wraparound Fuel-to-Air Radiator.

[redacted]

TABLE III

Thickness of Total Neutron Shield for CFR
with Wraparound Radiator

Dose rate: 10^3 or 10^5 rep/hr at 50 ft

Shield Section	Shield Thickness (in.)
Reactor (water)	
θ* = 0 to 15 deg	19.3
θ = 15 to 45 deg	15.6
θ = 45 to 75 deg	9.1
θ = 75 to 105 deg	5.8**
θ = 105 to 180 deg	0 *
Crew Compartment (plastic)	
Side	8.3
Front	8.3
Rear	17.3

** Augmented to 7.9 in. as a safety factor.

* Polar angle increment.

[redacted]

[redacted]

$$D_P = \frac{r_c r_s}{d^2} \frac{P_R/4\pi r_c^2}{P_{LT}/\pi a^2} H(a,z) D_{P,LT}(z) C_{HX} C_R$$

where

D_P = primary gamma-ray dose rate at a distance d from the radiator,

P_R = power of the reactor,

P_{LT} = power of the LTSF source plate,

$H(a,z)$ = conversion from finite disk to infinite plane source

$$= \frac{E_1(\mu z)}{E_1(\mu z) - E_1(\mu\sqrt{z^2 + a^2})}$$

$$E_1(x) = \int_x^\infty \frac{e^{-y}}{y}\, dy$$

μ = effective linear absorption coefficient for the reactor shielding materials based on a gamma-ray energy of 6 to 8 Mev,

$D_{P,LT}$ = primary gamma-ray dose rate at distance z from the LTSF source plate,

C_{HX}, C_R = corrections as defined previously except they are based on an effective linear absorption coefficient for a gamma-ray energy of 6 to 8 Mev.

The fission-product decay gamma-ray dose rate was computed as follows:

$$D_{HX} = N v_f \frac{P_R}{V_f} \frac{r_{HX_o} r_s}{d^2} \lambda(\bar{E}) \int_0^\infty \frac{B(\mu t) E_1(\mu t) N(E)\, dE}{2\, c(E)}$$

where

$N = 3.1 \times 10^{10}$ fissions/sec-watt,

D_{HX} = fission-product decay gamma-ray dose rate at distance d from the reactor,

v_f = volume fraction of the radiator that contains fuel,

V_f = total volume of fuel in system,

r_{HX_o} = outside radius of the radiator,

$\lambda(E)$ = effective mean free path of the radiator based on a gamma-ray energy of 2.7 Mev,

[redacted]

[redacted]

μt = number of mean free paths of lead and water shielding as well as Inconel (shells) outside the radiator for gamma rays of energy E,

$B(\mu t)$ = dose buildup factor for ut mean free paths,

$N(E)$ = number of photons per fission of energy E per unit energy interval

$= 7e^{-1.2E}$,

$c(E)$ = flux-to-dose conversion factor.

The optimization procedure mentioned above assumes the lead shadow shield to be tapered by a 12.5-deg relaxation angle coupled with a disadvantage angle of 15 deg. This permits the dose rate emission per unit polar angle to increase exponentially to compensate for the exponential decrease in the probability of scattered radiation penetrating the crew compartment sides. The tapering is based on a gamma-ray energy of 6.8 Mev.

The basic lead shield required to maintain 10^3 rep/hr at a distance of 50 ft is given in Table IV. This shield plus the shadow shield was divided so that lead and water shield layers could be alternated to cool the lead and to suppress capture gamma-ray production in the lead. For the 10^3-rep/hr case there was first an annulus of water 0.375 in. thick. The rest of the lead varied with polar angle. For the 10^5-rep/hr case, where only the shadow shield was required, the lead was separated from the radiator by a water thickness of 0.375 in. The variation with polar angle for the two cases is shown in Table V and Fig. 2.

SHIELD DESIGN FOR CRR WITH TANDEM RADIATOR

The arrangement for the fuel-to-air radiator in tandem with the reactor is shown in Fig. 2. It was assumed that a reasonable radiator shape would be a 6-ft-dia cylinder 7 ft long. The reactor acts as a shield at one end. The shield around the remainder of the radiator was assumed to be a shell with no penetrating holes. The resulting total weight for this idealized system might be considered a lower limit. However, it must be remembered that the total shield weight was based on a radiator volume that allowed for ducting and that it also included patch weights. Thus two major problems were left unexplored -- radiator design and duct design.

Reactor Shielding. As for the wraparound radiator design, the shielding on the reactor was determined by the comparison method. The most recent LTSF data were employed, correcting for the attenuation by the radiator by using neutron removal cross section and gamma-ray absorption coefficients. It was

[redacted]

[redacted]
2-01-059-71

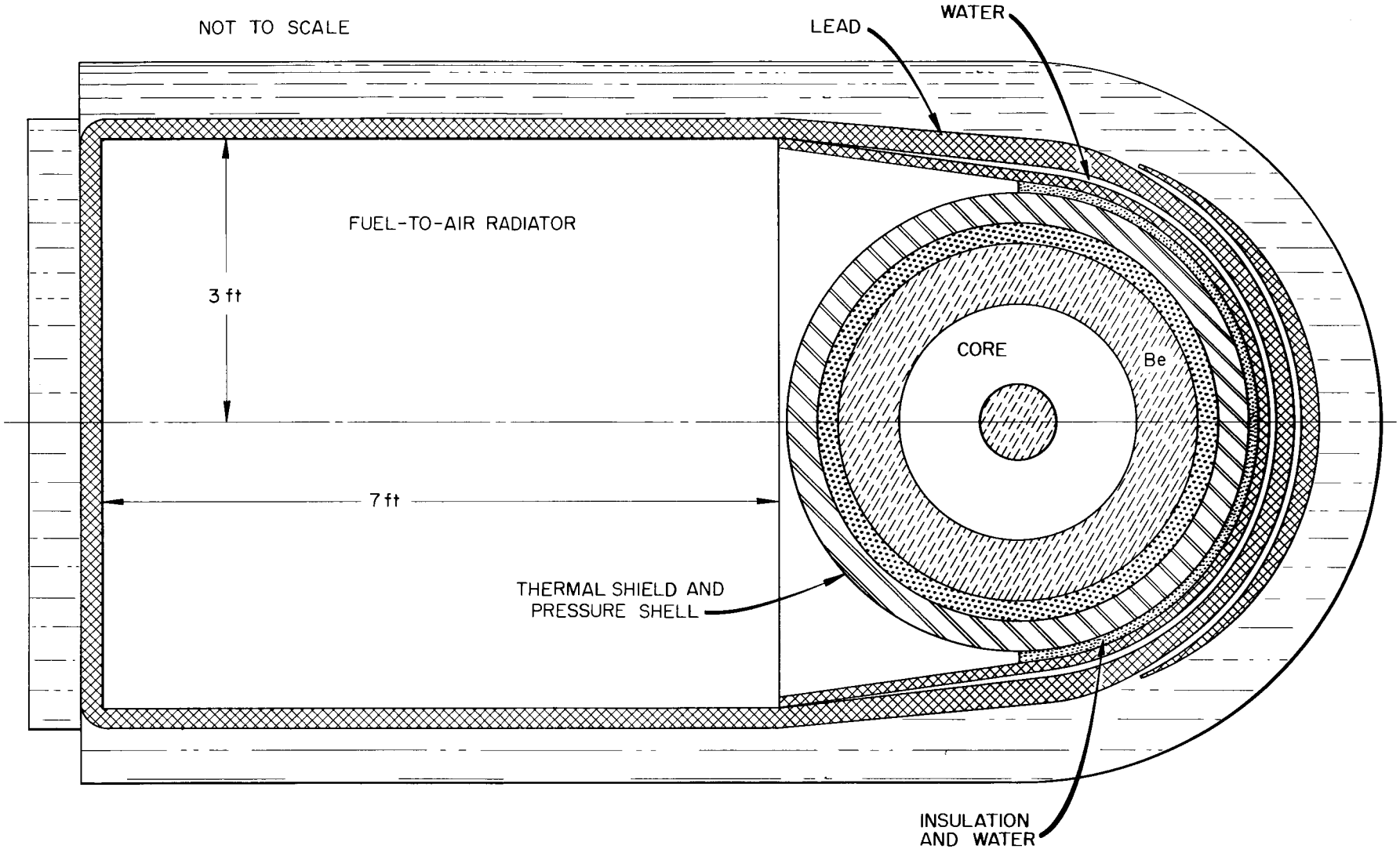

Fig. 2. Shield for a Circulating-Fuel Reactor with a Tandem Fuel-to-Air Radiator.

[redacted]

TABLE IV

Thickness of Basic Gamma-Ray Shield for CFR with Wraparound Radiator

Dose rate: 10^3 rep/hr at 50 ft

θ, Polar Angle Increment (deg)	Lead Thickness* (in.)
0 - 15	1.35
15 - 45	1.85
45 - 75	2.25
75 - 180	2.4

* Excluding shadow shield.

[redacted]

[redacted]

TABLE V

Thickness of Total Gamma-Ray Shield for CFR
with Wraparound Radiator

Shield Section	Lead Thickness (in.)			
	10^3 rep/hr at 50 ft			10^5 rep/hr at 50 ft*
	First Layer	Second Layer**	Total	
Reactor				
θ*** = 0 to 15 deg	1.35	4.32	5.67	4.47
θ = 15 to 27.5 deg	1.35	3.99	5.34	3.64
θ = 27.5 to 40 deg	1.35	3.17	4.52	2.82
θ = 40 to 52.5 deg	1.35	2.74	4.09	1.99
θ = 52.5 to 65 deg	1.89	1.35	3.24	1.16
θ = 65 to 77.5 deg	1.35	1.07	2.42	0.335
θ = 77.5 to 180 deg	1.35	1.05	2.40	0.0
Crew compartment				
Side			0.125	0.125
Front			0	0
Rear			0.478	2.46

* Only one layer required.
** Part of basic shield plus all of shadow shield.
*** Polar angle increment.

[redacted]

[redacted]

that 1/4 of the total gamma-ray dose rate in the central vertical plane of the reactor-radiator system came from the reactor. This was based on the ratio of the projected areas of the reactor and radiators.

Radiator Shielding. In calculating the gamma-ray shield for the radiator it was assumed that the fuel circulation time was so fast that the gamma-ray sources were uniform over the system. A surface source strength was then determined. Two methods of attenuation through the shield were used, which can be summarized as follows:

Method 1:[5]
$$D_1 = \frac{P_o \lambda}{c} \frac{r_s^2}{d} \sqrt{\frac{r_{rad}}{r_s}} \frac{E_1(\mu t)}{2} B(\mu t)$$

Method 2:[6]
$$D_2 = \frac{P_o \lambda}{2c\pi} \frac{r_{rad}^b}{d^2} \frac{\mathrm{erf}(\sqrt{\alpha})e^{-\mu t}}{\sqrt{\alpha}} B(\mu t) \qquad (2)$$

where

D_1, D_2 = gamma-ray dose rate at a distance d from the reactor,

P_o = photon source density

$$= \frac{P_R}{V_{f(sys)}} \frac{V_{f(rad)} \Gamma N}{V(rad)}$$

P_R = power of the reactor,

$V_{f(sys)}$ = volume of fuel in the system,

$V_{f(rad)}$ = volume of fuel in the radiator,

V_{rad} = volume of radiator,

Γ = number of photons per fission,

N = 3.1×10^{10} fissions/sec-watt,

λ = gamma-ray mean free path in the radiator,

r_s = outer radius of the lead shield,

r_{rad} = outer radius of the radiator,

$t = r_s - r_{rad}$,

[redacted]

[redacted]

$$E_1(ut) = \int_{ut}^{\infty} \frac{e^{-y}}{y}\, dy,$$

c = flux-to-dose conversion factor,

$2b$ = heat exchanger length,

$$\alpha = 1/2 \int_{r_{rad}}^{r_s} \frac{(r_{rad})^2}{r^2}\, \mu\, dr = \frac{(r_{rad})^2 \mu}{2}\left(\frac{}{r_{rad}} - \frac{1}{r_s}\right)$$

$$\mathrm{erf}(\sqrt{\alpha}) = \frac{2}{\sqrt{\pi}} \int_0^{\sqrt{\alpha}} e^{-\mu^2}\, d\mu \cong 1,$$

$B(\mu t)$ = dose buildup factor in lead.

The equations imply that the effective number of photons per fission, the source average mean free path, and the average absorption coefficient in the shield are known. These uncertainties may be removed by integrating over the spectrum of gamma-ray energies. Thus Eq. (1) may be written

$$D_1 = \frac{P_R}{V_f} \frac{V_{f(rad)}}{V_{rad}} \left(\frac{r_s}{d}\right)^2 \sqrt{\frac{r_{rad}}{r_s}}\, \lambda A \qquad (3)$$

where

$$\lambda A = \frac{N}{2} \int_0^{\infty} \frac{N(E) E_1(\mu t, E)\, B(\mu t, E)\, dE}{c(E)\, \mu(E)},$$

$N(E)$ = number of photons per fission of energy E per unit energy interval

$= 7e^{-1.2E}$

$\mu(E)$ = gamma-ray absorption coefficient in the radiator.

Also

$$N \frac{B}{c} \frac{}{2} = \frac{A}{E_1}$$

[redacted]

[redacted]

Then

$$D_2 = \frac{P_R}{V_f} \frac{V_f(\text{rad})}{V_{\text{rad}}} \frac{r_{\text{rad}}{}^b}{\sqrt{\pi}\, d^2} \frac{\text{erf}\sqrt{\alpha}}{\sqrt{\alpha}} e^{-\mu t} \frac{A}{E(\mu t)} \tag{4}$$

Thus a check may be obtained on the estimation of the dose resulting from Method 1 (Eq. 3) by use of Method 2 (Eq. 4). Method 2 yielded a slightly thicker gamma-ray shield for the case of 10^3 rep/hr at 50 ft. This thickness was used in the design in order to be conservative. Method 2 failed for the case of 10^3 rep/hr at 50 ft and thus the thickness given by Method 1 was used.

In the calculation of the lead shield delayed neutrons from the fuel were not considered since it is very difficult to estimate the source strength of delayed neutrons at the surface of the radiator and also to calculate their attenuation through the shield. Therefore, the maximum dose rate from delayed neutrons was calculated assuming zero circulation time and no attenuation from a point source. The dose at 50 ft under these conditions is about 30,000 rep/hr. LTSF data indicate a very short relaxation length in water for delayed neutrons. If a reduction by a factor of 10^4 is desired, 10 in. of water will be required. With the water placed at the outside and replacing the same number of gamma-ray mean free paths of lead, the additional weight is only 590 lb in the 10^3 rep/hr case. If, in the 10^5 rep/hr case, a reduction of 10^4 is desired, the additional weight is 4,470 lb.

The plastic on the crew compartment was determined from air scattering considerations outlined previously.[7] The thickness on the side and front is given by:

$$t_{ps} = 1.77 \ln 2\pi \left(\frac{\bar{K}}{\ell}\right) d \frac{I_{dn}}{\phi_{sn}}$$

where

d = reactor-crew compartment separation distance (cm),

I_{dn} = direct neutron dose rate outside the crew compartment,

ϕ_{sn} = desired crew compartment scattered dose rate,

$2\pi\left(\frac{\bar{K}}{\ell}\right) = 1.695 \times 10^{-4}$ for a symmetric shield.[b]

The thickness on the rear is given by:

$$t_{pr} = 2.84 \ln \frac{I_{dn}}{\phi_{dn}}$$

b. This term is defined in Ref. (7).

[redacted]

[redacted]

TABLE VI

Thickness of Total Neutron and Gamma-Ray Shield for CFR with Tandem Radiator

Shield Section	Shield Thickness (in.)	
	10^3 rep/hr at 50 ft	10^5 rep/hr at 50 ft
Reactor		
Lead at front	2.25	0
Lead at side[a]	3.2	0.2
Water at front and side	21.5 -- Lead Thickness[b]	
Shadow shield at centerline	5.16	6.66
Radiator		
Lead at front and side	3.9[c]	0.5[d]
Water at front and side	e	e
Crew Compartment		
Lead at front and side	0.125	0.125
Lead at rear	0.125	2.08
Plastic at front and side	8.18	8.18
Plastic at rear	20.2	20.2

a. Larger than the front thickness because the radiator contributes to the side gamma-ray dose rate.
b. I. e., total shield thickness = 21.25 in.
c. Obtained by Method 2 (Method 1 gives 3.4 in.). This thickness is reduced to 3 in. if 10 in. of water is added as a delayed neutron shield.
d. Obtained by Method 1 (Method 2 fails at small lead thicknesses). This thickness is eliminated if 10 in. of water is added as a delayed neutron shield.
e. 10 in. of water can be added as a delayed neutron shield in which case the lead thickness would be reduced (see c and d).

[redacted]

[redacted]

TABLE VII

Reactor and Shield Weights for Circulating-Fuel Reactors with Wraparound and Tandem Radiators

Component	Weight (lb)			
	10^3 rep/hr at 50 ft		10^5 rep/hr at 50 ft	
	Wraparound	Tandem[a]	Wraparound	Tandem[a]
Reactor[b]	44,400	31,500	44,400	31,500
Reactor lead shield[c]	37,400	18,200	12,600	9,900
Reactor water shield	9,000	8,600	9,200	9,800
Radiator lead shield	- -	38,400[d]	- -	4,800
Structure[e,f]	2,500	2,500	2,400	2,500
Patch[f]	5,000	5,000	5,000	5,000
Crew compartment lead shield	2,700	1,700	6,700	3,000
Crew compartment plastic shield	14,400	14,700	14,400	14,700
Total	115,400	120,600	94,700	81,200
Delayed neutron shield[g]		600		4,500
Total		121,200		85,700

a. Weights for shield specified in Table VI.
b. Includes estimate for decking, pumps and drives, control rod, island support, radiator (20,000 lb), etc.
c. Includes shadow shield.
d. Method I gives 33,200 lb.
e. Includes neutron shield container.
f. Estimated from information given in ORNL-1575, Report of the 1953 Summer Shielding Session, E. P. Blizard and H. Goldstein, Eds. (June, 1954).
g. Additional weight incurred if lead is replaced by water as described on p. 17 in this master.

[redacted]

[redacted]

where

ϕ_{dn} = desired crew compartment direct dose rate.

The resulting plastic thicknesses were used in the gamma-ray shield optimization procedure mentioned above to determine the lead thicknesses on the crew compartment and in the shadow shield.

The shield thicknesses for the tandem arrangement are given in Table VI.

TOTAL WEIGHTS

Total weights of the two systems given in Table VII do not appear to be excessive. Before conclusions with any degree of certainty can be reached, however, a more thorough study must be made in which consideration is given to the fuel-in-air radiator design and to the increase in engine efficiency obtained by elimination of an intermediate heat exchanger. The reactor for the tandem case is less because the Inconel shells have a much smaller diameter.

[redacted]

[redacted]

REFERENCES

1. Fraas, A. P. and Savolainen, ORNL Aircraft Nuclear Power Plant Designs, ORNL-1721, Series B, p. 72 (Jan. 28, 1955).

2. Farmer, W. S. Fraas, A. P., Stumpf, H. J. and Whitman, G. D., Preliminary Design and Performance Studies of Sodium-to-Air Radiators, ORNL-1509,

3. Valerino, M. F. and Keller, F. L. ANP Quarterly Progress Report September 10, 1955, ORNL-1947, p. 205.

4. Dee, J. B. et al., ANP Quarterly Progress Report December 10, 1955, ORNL-2012, Part IV, p. 25.

5. Blizard, E. P. and Goldstein, H., Report of the 1953 Summer Shielding Session, Eds., ORNL-1575, p. 92 (June, 1954).

6. ORNL-1575, op.cit., p 83.

7. ORNL-1575, op. cit., pp. 221, 355.

[redacted]

Paper III-F

SHIELDING MATERIALS FOR AIRCRAFT APPLICATION

S. A. Szawlewicz and H. C. Sullivan
Materials Laboratory
Wright Air Development Center

[redacted]

SHIELDING MATERIALS FOR AIRCRAFT APPLICATION

by

S. A. Szawlewicz and H. C. Sullivan

Materials Laboratory
Wright Air Development Center

The Materials Laboratory, Wright Air Development Center, is the Air Force organization responsible for developing and evaluating materials for operational use. Emphasis in the development of nuclear shield materials is placed on materials which are structually compatable with airframes, have acceptable fabrication and thermal properties, and will be available in time to support present weapon system projects. Studies at WADC have been completed on radiation stability of liquid ammonia and physical properties of linear-polyethylene for neutron shielding. Properties of lead epoxide resin compacts and creep properties of precipitation hardened lead alloys have been investigated for gamma-ray shielding. Contractors are investigating material combinations and mixtures, fabrication of LiH, and inelastic scatter in lead and tungsten. Further work is planned on tungsten alloys and cermets, uranium alloys with low thermal deformation, high melting point silanes and epoxides, and fabrication of a high temperature boron vehicle to replace boral.

INTRODUCTION

One of the most challenging problems now facing aircraft engineers is the design and fabrication of materials which will be suitable for aircraft utilization and which can simultaneously serve as adequate nuclear shielding materials. The operational requirements of aircraft materials, and the materials considered for nuclear shielding are almost mutually exclusive. The coordination of shielding physics and the materials engineering required to design an aircraft suitable for nuclear powered flight creates a broad new technical area which will require the complete cooperation of physicists and engineers. In order to accomplish these goals within the time limits specified aggressive programs must be initiated. The general problem of accomplishing this over-all task and the specific problems of materials and aircraft shielding have been the subject of a survey by engineers within Materials Laboratory, Directorate of Research, Wright Air Development Center.

[redacted]

[redacted]

DISCUSSION

Air Force Materials Approach

In order to better understand the general approach taken to the aircraft problem a brief discussion of the position of Materials Laboratory in Air Force research and its position in weapons systems development would be valuable. Materials Laboratory, Wright Air Development Center is the only materials organization within the Air Force. It has the general responsibility for developing and evaluating materials for operational use. It approaches this responsibility in two ways: through a research and development program for advanced materials and a program which might be termed production and operational engineering. The research and development program has been an aggressive program in progress for the past 30 years. It has been devoted to the development of materials in all areas of metallurgy. More recently emphasis has been shifting to requirements in high-temperature steels and the various alloys of nickel, chromium, and molybdenum. Of general interest is the observation that Materials Laboratory was one of the first metallurgical organizations in this country to develop the metallurgy of zirconium. Aircraft construction imposes severe requirements upon the physical and mechanical properties of metals. For this reason, the Air Force has put special emphasis on the program which develops mechanical criteria and the strength properties of materials. Design data development has been one of the outstanding contributions of Air Force engineers to the materials industry. Concurrent with the metallurgical program, a program for the development of organic materials has been a part of this approach. Many of the commercially available plastics both transparent and structural have resulted from aircraft requirements. In addition, programs are in progress to develop high-temperature lubricants, high-performance fuels, and experimental polymers for advanced plastics.

The production and operational side of materials development within the Air Force requires that research and development methods be integrated into production. Materials engineers must stay closely associated with the problems generated by the operation of advanced aircraft.

Shielding Materials Survey

Perhaps the most important consideration of a material for aircraft utilization is availability and the lead time necessary for materials development in support of any weapons systems approach. In order to evaluate existing materials, materials were examined from the point of view of lead time. This was accomplished by listing materials which could be available in order to begin construction on an airplane within the week. This framework was then extended to two years and then to five years.

[redacted]

In superimposing aircraft requirements upon shielding materials, the only starting point that could be assumed was existing aircraft competence for the use and fabrication of materials. The most important criteria in these considerations were fabricability, structural integrity, and reliability. Considerations of the high temperature creep of lead, poor fabricability of tungsten, and the thermal instability of uranium, to say nothing of the problems associated with lithium hydride and the poor temperature characteristics of the organic materials indicate that this was not too early a start. The required lead time for materials development in support of a 125-A had been drastically reduced. The study was directed toward the compilation of available design data and possible methods of fabrication.

In order to avoid unnecessary duplication of effort, a program was directed toward the use of present Air Force competence in design and fabrication for the development of shielding materials which could be used within the requirements of present day airframes. The survey shows that any significant weight savings would come from developments which could lend the shielding materials significant structural integrity. In other words the material would be more adaptable for aircraft utilization if it had some measure of self support. The most profitable approach to aircraft shielding materials results in combinations of materials and compromises in their various nuclear and physical properties. Another significant concept is the separation of the materials concept in the reactor shield and the crew shield. This separation of functional consideration was based primarily upon the temperature requirements of the crew shield and the reactor shield, respectively.

Shielding Materials Program

The program now in progress for development of aircraft shielding materials is divided into two phases: a contractual program and an internal program. Five contracts are now in progress under the joint cognizance of the Analysis and Measurements Branch and other branches within the Materials Laboratory. The first program is directed toward the generation of data on inelastic scattering cross sections and secondary gamma-ray production of uranium and tungsten. This data is urgently needed to refine shielding design calculations. Westinghouse Research Laboratory is conducting this study. Another program is directed toward the survey and evaluation of new materials and materials combinations for aircraft shielding application. This is presently in progress with Technical Research Group. This is a study of new and unique materials, those used commonly in aircraft and those proposed for use, and a study of shielding characteristics of these materials or their combinations. A third approach involves the fabrication and compatibility of materials mixtures (organic materials and high density elements) for application in the crew shield. Emphasis is placed on unique aircraft fabrication methods such as lamination, plastic and inorganic mixtures, and honeycomb construction for improving strength to weight ratios and the possibility of incorporating advanced

[redacted]

shielding materials into existing plastics. The Metals Branch is directing a program associated with the study of metal hydrides. This will involve not only hydriding techniques but fabrication and problems associated with canning and cladding. Some preliminary results have been reported on the design data of shield materials. This work is performed by Batelle Memorial Institute under contract.

The internal program at Wright Field is also subdivided into two areas and they shall be discussed in terms of neutron shielding materials and gamma shielding materials. Materials Laboratory and Oak Ridge National Laboratory have been involved in a study of lead and the addition of calcium or copper to prevent creep. The addition of calcium to lead results in a precipitation hardened alloy as shown in Table I. The addition of minor amounts of calcium with heat treatment results in significantly enhanced creep characteristics. Best results were obtained at a temperature of 295°F (240 hr at 300 psi). At this point there appears to be some tendency toward over-aging and studies are now in progress to determine these factors.

One of the investigations was a study of a homogeneous mixture of 93% lead powder and an organic epoxide resin binder. The use of lead, particularly in laminate construction, creates problems associated with cold flow, expansion and thermal conductivities. Figure 1 demonstrates some results of experiments on commercial Leadcast in terms of original properties, irradiated properties and a comparison with lead. Radiation does not significantly affect the mechanical properties and in some cases improves them. One of the anomalies of the study was the increase in shear strength as a result of radiation, since the indicated shear strength of the irradiated Leadcast is higher than the tensile strength of the irreadiated Leadcast. Better high temperature plastics can be obtained with perhaps better hydrogen contents. In addition to this, other materials are now attractive for incorporation with the plastics. The promise of these materials particularly for applications in crew shields is tremendous. Not only do they have excellent physical properties but fabrication is much easier than that of metals.

Some preliminary work has been initiated with the study of tungsten, its cermets, and alloys. One of the drawbacks to the use of these metals has been difficulty in fabrication. Present materials available are not true alloys but sintered products which have a number of disadvantages both in homogeneity, fabrication, and thermal shock properties. However, these tungsten materials in comparison to lead seem to offer significant advantages. Commercial tungsten composites have a density of 17.8 compared to a lead density of 11.3. The modulus of elasticity of the composites is 20 times as large as the lead. Tensile strengths are 30 times those available in lead. In addition, manufacturers are now promising billets which are 20 in. in diameter and 18 in. thick. In general, these materials are

[redacted]

[redacted]

TABLE I. SHORT-TIME CREEP OF A LEAD-CALCIUM ALLOY
(0.016 w/o Calcium)

Sample	Temperature (°F)	Stress (psi)	Time (hr)	Elongation (%)
As received	295	300	260	34.0
Heat treated	295	300	242	0.14
Heat treated	295	400	144	40.

[redacted]

Fig. 1. MECHANICAL PROPERTIES OF LEAD AND LEADCAST

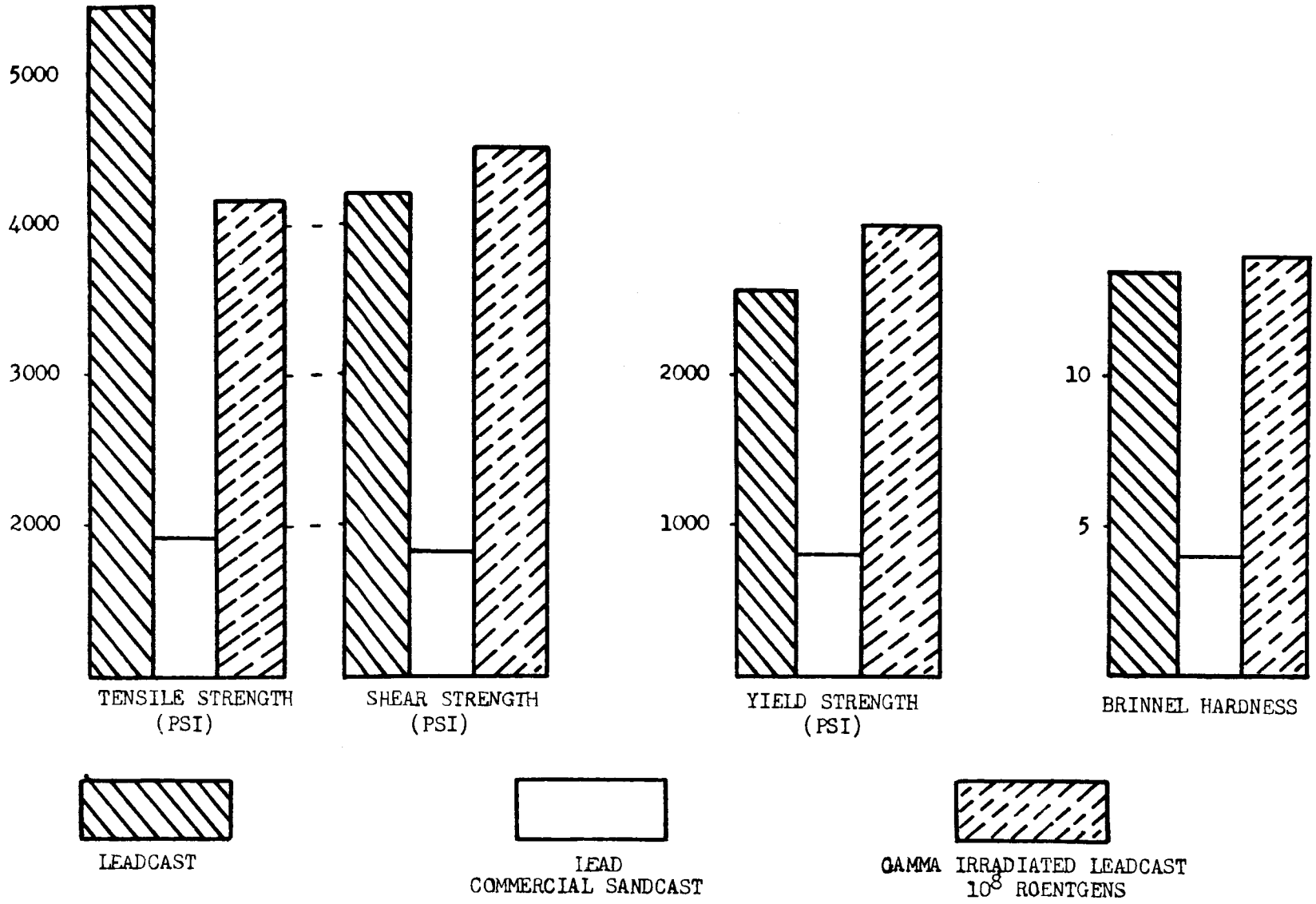

[redacted]

quite easy to work or machine. It is now indicated that the thermal shock properties can be significantly improved by grain size control. However, additional work must be performed on tungsten alloys before they can be acceptable for aircraft application.

Additional work is planned to improve alloys of uranium. While alloy development has been most extensive with this particular metal there are some significant gaps in these developments. Structural application of uranium is limited by thermal deformation as a result of thermal cycling. This can amount to as much as 25% deformation. Alloy development will be directed toward overcoming this shortcoming. The advantages of uranium alloys in terms of workability and fabrication make a development program most desirable.

The original work performed at Wright Field with respect to neutron shielding materials was accomplished with liquid ammonia. This work, which was directed toward the stability of liquid ammonia as a function of temperature and gamma radiation, has been completed and is now available in a WADC technical note. A significant program has been the program associated with studies of polyethylene, its physical properties and the effect of radiation on these physical properties. Original work was performed with commercially available polyethylene two years ago. At the time this work was completed, a new type polyethylene was becoming available, a so-called linear polyethylene or polymethylene. Since then, commercial production has been expanded and linear polyethylene is beginning to compete with the older type. Table II presents some of the comparative properties of conventional polyethylene and the new polyethylene. The higher melting point and the improved densities at higher temperatures make polyethylene desirable as a neutron shielding material. It has an excellent hydrogen content. While it is attractive as a shielding material, its main limitation is its melting point. Table III presents the effects of radiation on linear polyethylene. The conclusion is that radiation does not significantly affect the general engineering properties of this plastic. This work will be presently published in a WADC technical report. Other programs are in progress and under consideration. These involve high melting point organic silanes developed by the Aeronautical Research Laboratory at Wright Air Development Center. High temperature epoxide resins and other organic materials are being considered for possible matrices for gamma-ray shielding materials such as uranium, tungsten and lead.

CONCLUSIONS

In this controversial area of shielding and materials development the best approach toward a conclusion would be a summary of the problem areas involved in the intended development. This is as follows:

[redacted]

[redacted]

TABLE II. SOME PROPERTIES OF POLYETHYLENE AND LINEAR POLYETHYLENE

	Polyethylene	Linear Polyethylene
Density at 77°F, g/cc	0.92	0.96
Density at 210°F, g/cc	0.84	0.91
Melting point, °F	230	266

[redacted]

[redacted]

TABLE III. RADIATION EFFECTS ON LINEAR POLYETHYLENE

Temperature (°F)	Non-Irradiated		Irradiated 10^9 r	
	Density (g/cm^3)	Volume Increase (%)	Density (g/cm^3)	Volume Increase (%)
77	.96	0	.95	0
210	.91	5.6	.91	5.4
257	.83	15.7	.80	18.9

[redacted]

[redacted]

1. Lithium hydride

   a. Engineering data on the effects of thermal cycling and vibration. The determination of nuclear properties after such tests.
   b. Fabricability.
   c. Substitutes of equivalent nuclear and improved thermal properties.

2. Metals

   a. Development of uranium and tungsten alloys for high temperature gamma shielding.
   b. Improvement of lead by alloying or blending with organic resins.
   c. Means of incorporating $boron^{10}$ into a high temperature, structural material.
   d. High temperature design data.

3. Nuclear tests for obtaining data on shield materials and designs.

Lithium hydride has been widely considered as a very desirable shielding material particularly for neutrons. As an engineering material, however, it is still a long way from effective utilization. Thermal shock properties and the effect of thermal cycling of lithium hydride requires additional investigation. Still another broad area in the development of lithium hydride as a shielding material concerns its fabricability. Advances will have to be made both in the cold pressing and casting of lithium hydride as well as canning and containment before it will be an adequate aircraft material. A simultaneous program should be entertained in order to investigate other materials which would complete favorably with lithium hydride in terms of nuclear and improved thermal properties. Many of the development areas associated with metals, their development for high temperature use in gamma shielding, the use of metals in organic resins, and high temperature design data are self explanatory. Some explanation might be appropriate with respect to borbn. Boron will undoubtedly be used with aircraft nuclear reactor shields for absorbing thermal neutrons. The only material available of this type is boral, a mixture of boron carbide and aluminum. Aluminum is not suitable for high temperature application. It is, therefore, desirable that methods be investigated for incorporating boron in high temperature metals.

A number of materials are now available which will fill the requirements of neutron and gamma-ray shielding, but some reasonable doubt may be expressed concerning the ability of these materials to meet the requirements of aircraft construction. A significant payoff may be realized in developing

[redacted]

[redacted]

greater strength-to-weight ratios of shield materials, adding structural integrity, and providing them with the compatibility to meet the various aircraft environments. This predicts an expanded and progressive effort which will demand the best integration of competence in nuclear engineers and materials development.

[redacted]

Paper III-G

FULL SCALE TURBOJET ACTIVATION EXPERIMENT -- PRELIMINARY RESULTS

J. Moteff
General Electric Company - ANP Dept.
Evendale

[redacted]

[redacted]

FULL SCALE TURBOJET ACTIVATION EXPERIMENT -- PRELIMINARY RESULTS

by

J. Moteff

Aircraft Nuclear Propulsion Department
General Electric Company
Evendale, Ohio

In an effort to obtain full scale experimental data on induced activity, a standard production line J-27 turbojet was irradiated at the Tower Shielding Facility in Oak Ridge. The selected engine was a J-47 Model E. Preliminary results indicate that the activity to about 2 days is due to Manganese. From 2 to about 500 days the Tantalum activity dominates. Finally the cobalt activity is the sole contributer beyond 500 days after exposure.

INTRODUCTION

In an effort to obtain full scale experimental data on induced activity, a standard production line J-47 turbojet was irradiated at the Tower Shielding Facility in Oak Ridge. The selected engine was a J-47 Model E.

The experiment was performed during the third week of April, 1955. The engine was then shipped back to General Electric at Evendale for further measurements, by commercial vehicle, about two days after the last exposure. A more detailed report on the results of this experiment will be issued by GE-ANPD in the near future.

EXPERIMENTAL PROCEDURE

The engine was irradiated twice. On both occasions the reactor was brought as close as possible to the tank wall (15 cms) to give incident fluxes on the engine which would approximate as closely as possible in flight dose rates. Each irradiation period was 4 hours long. In the first irradiation which resulted from reactor operation at 0.4 MW a 1/8 inch boral box, open at both ends, was placed around the engine. Five days later, a second irradiation was performed without the boral box.

Following each irradiation period, the induced activity, as a function of time after shutdown, was obtained by means of hand counters and a previously established coordinate system. Height positioners were used to obtain geometrical consistency in measurement. All measurements were made in a plane thru the center line of the engine positioned in the dolly.

[redacted]

EXPERIMENTAL AND ANALYTICAL DATA

1. Neutron Flux

The intensity and profile of the neutron radiation is shown in Figure 2. The data plotted are for line AA' of Figure 1. The fast dose (with angular distribution) was obtained thru geometry correction from measurements made at 64 feet from the center of the reactor tank. The reactor was positioned about 15 cm from the side surface of the shield tank as shown in Figure 3.

The thermal flux in front of the midpoint of the boral box was obtained by a cadmium difference in gold foil and represents the thermal flux to the cadmium cut off. The distribution of the thermal flux was approximated from the induced activity of a 14 foot cobalt wire stretched along the boral box. The wire activity was normalized to the gold foil measurement, thus giving a relative distribution of the thermal flux over the surface of the side of boral box. In a similar manner, the apparent thermal flux distribution thru the side of the boral box was obtained and again normalized to a set of gold foils activated behind 1/8 inch boral.

TABLE I

Radioactivants used to obtain neutron spectrum

Reaction	Half - life	Resonance Energy (ev)	Threshold Energy* (Mev)	Cross Section ($x10^{-24}$)(saturation)
$Sn^{32}(n,p)^{32}$	14.3 d		2.9	0.300
$Al^{27}(n,p)Mg^{27}$	9.8 n		4.6	0.039
$Mg^{24}(n,p)Na^{24}$	14.9 h		6.3	0.048
$Al^{27}(n,\alpha)Na^{24}$	14.9 h		8.1	0.111
$Co^{59}(n,\gamma)Co^{60}$	5.2 y	120		
$Mn^{55}(n,\gamma)Mn^{56}$	2.59 h	260		
$Cu^{63}(n,\gamma)Cu^{64}$	12.8 h	570		
$Na^{23}(n,\gamma)Na^{24}$	14.9 h	1710		
$Cl^{37}(n,\gamma)CL^{38}$	37.3 m	1800		

* Effective threshold energy assuming a neutron fission spectrum.

[redacted]

2. Resulting induced activity

As an aid for determining the likely source of radiation, a cutaway drawing of a J-47 turbojet engine is given in Figure 3. The nomenclature and material compositions are given for the major components.

The isodose pattern measured about the engine at 6 hours after exposure (no boral) is shown in Figure 4. It is obvious that the pattern near the engine is strongly dependent on the specific locations of the radioactive sources within the engine. However, the radiation pattern at distances greater than about 10 feet appear to originate from a point source.

Isodose patterns about the engine at 300 days after exposure indicate that most of the radiation is in the region of the turbine. Figure 5 shows this centering of the radiation about the turbine region.

The engine was then disassembled to identify the source of radiation. This source was the nozzle diaphragm (See Figure 9) which has an isodose pattern as indicated in Figure 6. The hot spot is the edge of the diaphragm that was nearest the reactor.

Figure 7 shows the isodose patterns about the engine and about the nozzle diaphragm with the diaphragm superimposed on the position it would occupy in the engine. The dotted lines are those of the nozzle diaphragm.

Figure 8 is a close up photograph of the nozzle diaphragm and two turbine buckets. The marked areas of the diaphragm indicate the positions of samples taken to identify the radioactive isotope. These activities and materials are given in Table II. Gamma spectrometer measurements indicate that most of the radiation is from the Co^{60} in the partitions. The activity of the weld sample is probably due to traces of Co^{60}.

The dose rate measured at position A (between the 2nd and 3rd combustion can and near the turbine end) is shown in Figure 10. Preliminary analysis indicates that this activity is due to manganese, copper and tantlum. Beyond two to three days after exposure, the dominating activity is due to the tantalum isotope. The two experimental points of about two days after exposure are believed to be in error. They may, however, be due to a 28 day chromium activity. It is important, for future tests, to plot the data as it is being obtained with more emphasis on the knees of decay curves.

Table III gives some of the nuclear properties of these isotopes.

Since the reactor operating time of interest is somewhere between 40 and 400 hours, the dose rates at position A were corrected for these times and shown in Figure 11. From observing this plot, it appears that the activity has the greatest change in the first few days after exposure. Therefore, the waiting period beyond a few days after exposure would have to be about

[redacted]

[redacted]

Table II

Activity of Nozzle Diaphragm

Sample Number	Designation	Material	Activity
5	Weld		45 cts $min^{-1}gm^{-1}$
6	Band	347 S.S. 321	background
7	Partitions	Vitallium	2030 cts $min^{-1}gm^{-1}$
8	Band	347 S.S. 321	background

TABLE III

Element	Half Life	Abundance (%)	Gamma Radiations (Mev)	Cross Sections (barus)
$Mn^{55}(n,\gamma)Mn^{56}$	2.58 hours	100	.85, 1.8, 2.1, 3	13.3
$Fe^{56}(n,p)Mn^{56}$		91.6		0.013
$Cu^{63}(n,\gamma)Cu^{64}$	12.8 hours	69	1.34	4.4
$Ta^{181}(n,\gamma)Ta^{182}$	112 days	99.988	1.12, 1.22	22
$Co^{59}(n,\gamma)Co^{69}$	5.2 years	100	1.17, 1.33	37

[redacted]

[redacted]

112 days for the radiation to decay by a factor of two. The dose rate at position A, beyond two days after exposure, will probably not be much higher than one r hr^{-1} for the given neutron flux and 400 hours of exposure.

Figure 12 gives a plot of the dose rate at position A for very long times after exposure. This also indicates that the tantalum activity is prominent from about 2 days to about 600 days after exposure. The Co^{60} activity is important after 600 days. The experimental point at about 400 days after exposure was obtained after the nozzle diaphragm (and hence the Co^{60} activity) was removed from the engine.

The source of this tantalum activity is believed to be in the 347 stainless steel. Columbium and tantalum are added as a stabilizing agent to prevent intergranular corrosion in 347 stainless steel. Tantalum also has a fairly high thermal neutron absorption cross section.

[redacted]

[redacted]

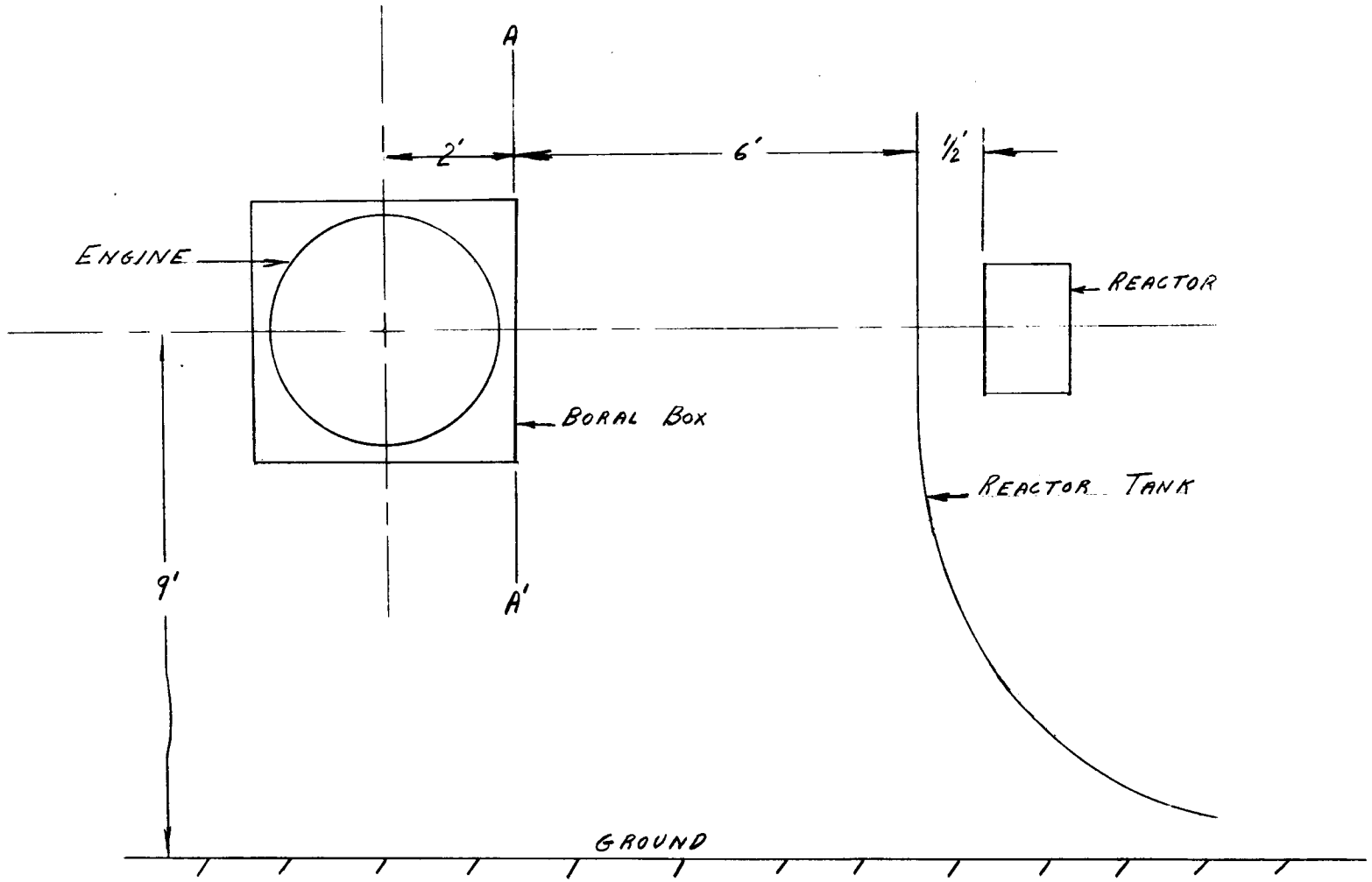

FIGURE 1

[redacted]

[redacted]

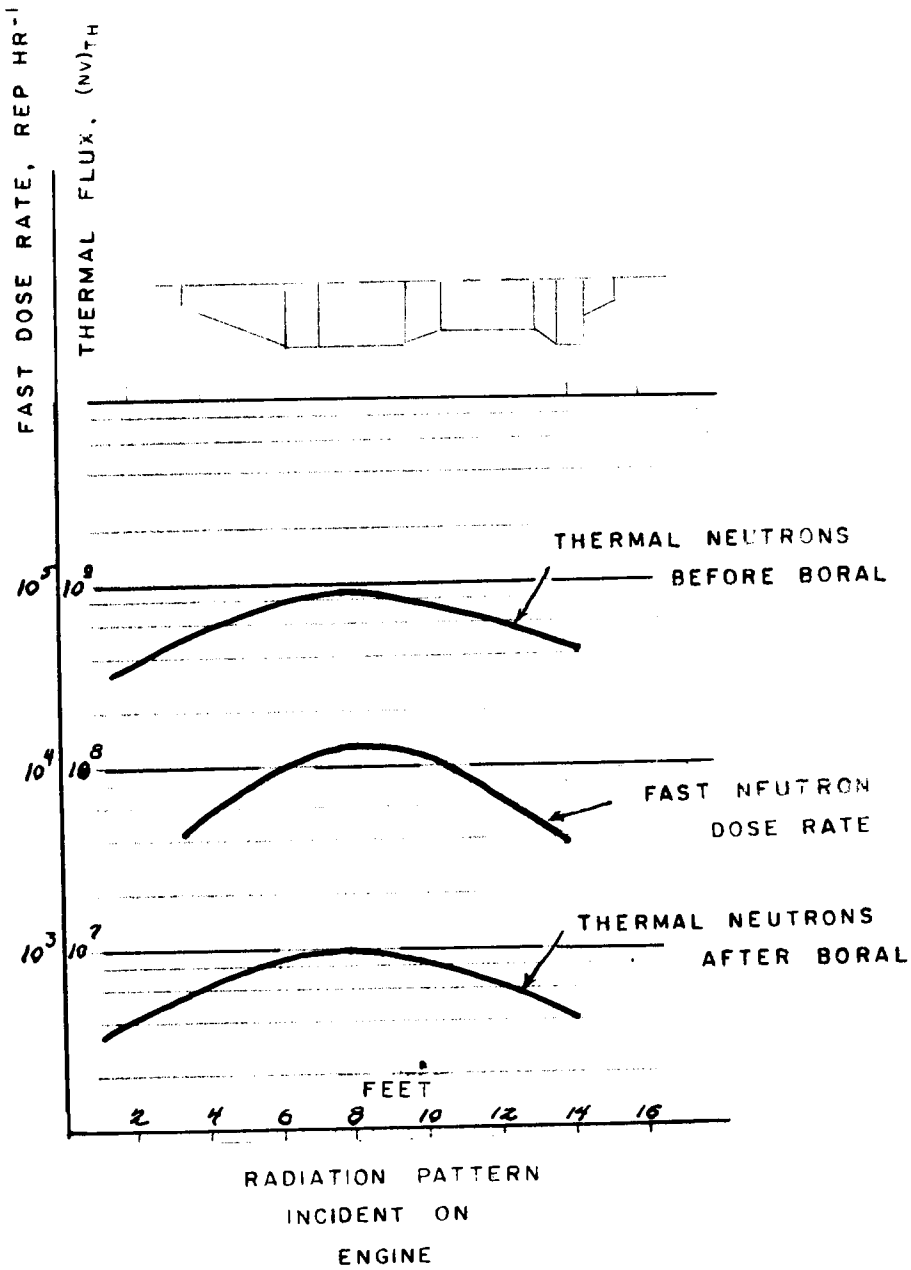

FIGURE 2

[redacted]

[redacted]

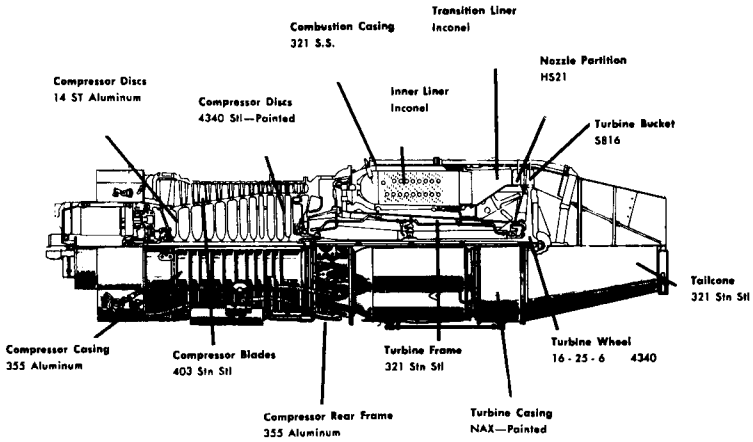

CROSS SECTION VIEW OF J-47

FIGURE 3

[redacted]

[redacted]

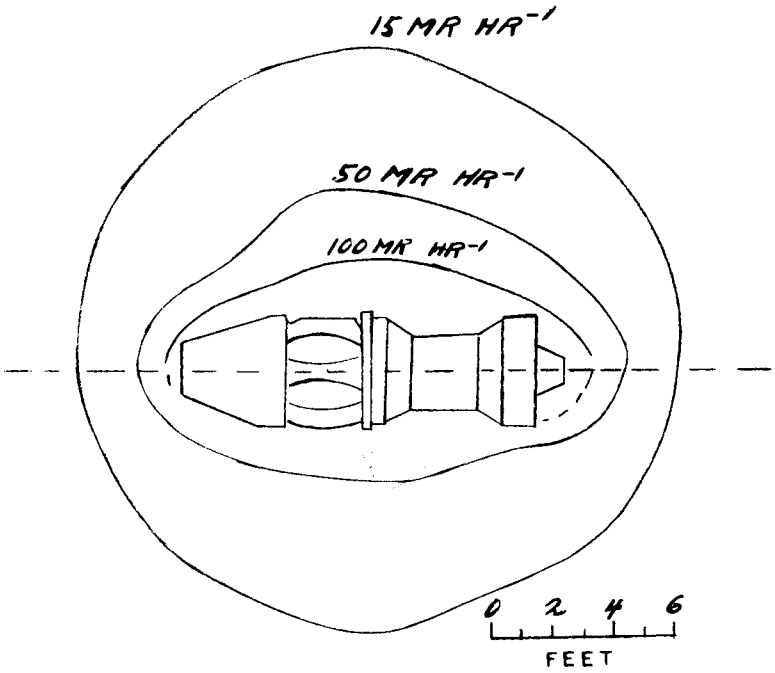

ISODOSE PATTERN ABOUT ENGINE, APPROXIMATELY 6 HOURS AFTER EXPOSURE.

FIGURE 4

[redacted]

[redacted]

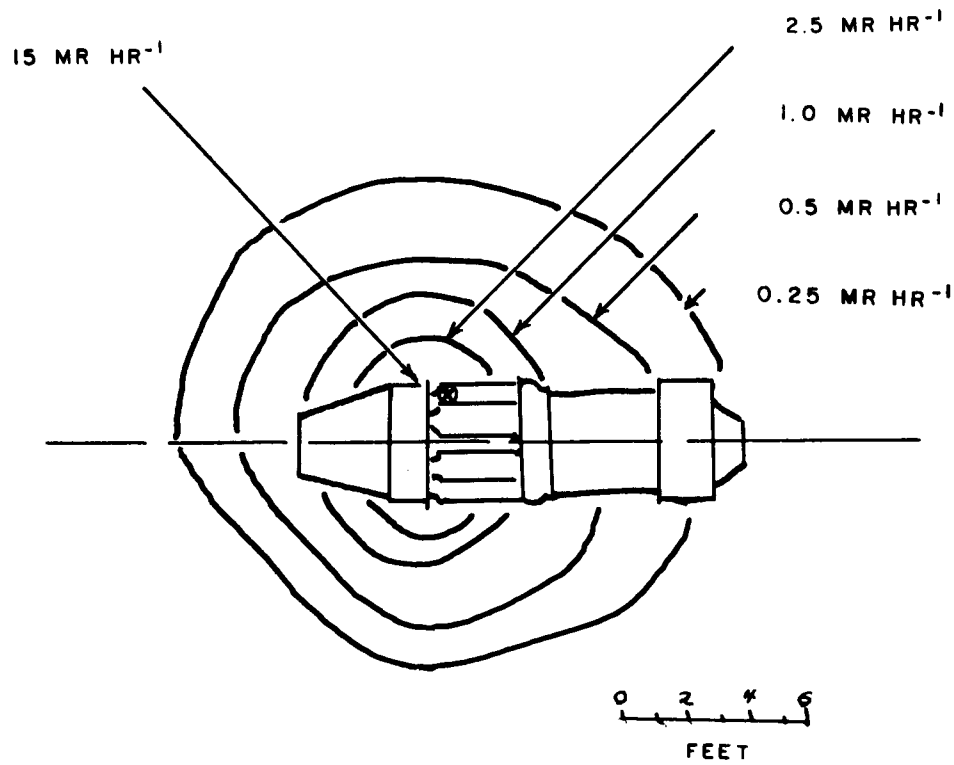

ISODOSE PATTERN ABOUT ENGINE AT APPROXIMATELY 300 DAYS AFTER EXPOSURE

⊗ POSITION A

FIGURE 5

[redacted]

[redacted]

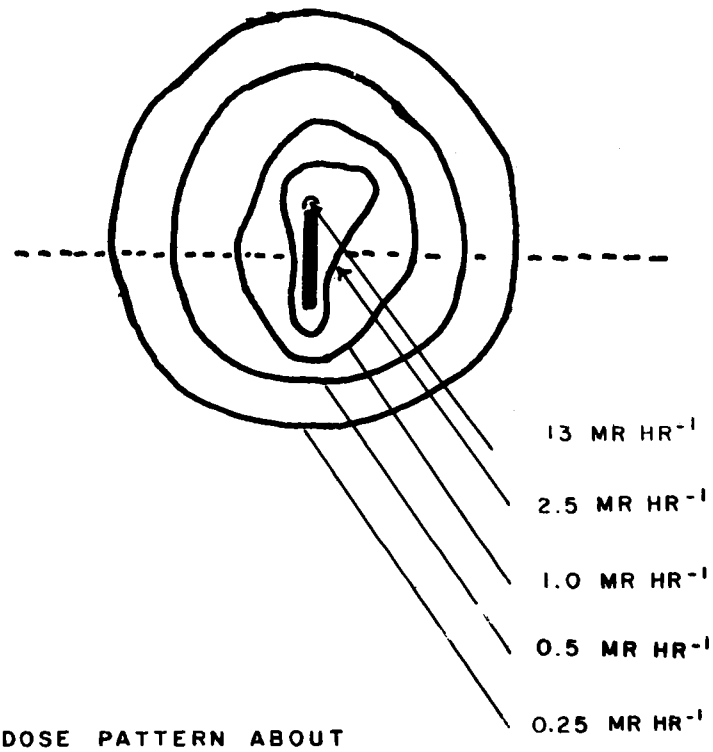

ISODOSE PATTERN ABOUT NOZZLE DIAPHRAGM AT APPROXIMATELY 300 DAYS AFTER EXPOSURE

FIGURE 6

[redacted]

[redacted]

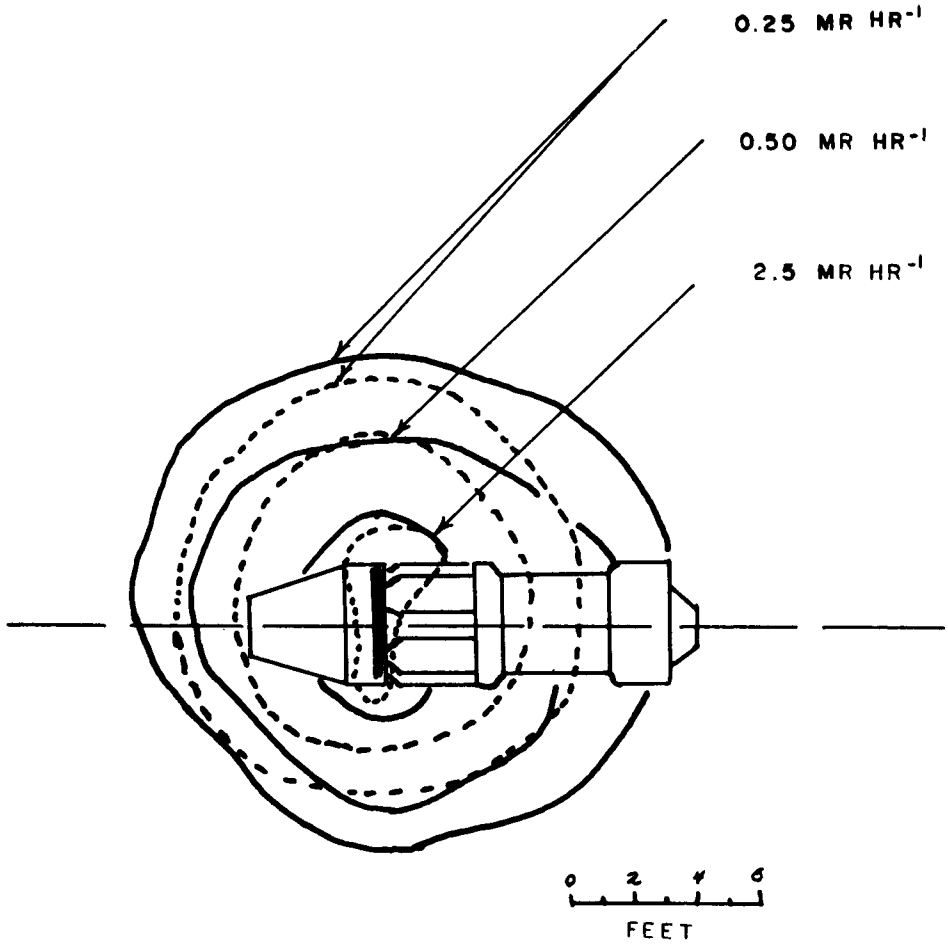

NOZZLE DIAPHRAGM ISODOSE PATTERN SUPERIMPOSED ON ENGINE ISODOSE PATTERN. APPROXIMATELY 300 DAYS AFTER EXPOSURE.

FIGURE 7

[redacted]

NOZZLE DIAPHRAGM AND TURBINE BUCKETS

FIGURE 8

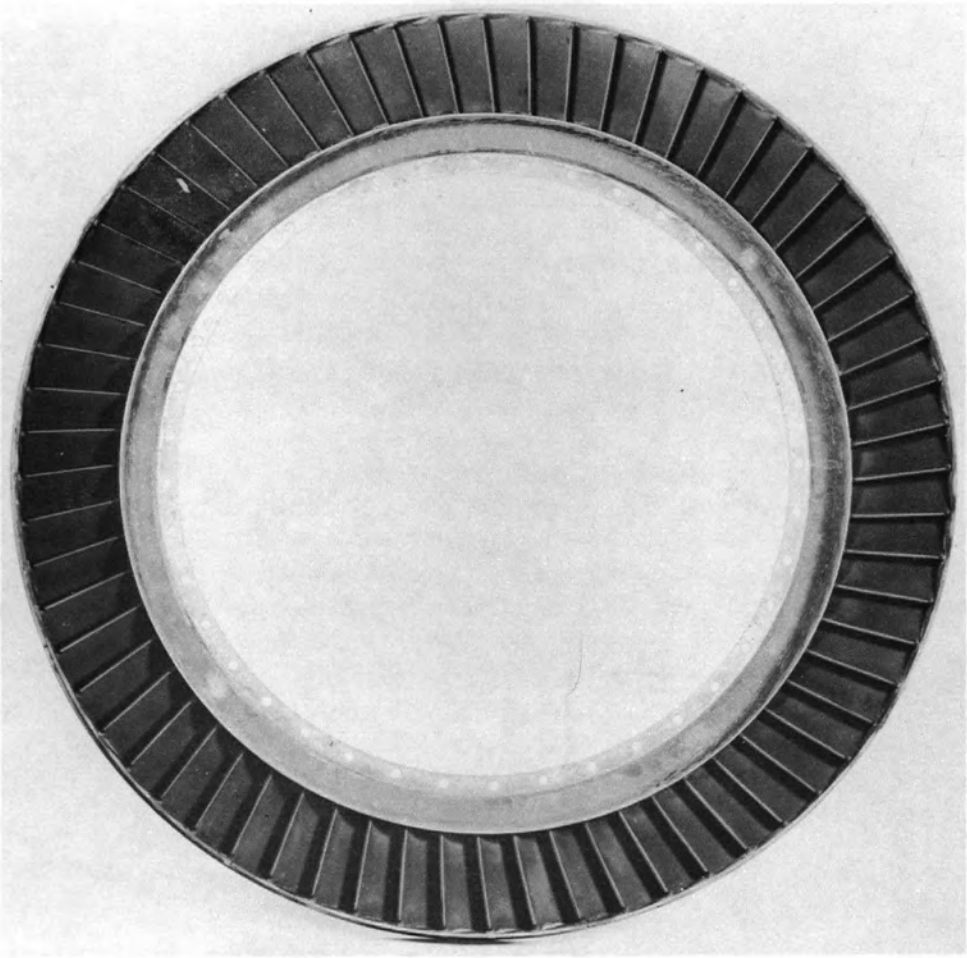

NOZZLE DIAPHRAGM

FIGURE 9

[redacted]

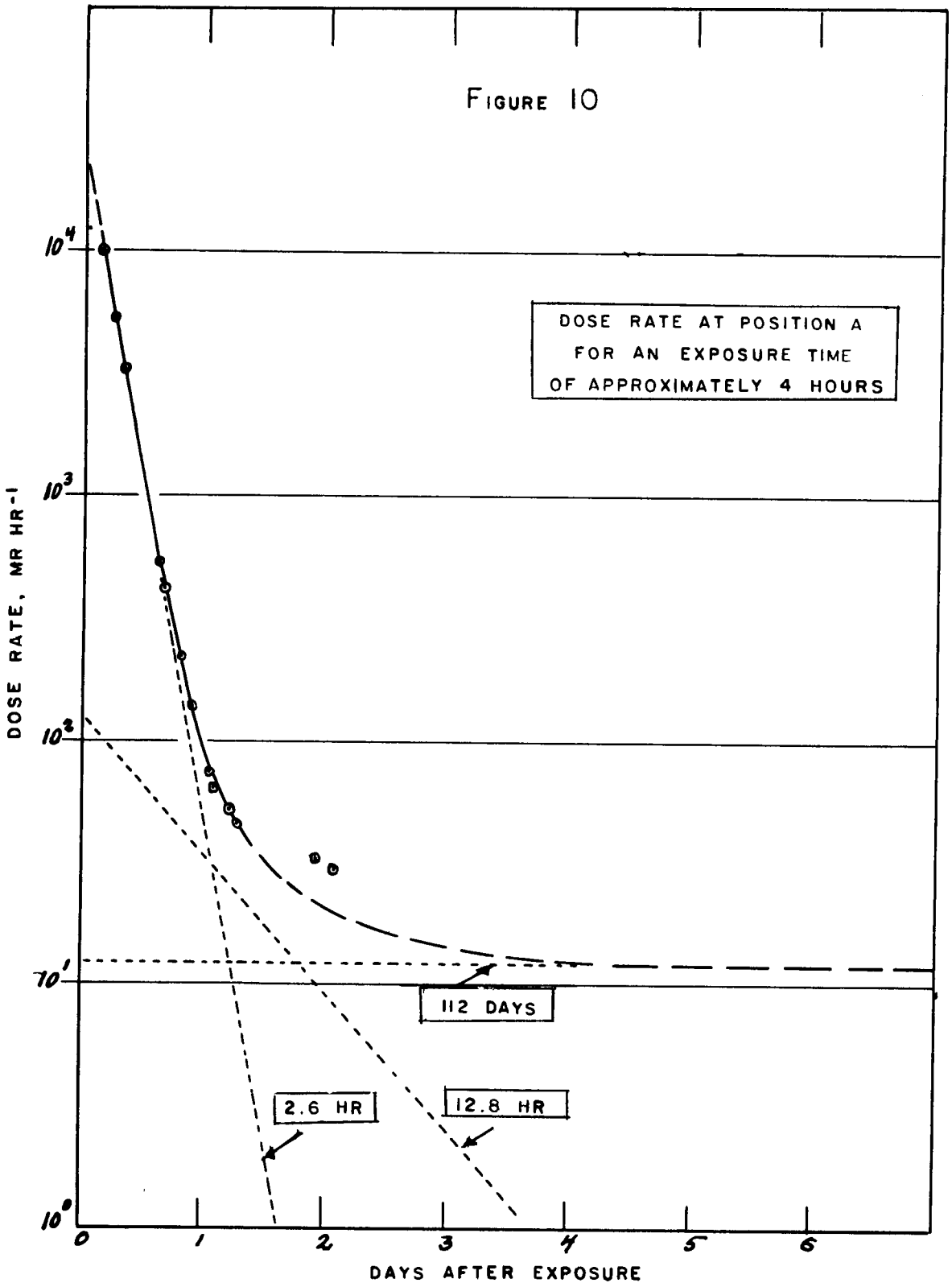

[redacted]

[redacted]

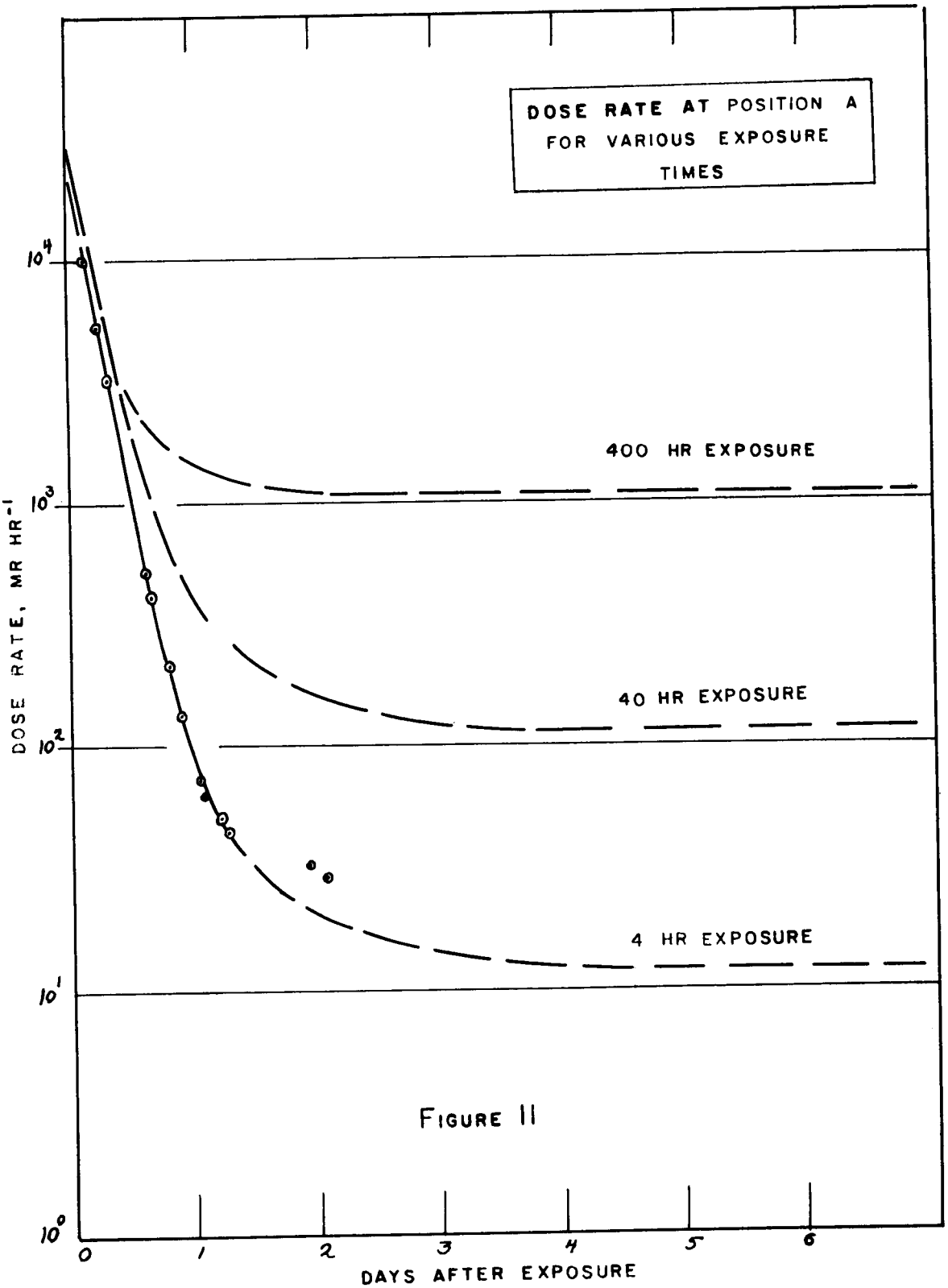

FIGURE 11

[redacted]

[redacted]

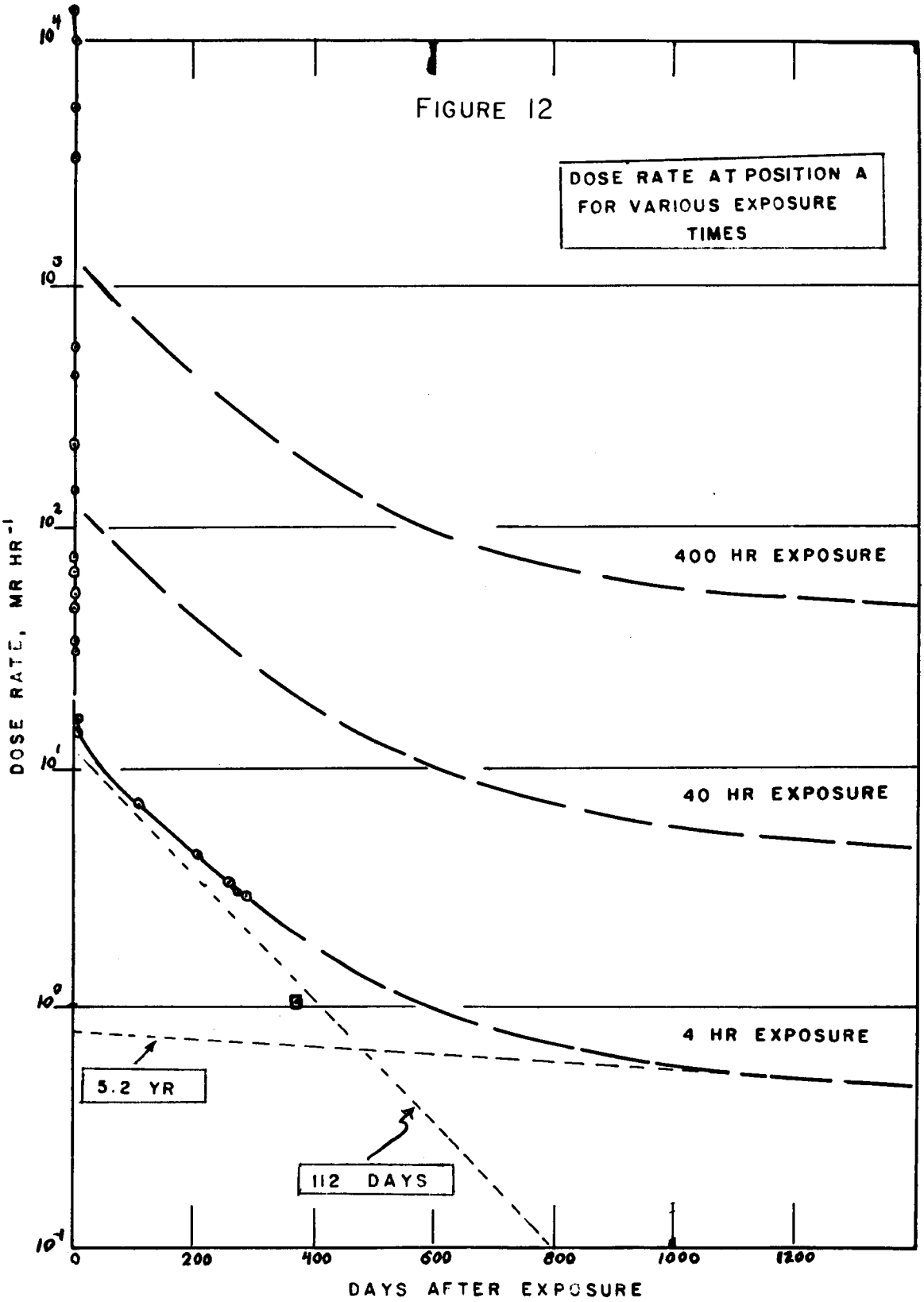

[redacted]

SECRET

Paper III-H

THE SHIELD MOCKUP REACTOR*

L. B. Holland
Oak Ridge National Laboratory

*Subsequent to the writing of this paper it was decided that this reactor will be called The Shield Mockup Core.

SECRET

[redacted]

THE SHIELD MOCKUP REACTOR*

by

L. B. Holland
Oak Ridge National Laboratory
Oak Ridge, Tennessee

Since a reflector-moderated circulating-fuel type reactor (CFR) is being considered for the nuclear-powered aircraft, it was proposed that shielding experiments should be performed with a reactor which simulates the radiation leakage of this reactor configuration in as much detail as possible. A preliminary design and cost estimate have been prepared for a reflector-moderated reactor using fixed-fuel elements. The reactor, which will be called the Shield Mockup Reactor (SMR), will correctly mock up all the radiation from the Pratt and Whitney CFR except the decay gamma rays and neutrons from the circulating fuel in the heat exchanger. The decay gamma rays would contribute approximately 30% to the total gamma radiation from a CFR for present reactor shield designs. The SMR will use a beryllium reflector shaped as specified for the CFR, and nuclear calculations by Pratt and Whitney indicate that the desired flux distribution in the beryllium can be obtained. The shield will be Lockheed's latest design.

Currently, tests of an optimized reactor shield design are made with a full-scale mockup of the shield and a known source. The effectiveness of the shield in its final application is then predicted by making source corrections. To date the source has often been a swimming pool type reactor. For the reflector-moderated circulating-fuel type reactor now being considered by the Aircraft Nuclear Propulsion Program it becomes increasingly more difficult to correct for the differences in sources. Thus a shield test with a reactor that more nearly mocks up a CFR is required.

Oak Ridge National Laboratory has proposed a 5-Mw reactor using fixed-fuel elements which will correctly mock up all the radiation expected from the Pratt and Whitney reflector-moderated CFR except the decay gamma rays and neutrons from the circulating fuel in the heat exchanger. A program has been initiated to prepare a preliminary design and cost estimate of its construction which will be included in a formal proposal to the Atomic Energy Commission. The reactor will be called the Shield Mockup Reactor and will be used with the latest optimized shield at the Tower Shielding Facility to determine

*Subsequent to the writing of this paper it was decided that this reactor will be called The Shield Mockup Core.

[redacted]

whether the calculated dose in the crew compartment agrees with the measured dose. It will also be used at the Bulk Shielding Facility where measurements will be made of the spectra of neutrons and gamma rays emerging from the reactor shield.

Calculations for the SMR thus far have been directed toward obtaining a good nuclear mockup; the design effort has been directed toward making a simple yet flexible over-all design. In this paper the SMR is described as it is now planned and the differences between it and the present CFR designs are noted. The SMR sources are then compared to the CFR to show how closely they agree.

THE REACTOR

When a shaped reactor shield is used, the source geometry becomes an important factor. Every attempt has been made to preserve the geometry of the CFR in the SMR (see Fig. 1). The central beryllium island will be cylindrical, and its center will be removed for the inlet cooling line. The CFR has a control rod of slightly smaller diameter in this position, but calculations have shown that the effect of the cooling line is not significant. The SMR will be controlled by using thin, curved, plates containing boron-10 at the outer edge of the island between the fuel plates and the beryllium. In the core region it is proposed to use fixed fuel plates of UO_2 and stainless steel which will be similar in cross section to the Army Package Power Reactor fuel plates. The shape of the plates will be peculiar to the SMR. The feasibility of this shape has already been determined with test fuel plates. There will be a total of 200 fuel plates placed radially around the beryllium island with light water used as the coolant. The core region will be separated from the beryllium island and reflector by inconel shells required by the CFR.

The region above the CFR reactor core will be difficult to mock up. Since it constitutes a small total angle it seems best in the SMR to attempt to black out radiation from this region. Another feature in favor of this idea is that the control rod drives and control chamber leads will be in this region.

The reactor is being designed so that it can be transported between the Tower Shielding Facility and the Bulk Shielding Facility with the minimum amount of dismantling. The fuel can be removed without disturbing the control rods or the control chambers. This will be accomplished by placing the elements in a rotating rig that can be locked in position. A removable plug in the rig will allow removal of the elements.

[redacted]
2-01-059-79

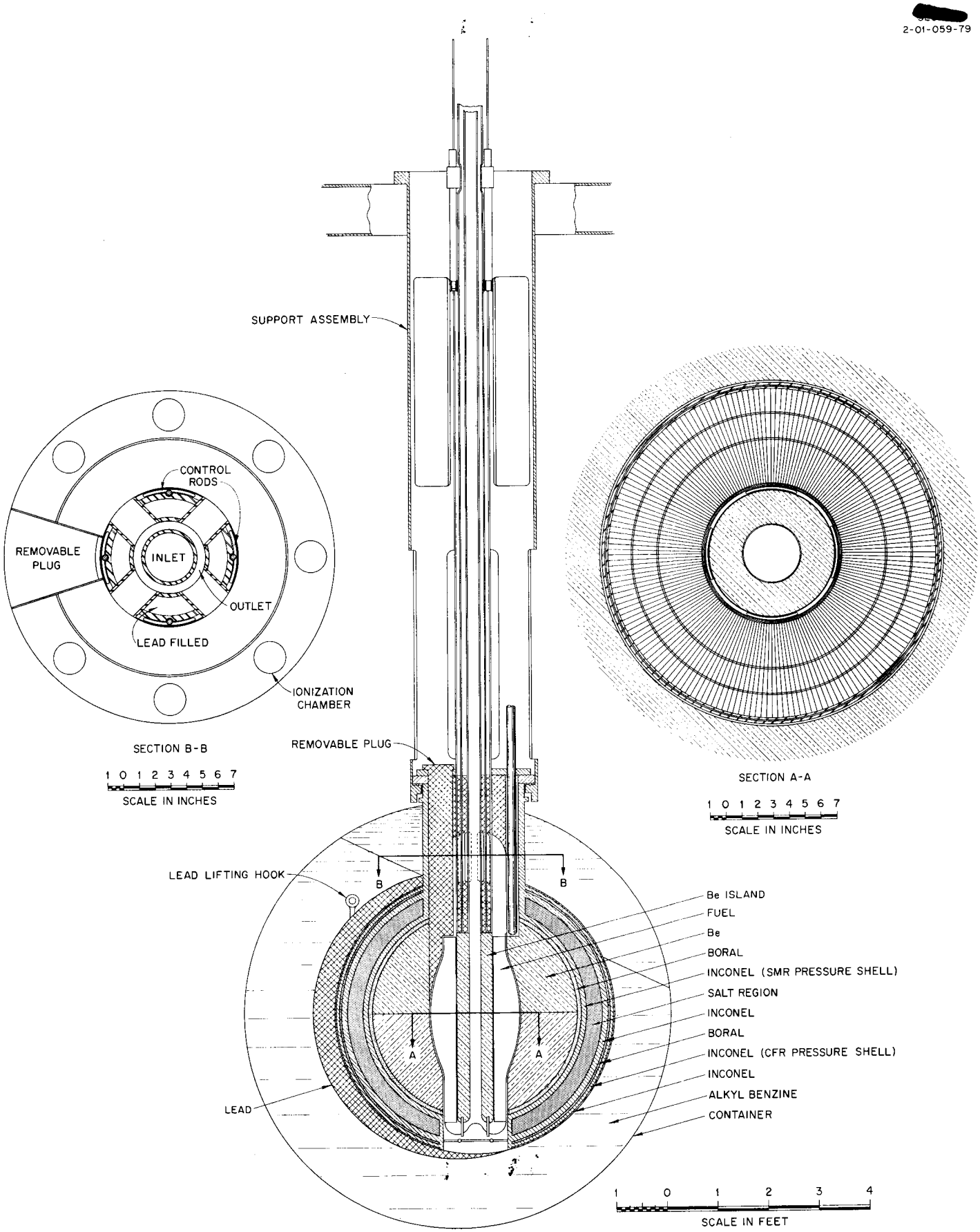

Fig. 1. The Shield Mockup Reactor (SMR)

[redacted]

THE REFLECTOR

The beryllium reflector of the SMR will be similar in shape to the CFR except at the tip of the beryllium where the question of hydraulics greatly influences the CFR design. The sodium coolant in the beryllium will be simulated with aluminum. If cooling is required in the beryllium of the SMR light water will be used, and it will be kept at a minimum.

REGIONS OUTSIDE THE REFLECTOR

The first region outside the beryllium reflector will be the first boron curtain. In the CFR it consists of a layer of sodium, followed by inconel and a complicated boron-copper layer. Considering the radiation as seen outside the shield, this region can be adequately simulated in the SMR with a shell of inconel followed by layers of boral to give the proper density in g/cm^2. Calculations are being carried out at Pratt and Whitney Aircraft Company to determine the importance of each region as a source of radiation.

The heat exchanger region just beyond the first boron curtain affects the crew compartment dose rate in several ways: (1) It attenuates the radiation from the core and the beryllium; (2) it is a source of some capture gamma radiation due to core neutrons; and (3) it is a source of delayed neutrons and fission product decay gamma rays. In order to account for the first two effects, the heat exchanger region will be mocked up with fused salt together with the NaK (in the form of NaF and KF) as a homogenized mixture. This will be accomplished by heating the salt and can to about 1000°C in an evacuated furnace. The cans will be placed in two layers to eliminate leakage paths through the salt region between the cans. The inconel in the heat exchanger will be split and will form two shells around the salt region, the inner shell acting as the pressure shell for the SMR. Outside the outer heat exchanger shell will be the second sodium-cooled boron curtain which, like the first curtain, will be mocked up with boral.

The regular CFR pressure shell will follow the heat exchanger region. It is proposed that part of this shell be split off for use in mounting the lead shielding. This section is removable which allows the lead shield to be changed without dismantling the reactor.

The neutron shielding material will be contained in an aluminum tank. The optimized neutron shield will be a spherical shield which will be placed off-center with respect to the center of the reactor. It is proposed to permit lateral motion of the neutron shield while using water as shield material to check the present optimization. Later the shield container can be sealed in the optimized position and neutron shielding materials other than water can be used.

[redacted]

[redacted]

To facilitate the measurements at the TSF it is proposed to design the whole reactor and shield system so that it can be rotated about the vertical axis.

COMPARISON OF SMR AND CFR

An examination of some of the results of the calculations performed by Pratt and Whitney indicates how closely the SMR radiation simulates the CFR.

Neutron Captures in Beryllium

Since approximately 20% of the dose rate in the crew compartment originates from neutron captures in the beryllium this source should be accurately simulated. Figure 2 shows the captures that can be expected in the SMR beryllium with light water as the coolant in the core. The lower curve shows the absorptions in the SMR beryllium when the space between the fuel plates is completely filled with light water and the reactor is operated at room temperature. Comparing this with the calculations for the absorptions in the CFR reflector (this includes beryllium and sodium) operating at CFR temperature it can be seen that the absorptions in the SMR are low. By reducing the water volume in the core of the SMR with aluminum spacers (and thereby reducing the moderation in the core) the absorptions of neutrons in the beryllium can be increased. With 75% aluminum and 25% water in the spaces the tails of the absorption curves are in good agreement. The shape of the curve for the region near the core-reflector interface does not match as well as the rest of the curve, but it may be lowered by adding the water necessary for cooling and adjusting the amount of aluminum simulating the sodium. In this manner the curves can be matched throughout. Both curves are normalized to one fission per cubic centimeter in the core region.

Power Distribution

Some effort has been made to match the power distribution in the core. Figure 3 shows the power distribution in a CFR and the power distribution in the core of the SMR for various percentages of water in the core. Since a difference between the CFR and the SMR for the case of 75% aluminum and 25% water was noted some effort has been made to bring these into better agreement. A slightly different core (100 fuel plates rather than 200) was divided into five regions to determine the variation that can be obtained in the core power distribution (Fig. 4) by adjusting fuel in the five regions from the center out in the proportions of 2:2:3:3:4 and 1:2:3:4:5. These calculations are not final but indicate that the proper mockup of the source radiation in the SMR can be obtained.

[redacted]

[redacted]

2-01-059-77A

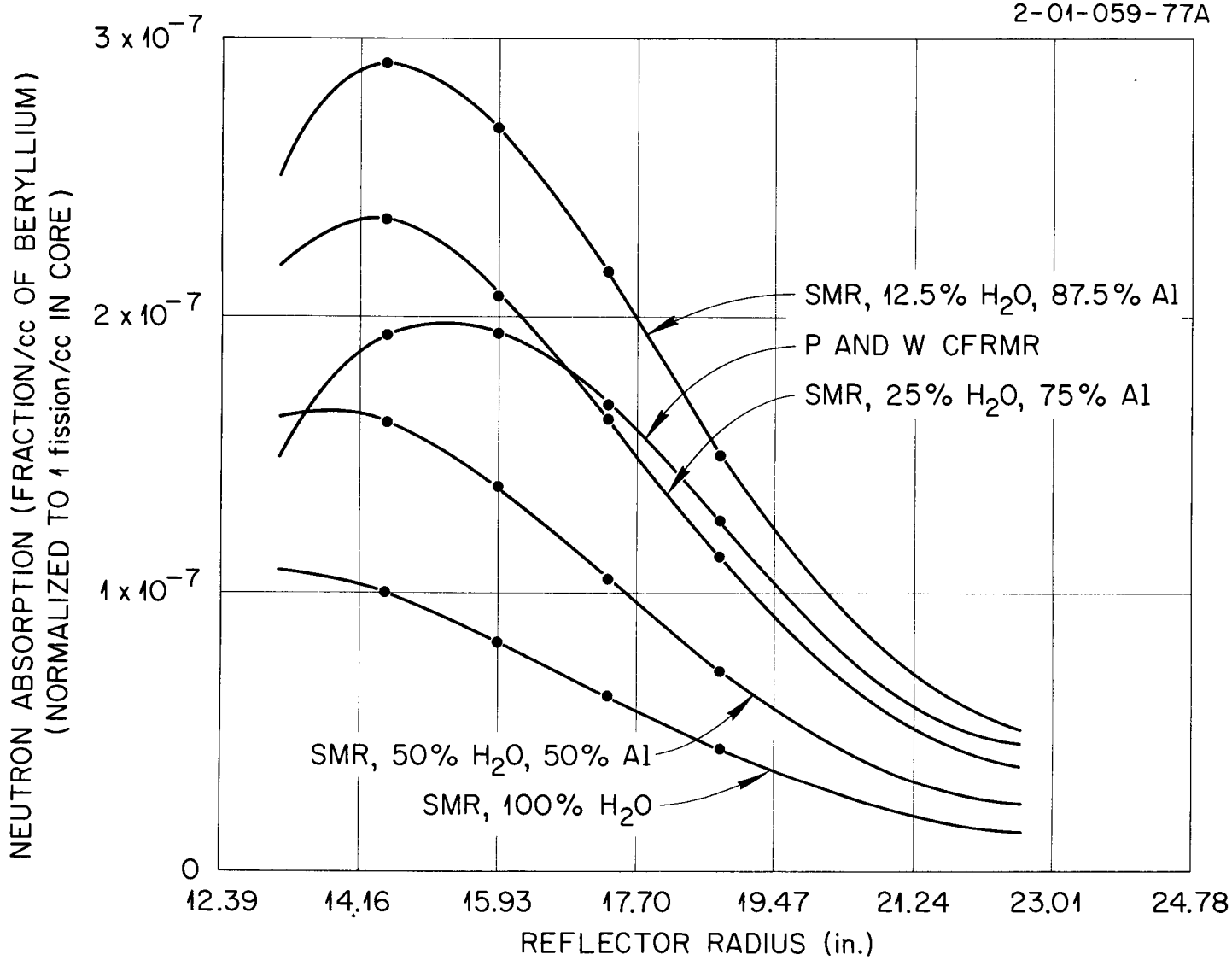

Fig. 2. Fraction of Neutron Absorption in Beryllium Reflector of SMR, Compared with Pratt and Whitney CFRMR.

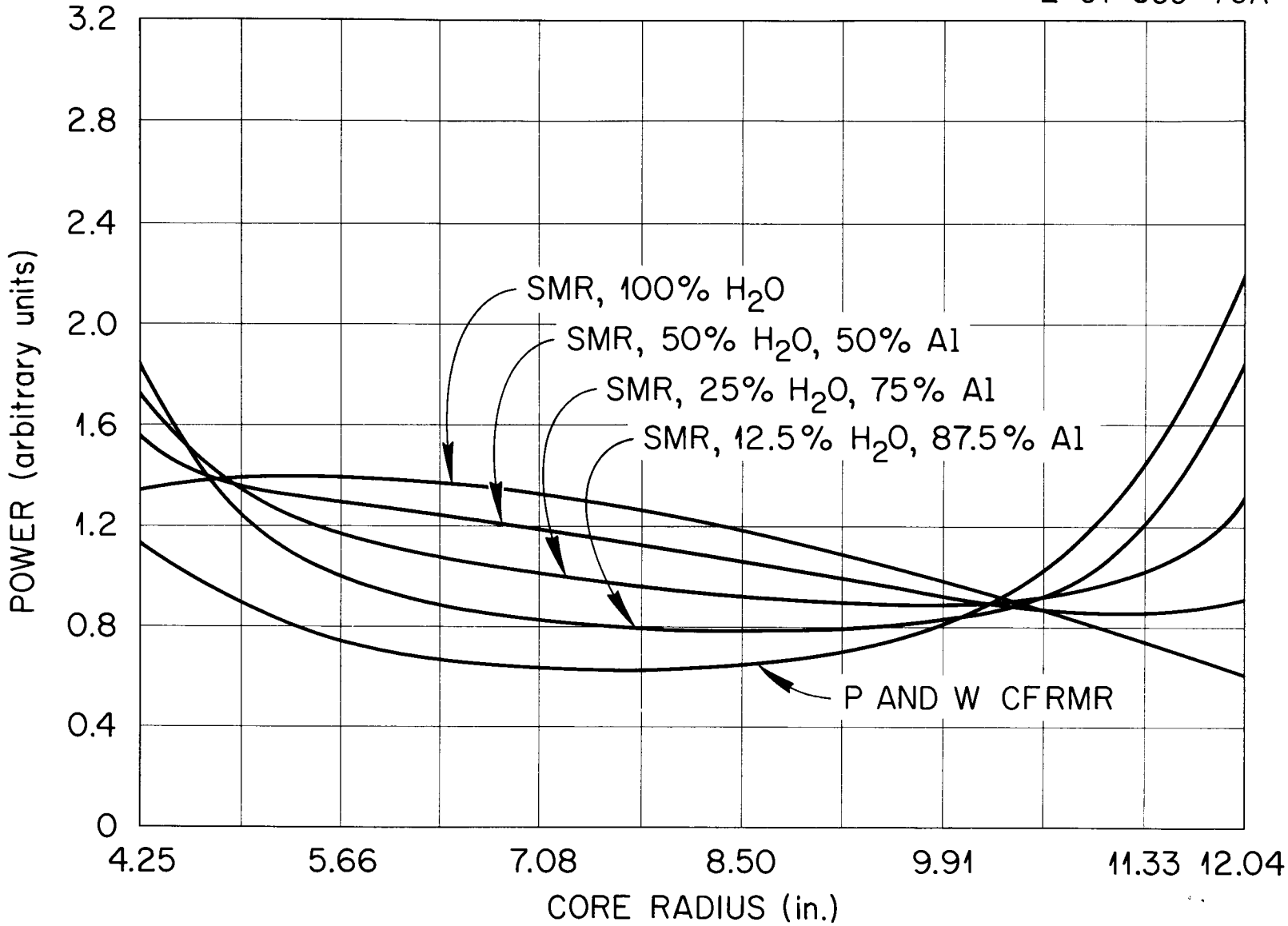

Fig. 3. Power Distribution in SMR Containing 200 Fuel Plates Compared with Pratt and Whitney CFRMR (Spherical Mockup).

[redacted]

2-01-059-75A

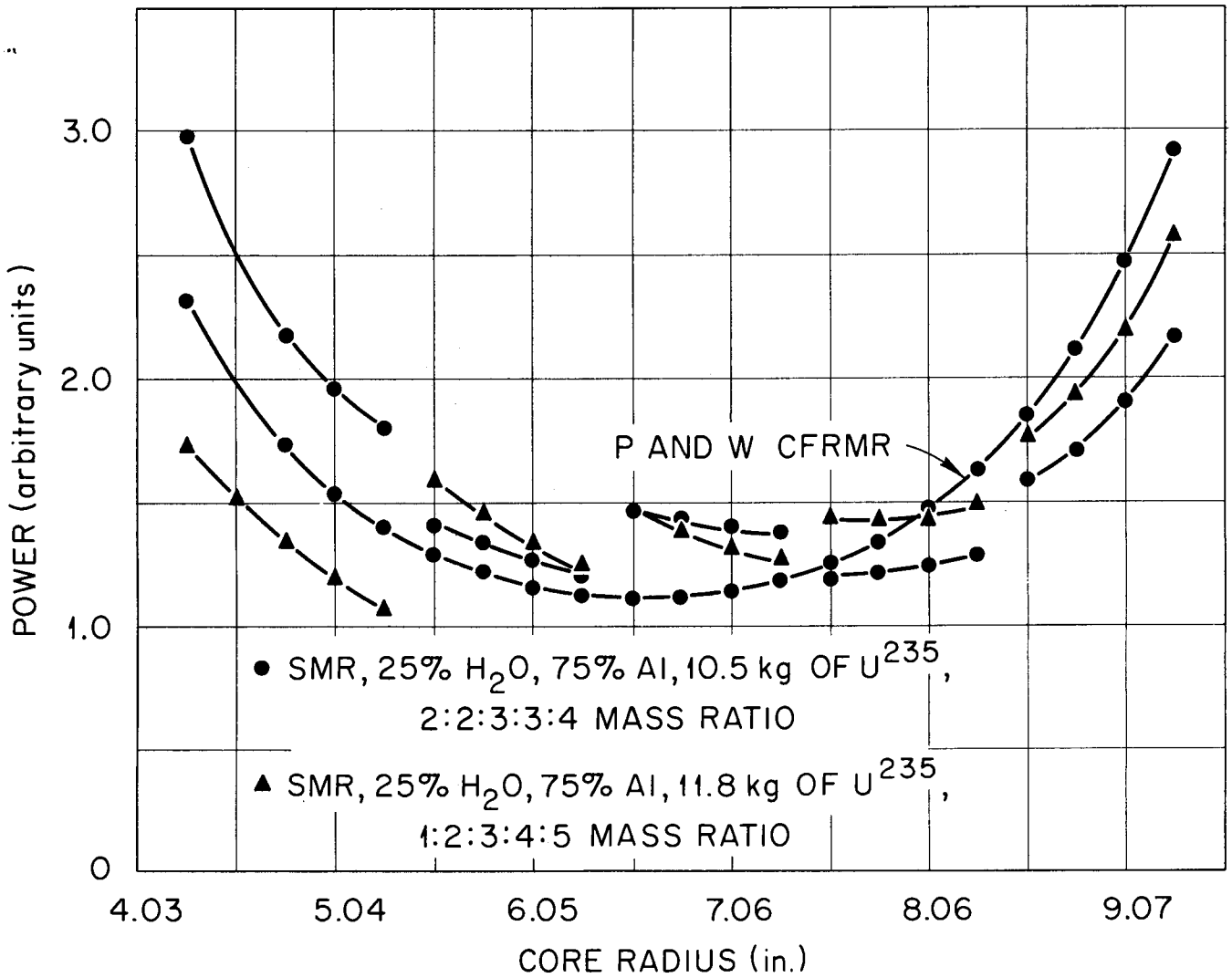

Fig. 4. Power Distribution in SMR Containing 100 Fuel Plates Compared with Pratt and Whitney CFRMR (Cylindrical Mockup).

[redacted]

Gamma-Ray Sources

Another calculation is being carried out at Pratt and Whitney to determine the importance of each region as a gamma-ray source. The reactor is being divided into shells and the gamma-ray intensity due to sources in each shell is being determined in a line of sight attenuation calculation. This is being done both for the CFR and the SMR as a basis of comparison of the source mockup.

The remaining region of importance that requires some further work is the heat exchanger. As previously mentioned the source due to the circulation of the fuel is not present. Previous Lid Tank Shielding Facility data[1] indicates that the gamma-ray source due to circulation of the fuel contributes approximately 30% of the gamma-ray dose rate outside the reactor shield. It is expected that further analysis of the fission-product gamma-ray data reported by Zobel and Love[2] will enable a calculation to be made by the Monte Carlo method to determine the gamma-ray dose rate due to the circulation of the fuel at least as well as the rest of the radiation from the SMR can be measured.

SCHEDULE

The Shield Mockup Reactor program is being scheduled so that criticality will be reached about May 1, 1957.

[redacted]

[redacted]

REFERENCES

1. H. C. Woodsum, ANP Quarterly Progress Report for Period Ending March 10, 1956, Chapter 13, ORNL-2061.

2. W. Zobel and T. A. Love, "Time Dependence of Fission-Product Gamma Radiation," this report.

[redacted]

SECRET

Paper III-I

CURRENT AND FUTURE ORNL SHIELDING PROJECTS

E. P. Blizard
Oak Ridge National Laboratory
Oak Ridge, Tennessee

SECRET

RESTRICTED DATA

"This document contains restricted data as defined in the Atomic Energy Act of 1954. Its transmittal or the disclosure of its contents in any manner to an unauthorized person is prohibited."

[redacted]

CURRENT AND FUTURE ORNL SHIELDING PROJECTS

by

E. P. Blizard
Oak Ridge National Laboratory
Oak Ridge, Tennessee

The LTSF is currently investigating laminated shields of interest to GE and utilizing LiH, Zr, Be, and U, and other materials; a rerun of some of the RMR tests is planned. Experiments performed at the BSF or at other locations by BSF personnel will include investigations of: angular distribution of fast neutrons behind H_2O and LiH; prompt fission gamma rays; density effects on hydrogenous shields; gamma-ray streaming in mocked-up penetrations of the ART shield; and shielding measurements at the ART during its operation. A series of radiation damage experiments at the BSF are also planned. The TSF will continue to investigate ground and structure scattering of radiation and total divided shield configurations. A pseudo optimized divided shield will also be tested. A Shield Mockup Reactor which will include many features of a CFR will be built for use in shielding tests at both the BSF and TSF. The Shield Design Group will continue to concentrate on the simultaneous optimization of neutron and gamma-ray shields, using experimental data. The several projects of the Shielding Theory Group will include: investigations of the air scattering of gamma rays and neutrons; the penetration of a cylindrical crew compartment by gamma rays; gamma-ray heating in a multilayered reactor and shield; and the response of a NaI crystal.

There are a few shielding projects currently in progress at the Laboratory which have not yet resulted in reportable information. These projects plus several investigations planned for the future are discussed in this paper.

LID TANK SHIELDING FACILITY

Currently in progress at the Lid Tank Shielding Facility is a series of experiments on laminated shields of particular interest to the General Electric ANP Project. The shield materials which are to be utilized include lithium hydride, zirconium, beryllium, depleted uranium, and several other lesser components. Determinations will be made of the attenuation of a pure lithium hydride shield, as well as a lithium hydride shield preceded by depleted uranium. Neutron and gamma-ray intensities will be measured.

[redacted]

[redacted]

A sequel to this will be a rerun of some laminated shield tests of particular interest to the reflector-moderated reactor, including the new shielding materials mentioned above. In addition, these tests will include a series of experiments to determine not only the sodium activation to be expected in the heat exchanger, but also to determine methods of reducing this factor by the addition of boron or other materials.

BULK SHIELDING FACILITY

The angular distribution of fast neutrons behind water and lithium hydride shields will be measured at the Bulk Shielding Facility. This information is of interest in the calculation of shaped reactor shields. Prompt fission gamma rays will also be measured. The interest in this experiment lies basically in the enigma that the gamma-ray spectra which have been measured to date, principally by Gamble,[1] show no line structure whatsoever and this is hard to understand on the basis of nuclear theory. A strong effort will be made to determine whether line structure actually exists.

As a check on the geometric transformations which are used in connection with the Bulk Shielding Reactor, measurements will be made in water at significant distances from the reactor as a function of the temperature of the water. This increase in temperature will change the attenuation of the water but will of course not affect the spreading factors. An attempt will be made to correlate theory and experiment.

The many penetrations in the lead shielding of the aircraft reactor tests introduce significant uncertainties in the shield design. By means of mockup experiments carried out by BSF personnel at the thermal column of the ORNL Graphite Reactor, some of these uncertainties are being reduced. A gamma-ray source will be produced by means of a layer of cadmium at the top of the thermal column. Above this will be the lead shield with the mocked-up penetrations. Measurements of gamma rays will be made in the water above the lead.

At the ART, scheduled for operation in calender year 1957, various shielding measurements will be made by BSF personnel. Among these are gamma-ray spectroscopy and angular distribution measurements at the surface of the reactor shield, NaK activation measurements, and the gamma-ray intensity outside the shield as a function of time after reactor shutdown.

RADIATION DAMAGE PROGRAM

It is anticipated that the Bulk Shielding Facility will be used as the site for a series of radiation damage experiments. To this end, a

1 R. L. Gamble, "Prompt Fission Gamma Rays from Uranium 235," Dissertation, University of Texas, Austin, Texas (June, 1955).

[redacted]

[redacted]

large tank will be installed in the pool so that the reactor can be placed adjacent to it, thus flooding the tank with neutron and gamma radiation. Various experiments are contemplated utilizing this source of radiation.

TOWER SHIELDING FACILITY

In an effort to determine the effect of ground scattering not only on experiments but on airplanes operating close to the ground, differential measurements will be made utilizing a beam of radiation aimed at various points on the ground. Measurements of neutrons and gamma rays will be made.

Differential studies of total divided shield configurations will be continued. These include measurements of the variation of radiation with position in the crew shield, variation with the reactor shield thickness, and the separation distance.

Structure scattering will be measured in differential-type experiments. In these small samples of structural materials of interest to airplane construction will be utilized as scattering media, and their effect will be measured on the radiation reaching the crew compartment.

It is anticipated that a complete test will be made of a pseudo optimized divided shield configuration using a crew shield and reactor shield of simple geometry. For these experiments the present Tower Shielding Facility Reactor will be used. Jet engine activation and radiation damage will also be studied early in calendar year 1957 with a Pratt and Whitney J-57. The engine will be run during the tests.

SHIELD MOCKUP REACTOR

A Shield Mockup Reactor will be built for use both at the Tower Shielding Facility and at the Bulk Shielding Facility. This reactor will encompass in its design as many features of a circulating-fuel reactor as is possible which are of interest to shield design itself. These include the beryllium reflector, capture gamma-ray sources such as the inconel shells at the edge of the fuel region, heat exchanger tanks with their boron protection layers, lead shadow shields, and hydrogenous neutron shields. This reactor is not completely designed at the present, but it is hoped that its power will be in excess of 1 Mw and that it will remove many of the uncertainties which are extant.

SHIELD DESIGN

Simultaneous optimization of neutron and gamma-ray shields utilizing the differential data obtained at the Lid Tank and the Tower Shielding Facilities will be carried out. The optimization will be extended to include the effect of ground and structure scattering when this information becomes available.

[redacted]

[redacted]

SHIELDING THEORY

In cooperation with Lt. R. E. Lynch of WADC, calculations will be carried out on the air scattering of gamma rays, extending the information to more than single scattering. The sources will be point monodirectional and monoenergetic. The detector will be a point detector. Complete angular distribution and energy spectra will be recorded for different conditions of separation, source energy, and direction at which the source points with respect to source-detector axis. In addition, it is hoped that the foregoing will be extended to include the penetration of a cylindrical crew box of finite length.

Air scattering of neutrons will be studied by the Monte Carlo method. In the first effort the scattering will be presumed to be isotropic in the center of the mass system. The source will be the surface of a sphere or a point; it can have any given angular distribution or can be monodirectional. The detector will be a point detector. Energy and angular distribution spectra will be determined as a function of the diameter of the source sphere, the separation distance, and the energy of the source neutrons. An extension of this, which it is hoped will be carried out with the collaboration of Boeing Airplane Company, will encompass the anisotropic scattering to be expected in air.

Gamma-ray heating will be calculated for the multilayered reactor and shield arrangement of the circulating-fuel reactor. This calculation will utilize the Monte Carlo method.

The response of a sodium iodide system will be calculated, using the Monte Carlo method, to determine the pulse height spectra for any size crystal and incoming gamma radiation. Bremsstrahlung and annihilation radiation will be accounted for.

[redacted]

Paper III-J

SOME ASPECTS OF THE LONG TERM EFFECTS OF RADIATION*

Nathaniel I. Berlin
Armed Forces Special Weapons Project
Washington, D. C.

*This material has been extracted from a study underway by N. I. Berlin and F. L. DiMaggio.

[redacted]

SOME ASPECTS OF THE LONG TERM EFFECTS OF RADIATION

by

Nathaniel I. Berlin
Armed Forces Special Weapons Project
Washington, D. C.

It is a pleasure to be here and to be permitted to participate in your program. The nuclear propelled aircraft is certainly a fascinating field of endeavor. Underlying many of the physical and engineering problems is that of the effect of radiation on man. At the outset, I would like to state that I shall confine myself to the presentation of a particular line of approach for estimating the hazard, without consideration of the problems that this poses for both the designer and for those concerned with the establishment of operational radiation exposures.

Radiobiological experiments indicate that all radiation is deleterious; the question then becomes "What is the magnitude of the injury produced?" The problem in the determination of a permissible radiation experience for individuals in a program where the dosage levels may be greater than the present "tolerance" levels is not easily resolvable. The present tolerance level for acute and chronic radiation is largely based upon the failure to observe in individuals so exposed changes which can be ascribed to radiation. However, most of our present methods for observation of radiation injury in both man and animals are relatively insensitive, and are changes observed in the blood. Unfortunately, the dose required to produce clear cut changes in the blood of man are rather large, probably at least 25 r of whole body irradiation when given as a single dose. In the case of low level chronic radiation -- if sufficient numbers of individuals are studied carefully -- small changes can be observed at present tolerance levels, but only by means of statistical analysis; the data are not clear cut. There is, however, one aspect which cannot be measured in the individual but which is a real effect, and that is shortening of life span. This requires a control and an irradiated population. For man there is only one opportunity to get such information, and that is from the data accumulated to date and that being gathered by the ABCC in Japan. However, this data will always be fragmentary. The actual collection of the data is difficult, but, more important, an assignment of radiation dose to any individual or group of individuals can be done only with considerable uncertainty. For this reason, we must turn to experimental animals. In the past 50-100 years much animal investigation has been carried out in many fields from which it has become evident that the over-all pattern of physiological behavior is similar in man to that observed in experimental animals, but caution must be used in extrapolating details from one species to another.

For the future, probably the most sensitive factor in determining levels of radiation exposure will be shortening of life span. This is not

[redacted]

[redacted]

to say that other deleterious effects of radiation should be neglected. The number of people that could be involved in your program is such that from the standpoint of the whole population, the genetic problem is minimal. This, however, neglects the individuals involved and their concern for the welfare of their own progeny. Because the data are limited, the genetic hazard, and others involving the individual irradiated, cannot be satisfactorily reduced to usable numbers. The choice then is that of using relatively insensitive changes observed in the blood or shortening of life span. Basically, shortening of life span is the most satisfactory criterion, since this is a measure of the total injury produced.

In 1825 Gompertz[1] observed that the mortality rate and distribution of the population by age groups could be treated mathematically. If the mortality rate is defined as

$$r(t) = \frac{1}{N} \frac{dN}{dt}$$

Gompertz found that

$$r(t) = r_o e^{mt}$$

which is plotted graphically in Fig. 1. From these equations, it is possible to derive an expression for the median life span

$$S_o = \frac{1}{m} \ln \left[1 + 0.693 \frac{m}{r_o} \right]$$

Simms[2] at Columbia University and lately Jones[3] at the University of California have shown that, for man, the Gompertz function for most diseases, and in particular for those that constitute the principal causes of death, are similar to the Gompertz function for all causes of death; that is, a plot of the logarithm of the mortality rate as a function of age is a straight line with the same slope for all causes of death. Thus, the population may be thought of as consisting of a number of subgroups in each of which the death rate is increasing in a regular manner as expressed by the Gompertz formulation. For our purposes, whether death is due to cancer, heart disease, kidney disease, or any other cause is immaterial.

Both Brues and Sacher[4] at the Argonne National Laboratory and Jones[5] at the University of California have approached the problem of the effect of radiation through use of the Gompertz functions.

[redacted]

Fig. 1. Graph of Gompertz Function.

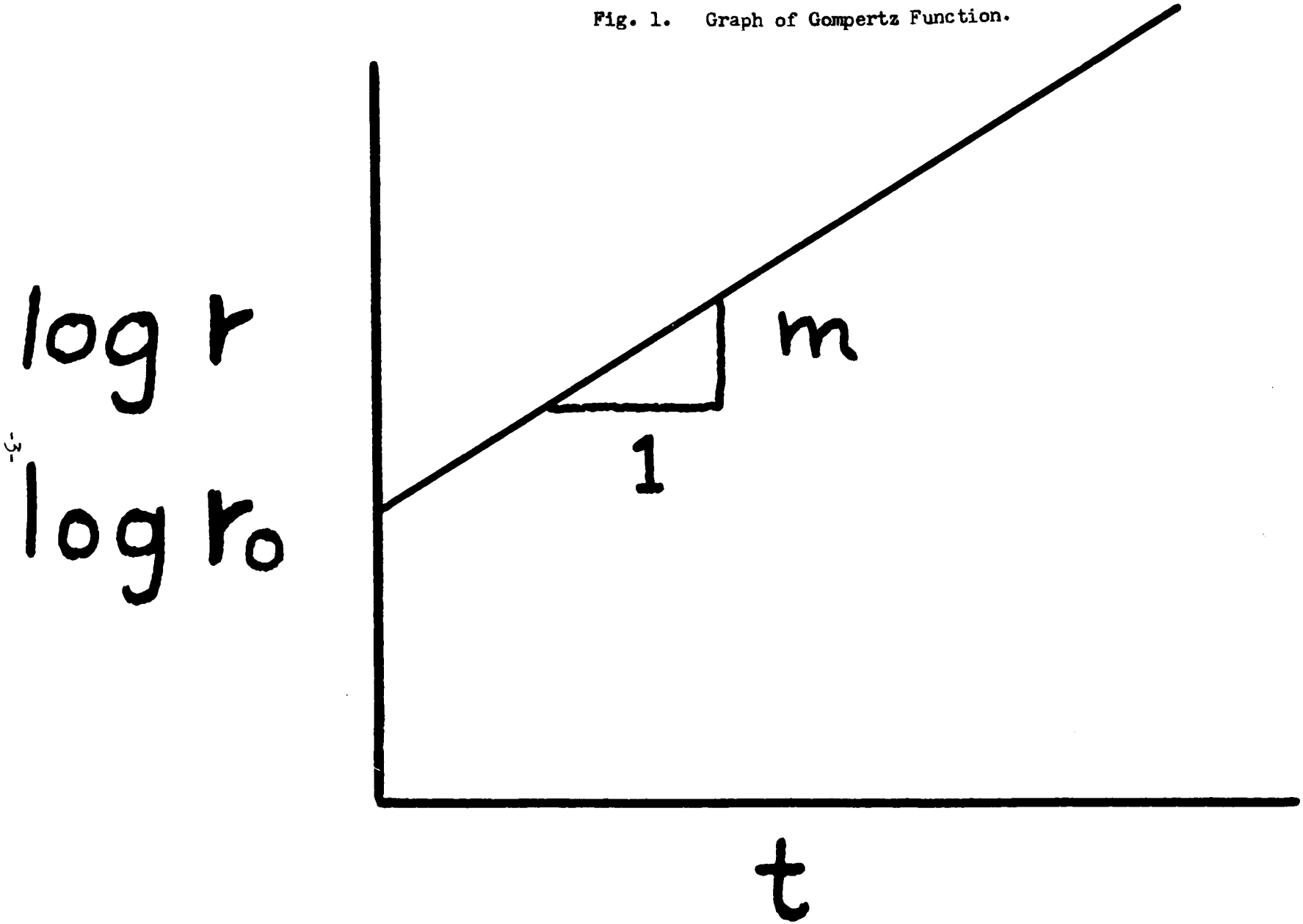

[redacted]

Brues and Sacher[4] postulate that the effect of a single dose of radiation "is an upward displacement without change in slope" and that for chronic radiation the "upward displacement is proportional to dose."

Jones' basic concept is that for any given species at any given chronological age the mortality rate is an index of physiological age, and that radiation, both acute and chronic, results in physiological ageing and consequently a shortening of life span.[5]

Then for a single dose delivered at any given time, the Gompertz function will be as shown in Fig. 2. The basic thought is that following a single dose of radiation there is produced an instantaneous physiological "ageing," causing the upward displacement, and that following this the animals continue to "age" at the same rate as do normal unirradiated controls. The experimental evidence indicates that relationship between r_σ and r_o may be described by

$$\frac{r_\sigma}{r_o} = e^{k\sigma}$$

where k is a constant and σ is the dose in roentgens.

In making this assumption regarding the displacement by radiation, which we shall return to later, it is tacitly implied that radiation results in a shortening of life span. Then the question -- "What is the magnitude of recovery from radiation injury?" -- becomes partially resolved. It has an upper limit, i.e., recovery is not complete. Unfortunately, analysis of the data by the use of the Gompertz function can define only the end result; the magnitude and rate of recovery cannot be calculated. There are, however, a number of interesting observations that can be derived from this type of approach. If the postulated effect of a second sublethal dose be the same as that for the first, then the effect of chronic irradiation can be arrived at from theoretical considerations; that is, to consider chronic irradiation as a series of acute doses, it can be seen in Fig. 3 that as the interval between doses becomes smaller, the Gompertz function becomes a straight line with a slope greater than that of the normal animals. From equations developed, the ratio P of the slope of the Gompertz function for the chronically irradiated animal to the slope of the Gompertz function of the normal animal is

$$P = 1 + k \frac{\gamma}{m}$$

where γ is the dose (r/day). We are thus able to predict the effect of chronic irradiation from the constant k observed in the analysis of the

[redacted]

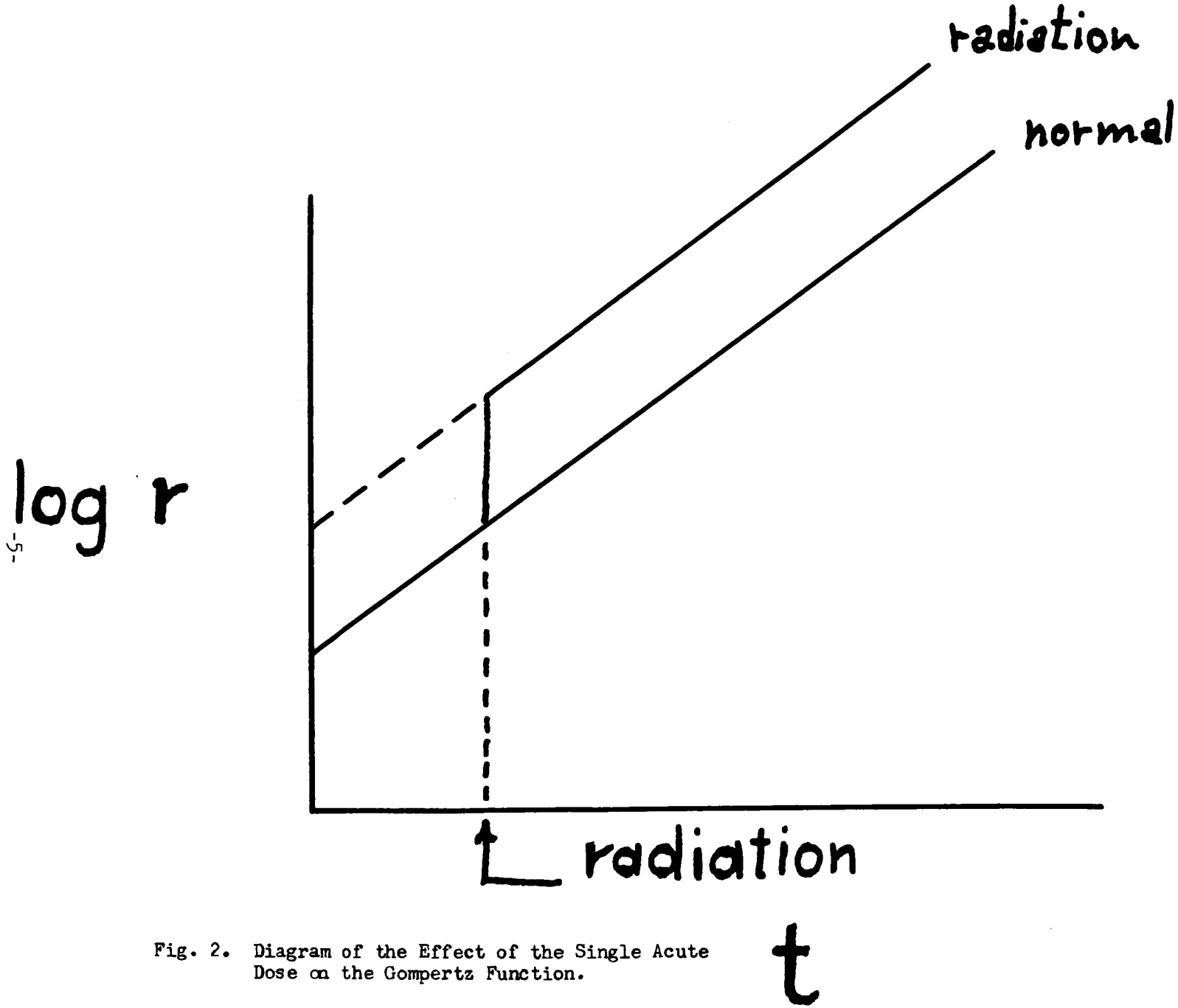

Fig. 2. Diagram of the Effect of the Single Acute Dose on the Gompertz Function.

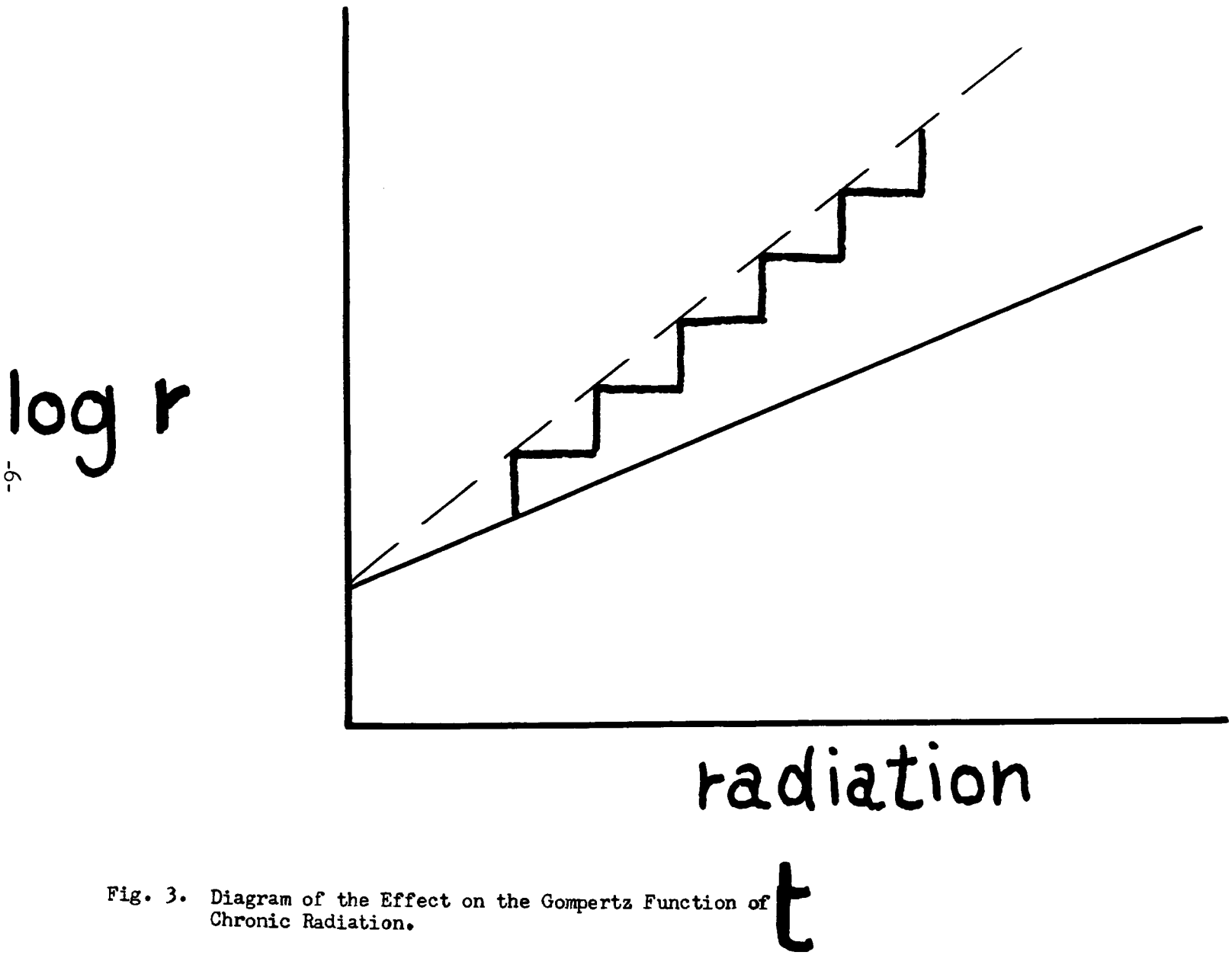

Fig. 3. Diagram of the Effect on the Gompertz Function of Chronic Radiation.

[redacted]

effect of a single exposure. Again the conclusion must be drawn that radiation results in a shortening of life span.

The experimental data available for analysis by means of the Gompertz function is limited. The number of experiments, the dose range for the single acute dose, and the number of animals involved in any given experiment are such that while the data can be treated in terms of the Gompertz function, the numbers arrived at should be viewed with considerable caution.

Table I shows the data from three experiments involving a single sublethal dose. The general concept that there is an upward displacement and that the slope of Gompertz function remains unchanged, is confirmed, although the data are not as clear cut with regard to r_o as would be desirable.

Table II shows the results of an analysis of three chronic irradiation experiments. Here the postulate that the slope should increase as the dose rate increases is borne out; however, theoretically r_o should be the same for all groups, and the observed variance may be ascribed to the small number of animals used.

From the equations developed for the calculation of the median life span and the observed k, the shortening of life span from either a single acute dose or from chronic irradiation can be calculated.

Figure 4 shows the predicted shortening of life span* from a single sublethal exposure, in rodents, at t = 0. It will be noted that there is predicted a 3.4% reduction in life span for a dose of 100 r of total body radiation. Actually for the three experiments in Table the predicted shortening of life span for a dose of 100 r varies from 2.4% to 3.4%. It should be pointed out that this applies only to young animals (8-12 weeks of age). If the relationship $r_\sigma/r_o = e^{k\sigma}$ holds throughout life, then the predicted percentage shortening of life span increases with age. Figure 5 shows the predicted and observed reduction in life span for chronic irradiation as a function of dose rate. The general similarity of these curves is such that further experimentation is warranted, particularly at low dose rates, between 0.1 and 1.0 r/day. The difficulty at low dose rates is that it is experimentally difficult to obtain good data, since small differences between large numbers must be determined.

---

*In discussing shortening of life span, the reduction mentioned at any place in the text is that occurring in the life expectancy at the time of irradiation for the single dose, or in case of chronic radiation, the reduction is in life expectancy from the time at which radiation is started.

[redacted]

[redacted]

TABLE I

Dose (r)	r_o(days^{-1})	m(days^{-1})
Control	0.0110/120	3.18×10^{-3}
300-400	0.0103/120	3.34×10^{-3}
Control	0.0454/120	2.43×10^{-3}
300	0.0566/120	2.60×10^{-3}
Controls	0.0122/100	2.40×10^{-3}
150	0.0109/100	2.79×10^{-3}
300	0.0160/100	2.15×10^{-3}

[redacted]

[redacted]

TABLE 2

	r_o	m
Control	0.0143	0.013/week
0.1 r/day	0.0053	020
0.5	0.0125	016
1.0	0.0055	021
10	0.0042	032
Control	0.00011	0.00286/day
5 r/day	0.000078	0.00435
Control	0.00159	0.0755/30 day
0.11 r/day	0.00039	0.0934
1.1	0.00049	0.103
2.2	0.00039	0.1203
4.4	0.00041	0.1294
8.8	0.00039	0.1625

[redacted]

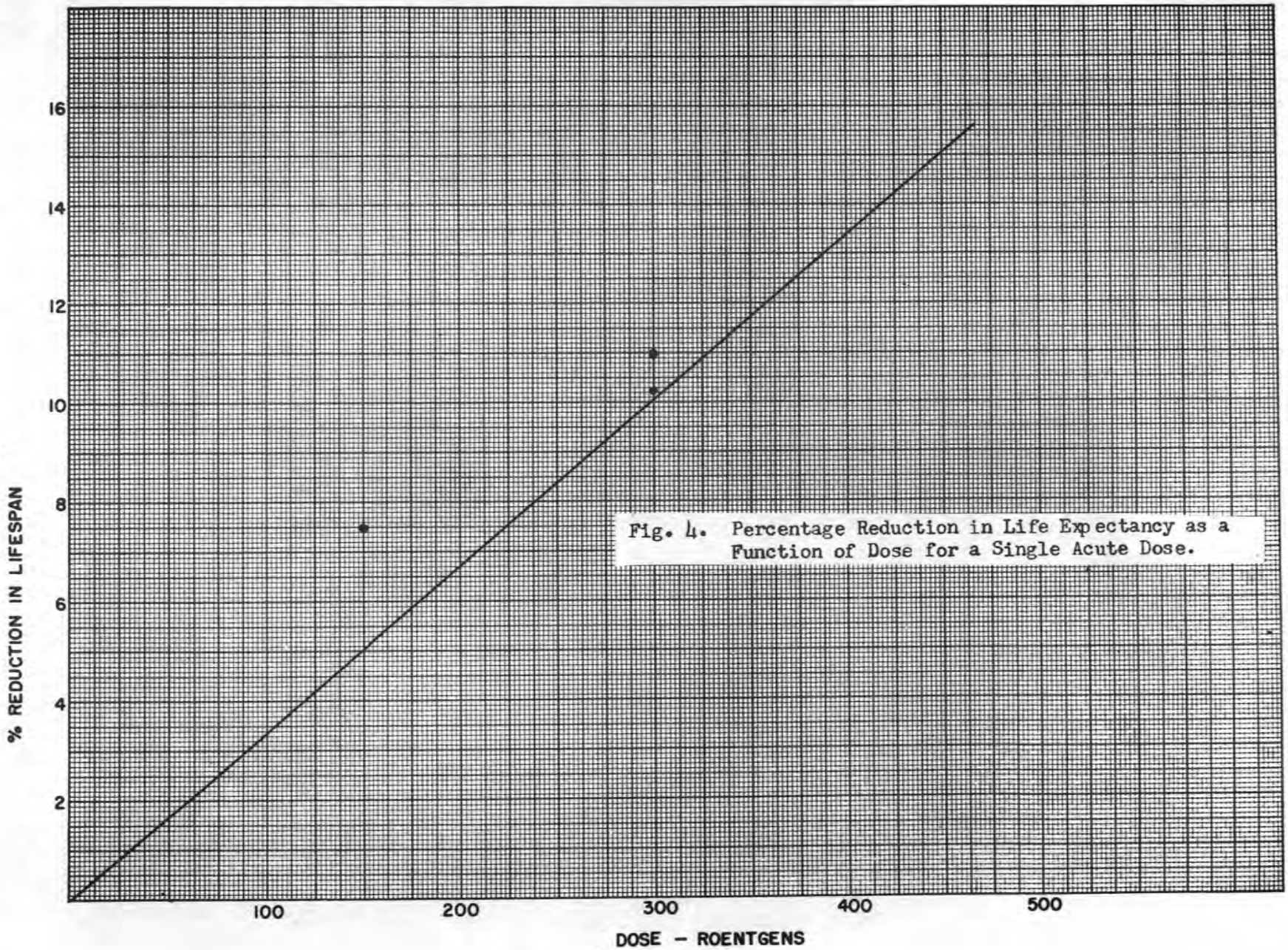

Fig. 4. Percentage Reduction in Life Expectancy as a Function of Dose for a Single Acute Dose.

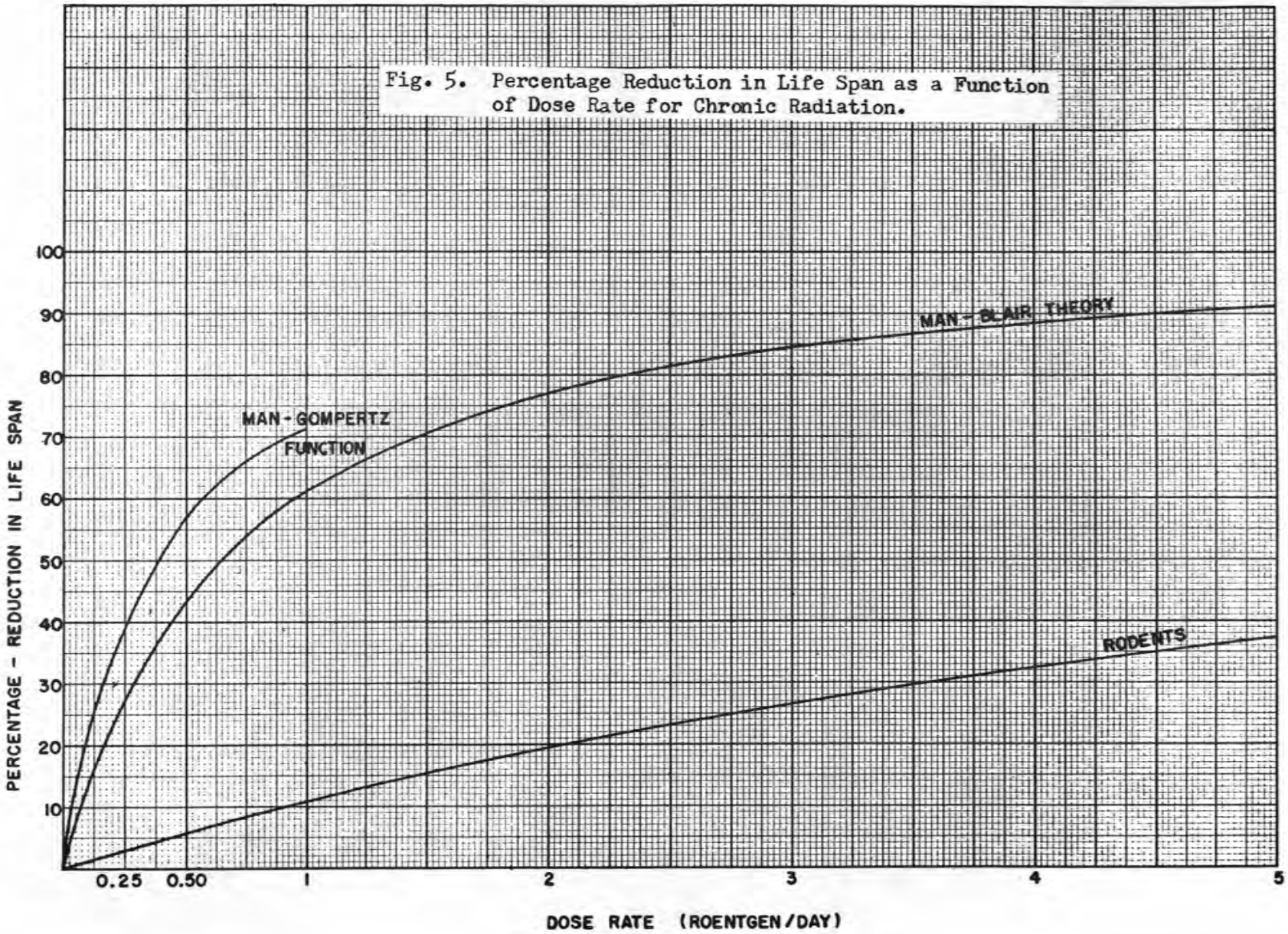

Fig. 5. Percentage Reduction in Life Span as a Function of Dose Rate for Chronic Radiation.

[redacted]

What can be said about man? At present there is only one potential opportunity and that is the experience at Hiroshima and Nagasaki. It is hoped that in the near future the ABCC will publish their findings. However, Brues and Sacher[4] have developed two postulates for the extrapolation from species to species. These are

1. For the single acute dose - the percentage reduction in life span is the same if irradiated at an actuarially equivalent age.

2. For chronic irradiation - to produce the same percentage reduction remaining in life span, the dose rate should be Y_γ, where

$$Y = \frac{\text{life span species 1}}{\text{life span species 2}}$$

The first postulate permits an extrapolation to man of the results of a single short term exposure. We shall return later to the results of application of the second postulate.

In summary, analysis of the effects of irradiation may be carried out by use of the Gompertz function. These indicate that for both acute and chronic radiation, shortening of life span occurs. In addition the equations developed permit a prediction of the effects of chronic radiation if the effect of acute radiation is known.

At present perhaps the most interesting theory describing the effect of radiation is that of Blair of the University of Rochester.[6] Blair assumes that recovery from radiation injury is not complete, that recovery may be described by a first-order process and that the injury may be expressed as shortening of life span. Blair then states that injury develops in proportion to the dose rate and repairs at at a rate proportional to its magnitude except for an irreparable fraction which accumulates in proportion to the total dose, from which Blair writes the following equation

$$\frac{dI}{dt} = A\gamma - \beta(I - \alpha\gamma t)$$

where I = injury; A, β, and α are constants; and γ is the dose rate. Blair then considers several different cases. For the purposes of this discussion, we shall consider only the case of low level chronic irradiations until death. Solution to this equation for that case is

[redacted]

[redacted]

$$I = \frac{\gamma}{\beta} (A - \alpha) + \alpha\gamma t$$

Now if injury be equivalent to shortening of life span, as Sacher assumes and the Gompertz function type of analysis shows, then with rearrangement of the terms,

$$S = S_o - \alpha \left[\frac{(A - \alpha)\gamma}{\alpha\beta} + \sigma \right]$$

A = constant

α = constant

β = constant

σ = dose

Experimentally, if S is plotted against total dose plus a quantity proportional to dose rate, a straight line with slope of $-\alpha$ will be obtained. Figure 6 indicates that for a particular experiment the observed data are well described in this equation. Blair has carried out this type of analysis for a number of experiments.[6] However, there are two features of Blair's theory and method of analysis that require further explanation. The Blair theory predicts that the acute dose LD_{50} decreases with age and that this decrease is linear. This has been tested in only a very limited way, and indeed the acute LD_{50} dose does decrease with age, but the data is not sufficient to determine the rate of decrease of the LD_{50} with age. The Gompertz function type of analysis also predicts that the LD_{50} should decrease with age. Since ageing and irradiation injury are additive, older animals will require less additional injury, whatever the source, to produce death if the injury produced is comparable to normal ageing.

Blair's analysis of the data does not permit evaluation of all three constants, α, β, and A. β, the rate of recovery from radiation injury, must be determined from a second experiment, generally from the results obtained from two or more sublethal doses administered at short intervals. There are two experiments from which this constant can be calculated -- they are those of Hagen and Simmons[7] and Patterson and her co-workers.[8] Basically, these experiments consist in giving a group of animals 1/2 of an LD_{50} dose and then at varying time intervals determining the additional radiation required to produce 50% lethality. As the interval between the first and second dose becomes greater, the second dose required to produce 50% lethality becomes larger. If there is plotted the difference between the single dose acute LD_{50} and the second dose required to produce an LD_{50} when the first dose is 1/2 LD_{50}, there is obtained a straight line with slope of $-\beta$ (see Fig. 7).

[redacted]

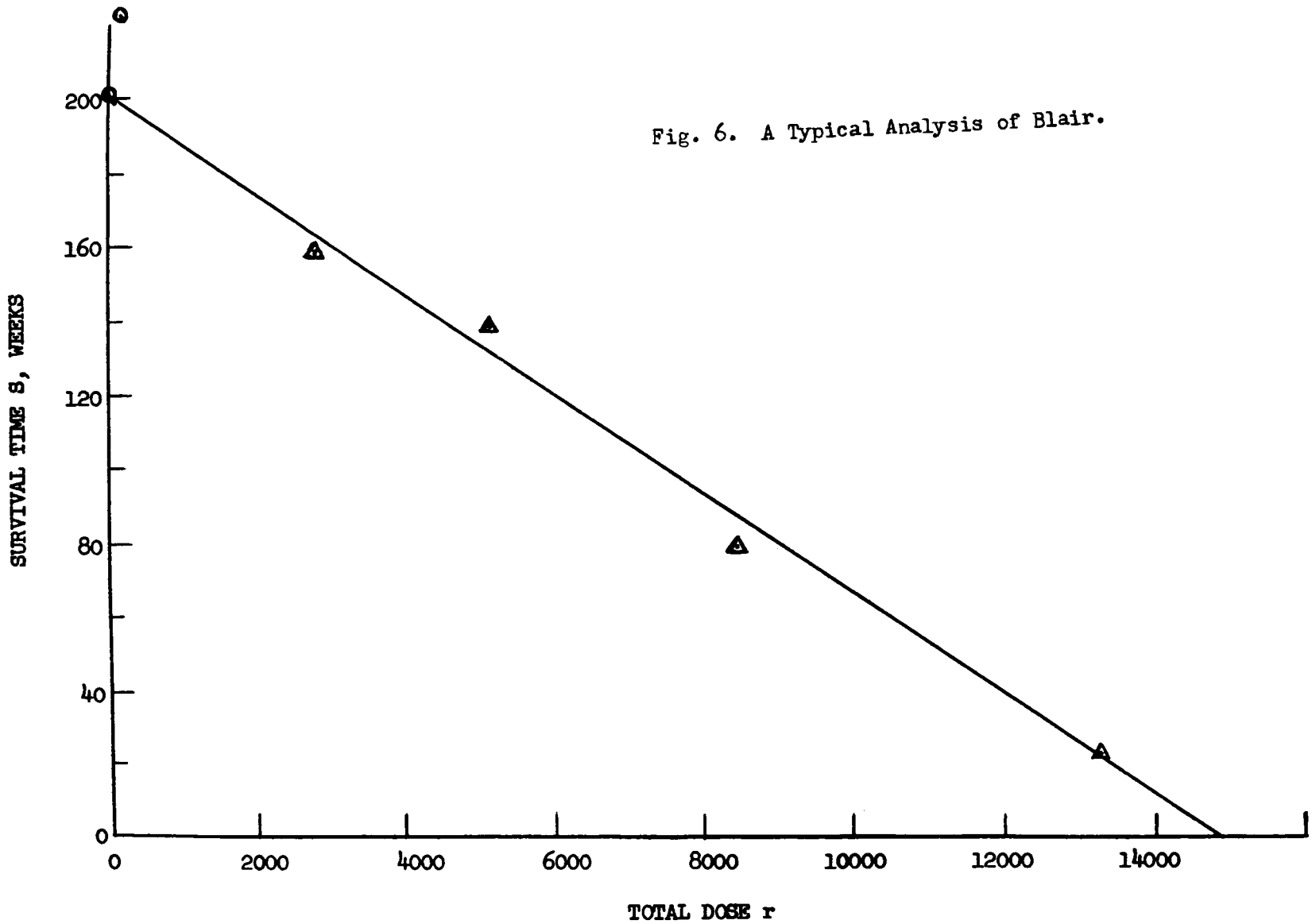

Fig. 6. A Typical Analysis of Blair.

Fig. 7. Measurement of Recovery from Radiation Injury.

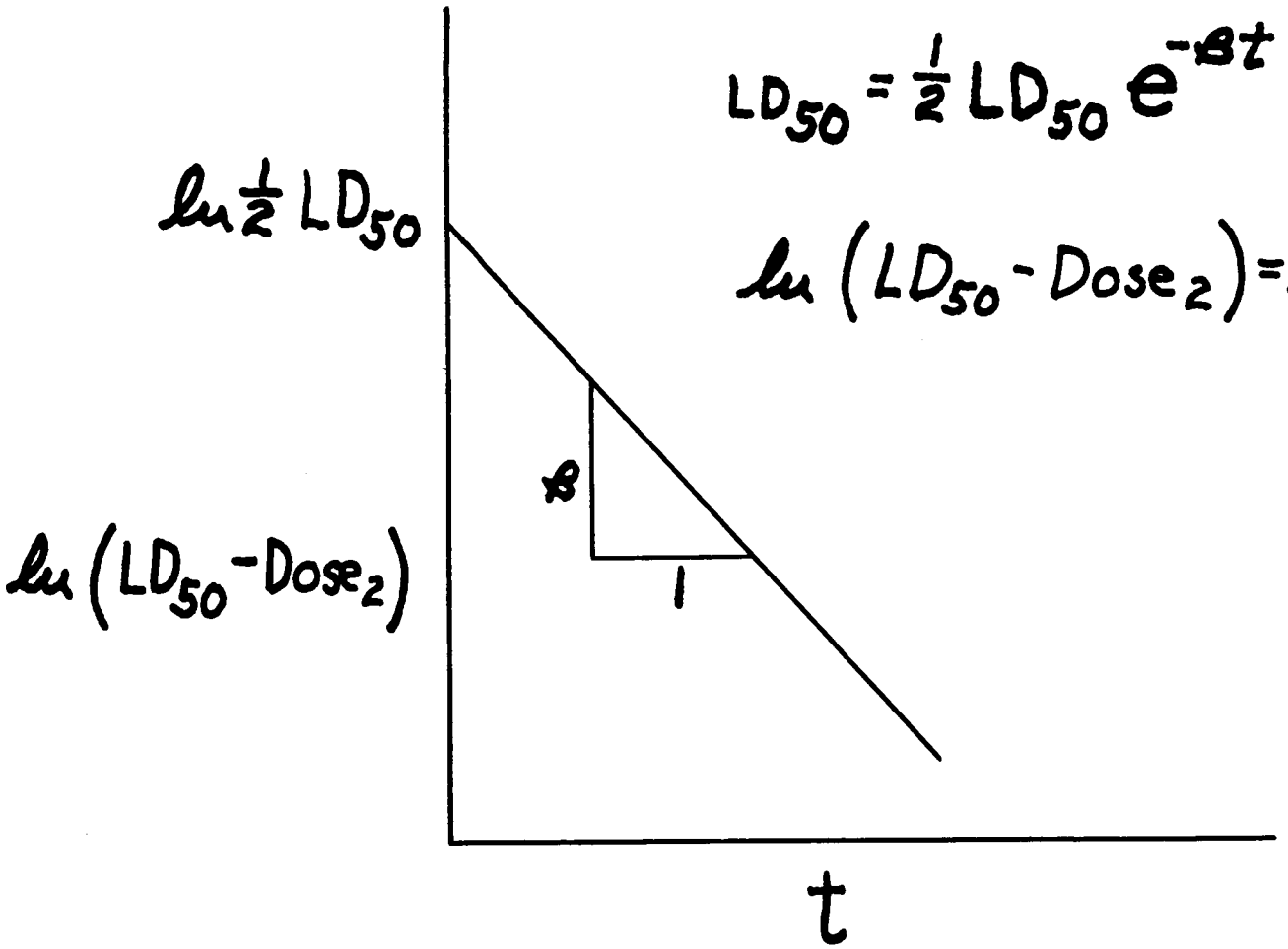

$$LD_{50} = \frac{1}{2} LD_{50} e^{-\beta t} + Dose_2$$

$$\ln (LD_{50} - Dose_2) = \ln \frac{1}{2} LD_{50} - \beta t$$

[redacted]

This postulate that rate of recovery can be represented by a first-order process is confirmed by these experiments.

What can be said about man? Three approaches to this problem have been carried out. They are:

1. Blair[6] has postulated that the constants α and A can be extrapolated from species to species by the relationship

$$\frac{\alpha}{S_o} = \text{constant}$$

$$\frac{A}{S_o} = \text{constant}$$

$$S_o = \text{life span of normal animal}$$

carrying out this extrapolation and for the case of chronic irradiation to death, and assuming a value for β based on experimental dog values, the results are as shown in Fig. 5.

2. Using the ratio m/r_o, as observed in man, and the k obtained from animal data, the shortening of life span from chronic radiation can be calculated (see Fig. 5, Gompertz function).

3. With the Sacher and Brues[4] postulate, the results (see Fig. 5) are almost identical to that predicted from the Gompertz function.

The next concept to be discussed is that of effective dose. It has long been known that fractionation and protraction of a given physical dose results in a smaller biological effect, at least with regard to lethality, than does a single dose of the same magnitude delivered in a short period of time, that is, minutes or hours. The effective dose is defined in terms of the results of a single dose, and is best illustrated by an example. If the dose to produce acute lethality, within 30 days, is 400r, then effective dose of any system of fractionation or protraction that produces 50% acute mortality is 400r, although the physical dose may be much greater than 400r.

From the Blair theory, for the particular case that the animals are young and that each dose is administered within a short period of time, such that $\beta t_1 <<< 1$ (where t_1 is interval between doses)

$$\text{Deff} = \Delta(nf) + (1 - f)\ \frac{(e^{-n\beta t_2} - 1)}{(e^{-\beta t_2} - 1)}$$

[redacted]

[redacted]

where

$f = \alpha/A$ in Blair notation,

n = number of dose,

Δ = magnitude of each dose,

t_2 = interval during which dose is delivered.

As I view your program the radiobiological problem can be divided into two aspects:

1. The long-term effect on life span -- when the dose per exposure and the interval between exposure is such that acute lethality is not encountered.

2. The magnitude and rate of recovery from radiation injury, for pulsed doses, when the physical dose accumulated, whether over a period of weeks or a few months, approaches the minimum lethal dose. For this case the expression for the results of fractionation would be pertinent.

In summary there is animal evidence that radiation produces shortening of life span and that this may be described in terms of the Gompertz function or Blair equations. For the case of chronic radiation, three independent extrapolations to man yield similar results, lending some degree of credence to the numbers arrived at. However, it must be emphasized that the animal data is not as extensive as desired and that extrapolations to man are hazardous. Even so, I have tried to present the results realizing the inherent weaknesses.

[redacted]

[redacted]

REFERENCES

1. B. Gompertz, Phil. Tran. Roy. Soc. (London) 1825, p. 513-585.
2. H. Simms, J. Gerontology, 1, 12, 1945.
3. H. B. Jones, Trans. N. Y. Acad. Sciences, Feb. 1956.
4. Brues and Sacher, Symposium on Radiobiology, John Wiley and Sons, New York, 1952.
5. H. B. Jones, personal communication.
6. N. A. Blair, University of Rochester Report 206 and 207.
7. Hagen and Simmons, CH 3895-(University of Chicago Report).
8. E. G. Patterson, C. W. Gilbert, and J. Mathews, Brit. J. Radiology 25.425, 1952.

[redacted]